DANMARKS OG GRØNLANDS GEOLOGISKE UNDERSØGELSE RAPPORT 2006/43

Composition, age, and geological and geotectonic significance of igneous rocks dredged from the northern Labrador Sea and the Davis Strait

Lotte Melchior Larsen & Finn Dalhoff

GEOLOGICAL SURVEY OF DENMARK AND GREENLAND
MINISTRY OF THE ENVIRONMENT

GEUS

DANMARKS OG GRØNLANDS GEOLOGISKE UNDERSØGELSE RAPPORT 2006/43

Composition, age, and geological and geotectonic significance of igneous rocks dredged from the northern Labrador Sea and the Davis Strait

Lotte Melchior Larsen & Finn Dalhoff

GEOLOGICAL SURVEY OF DENMARK AND GREENLAND
MINISTRY OF THE ENVIRONMENT

G E U S

Contents

Abstract

During the summers of 2003 and 2004, seabed sampling was carried out on a number of physiographic features on the West Greenland shelf. Recovered rocks were Precambrian gneisses, most but not all of which are ice-rafted debris, Palaeozoic and Palaeogene sediments, and many igneous rocks. Igneous rocks, mainly lavas, were recovered from the Davis Strait High (66°32′–66°34′N) and, south of 64°N, in a large submarine canyon (Canyon A) along the western side of the Fylla platform (63°07′–63°31′N), on three seamounts at 62°27′–62°51′N (Seamounts B, C, and H), and on a high area off South Greenland at 59°38′N (Seamount E). Igneous rocks constitute 7–20% of the recovered clasts and are either rafted with icebergs, dispersed by an earlier ice sheet, or derived from local outcrops.

In situ Precambrian basement was recovered on the eastern side of Canyon A, confirming the existence of exposed, upthrust basement as inferred from seismic sections. Zircons from a basement sample gave an Archaean age of 2740 Ma; thus the Archaean basement in West Greenland extends for nearly 200 km offshore.

A total of 95 igneous rock samples were chemically analysed and divided into 12 compositional groups. On the Davis Strait High, the only basalt type found is geochemically depleted basalt. South of 64°N, non-depleted and related basalts (the 'main group' *s.l.)* constitute 70% of the igneous rocks, but other groups are present including rhyolites, enriched basalts and basanites which may have formed part of the same volcanic succession.

Fourteen samples were dated by the $^{40}Ar/^{39}Ar$ step-heating method. Eleven samples were Palaeogene, 63–48 Ma, one was Cretaceous, 119 Ma, and one was Proterozoic.

The geochemically depleted basalts from the Davis Strait High are dated at 63.0 ±0.7 Ma. They are compositionally different from contemporaneous depleted basalts onshore West Greenland and Canada but similar to basalts drilled on the High itself, and they must be locally derived. Their REE patterns indicate mantle melting in spinel facies, i.e. beneath a lithospheric lid thinner than about 80 km. However, the presence of siliceous, crustally contaminated depleted basalts clearly shows that the Davis Strait High contains continental crystalline basement.

In the areas south of 64°N, 10 samples have ages in the range 59–48 Ma. The dredged basalts are geochemically similar to basalts from both central West Greenland and East Greenland. The ocean current pattern and the lack of similar basalts on the Davis Strait High speak against ice rafting from central West Greenland. The similar East Greenland basalts have a narrow age interval of 57–55 Ma, and five of the 10 dated dredged samples are outside of this. The Hecla High is suggested as a local source for the basalts in the southern areas, where the rocks could have been dispersed by a former ice sheet on the shelf, and by river transport. The REE patterns of the basalts indicate mantle melting in garnet facies, i.e. beneath a lithospheric lid thicker than about 80 km. The Hecla High clearly forms part of the West Greenland continental margin.

The volcanic Seamount B yielded rocks geochemically similar to those inferred to be derived from the Hecla High. If they originated on Seamount B, they indicate a lithosphere of similar thickness as at Hecla High. Two basanite samples from Seamount B are of indisputable local origin. They represent small-volume deep melts and confirm the existence of relatively thick lithosphere beneath Seamount B. The lithosphere could be of continental character or it could be abnormally thick oceanic lithosphere.

Seamounts C, H, and E are structural highs. No serpentinites were found on them.

Introduction

Sedimentary basins are situated on the continental shelves along Greenland and Canada in the Labrador Sea, the Davis Strait and the Baffin Bay. Because of their hydrocarbon potential, the basins have been investigated extensively since the early 1970s on both the Greenland and the Canada sides (e.g., overwiews by Henderson et al. 1981; Balkwill et al. 1990; Keen et al. 1990; Chalmers & Pulvertaft 2001). The geotectonic development of the region is very complex, and despite the extensive research which has included geophysical surveys, drilling, and dredging, there has been no unanimous agreement on a model for the history of stretching, rifting, and sea floor spreading in the region. Most importantly from a hydrocarbon exploration point of view, there has been uncertainty with regard to the character of the continent-to-ocean transition zone and the extent of true ocean floor on the Greenland side. In the spreading models of Srivastava (1978) and Roest & Srivastava (1989), true oceanic crust with linear magnetic anomalies dating back to anomaly 33 extended over large areas of the Greenland shelf, leaving little room for Mesozoic sedimentary basins. On the other hand, Chalmers (1991) and Chalmers & Laursen (1995) were unable to model the linear magnetic anomalies older than anomaly 27 within a large section of anomalous crust and suggested that thinned continental crust with sediment accumulations extends a considerable distance into the Labrador Sea (see review by Chalmers & Pulvertaft 2001). More recent work, including drilling of the Qulleq-1 well, has demonstrated the existence of thick Mesozoic sediment accumulations in the anomalous area (Christiansen et al. 2001). None the less, the model of Roest & Srivastava (1989) has maintained its popularity with many researchers and is still in use despite the clear refutation of its version of the pre-anomaly 27 part of the spreading history. There is, in contrast, general agreement on the post-anomaly 27 spreading history.

In 2003 and 2004, a number of conspicuous physiographic features (seamounts, structural highs, and submarine canyons) on the West Greenland shelf were dredged by GEUS in order to obtain more data on the nature of these features many of which are situated in the anomalous area, and thereby to elucidate further the geological history of the shelf area. Besides Precambrian gneisses, most of which are ice-rafted debris, and Palaeozoic and Palaeogene sediments, many igneous rocks were recovered. The igneous rocks are mainly lavas and, although somewhat transported, many are considered to be of relatively local origin. This report presents the results of geochemical analyses and age determinations on the igneous rocks, identifies their source areas, and discusses the implications of the results for the history of the development of the shelf areas.

Dredge localities

In 2003, dredging was carried out from the Russian research vessel R/V Professor Logachev, as part of the UNESCO Training Through Research programme. In 2004, dredging was carried out from the Danish research vessel R/V Dana. The selection of dredge stations was guided by previously obtained geophysical (mainly seismic) data, and the detailed positioning was aided by on-board echo soundings, side scan sonar and sparker seismic data. Detailed technical information on the cruises is found in the cruise reports (Dalhoff et al. 2003; 2004).

In total for the two years, 33 stations were dredged, and igneous rocks were recovered at 29 of these. Site information for the 25 stations from which igneous rocks were analysed is given in Table 1, and the locations are shown in Fig. 1.

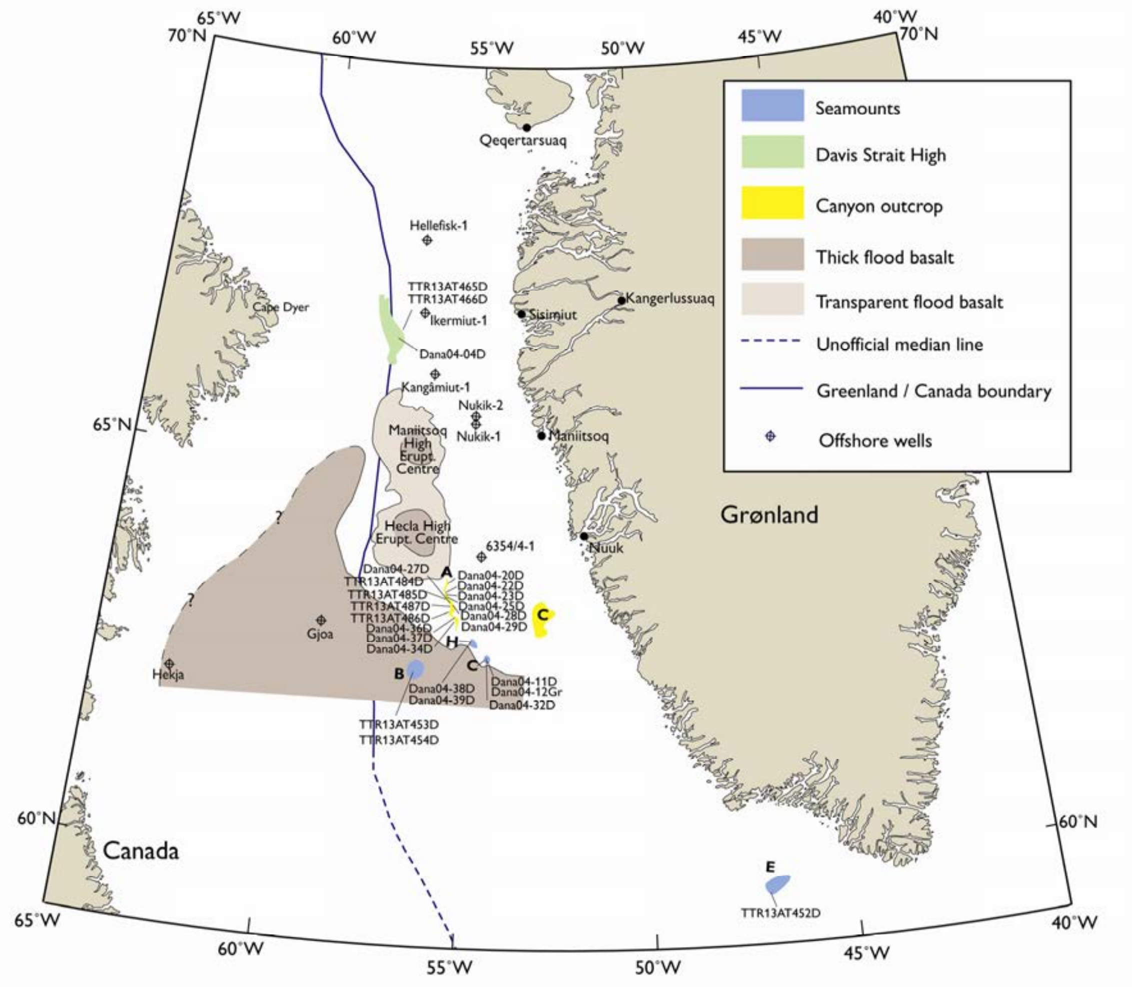

Fig. 1. The location of the dredged features in the Labrador Sea and the Davis Strait. Igneous rocks were recovered from the Davis Strait High, Canyon A, and seamounts B, C, E, and H. The dredges with analysed igneous rocks are indicated.

Table 1. Coordinates for dredges in the Labrador Sea and the Davis Strait

Station	Location	Latitude N	Longitude W	UTM Northing	UTM Easting	Depth, m
TTR13 AT452D	Seamount E	59°37.570	46°50.268	6653696	1071727	2555
		59°37.193	46°49.220	6653153	1072812	2130
TTR13 AT453D	Seamount B	62°27.550	56°26.529	6925458	528778	2398
		62°27.615	56°26.612	6925578	528705	2398
TTR13 AT454D	Seamount B	62°27.288	56°26.516	6924971	528793	2506
		62°27.545	56°25.965	6925453	529263	2302
TTR13 AT465D	Davis Strait High (E)	66°33.600	57°17.794	7382363	486836	679
		66°33.515	57°18.438	7382207	486358	678
TTR13 AT466D	Davis Strait High (E)	66°33.198	57°18.109	7381617	486599	675
		66°33.060	57°17.510	7381359	487041	680
TTR13 AT484D	Canyon Margin A (E)	63°19.833	55°25.239	7023393	579086	1921
		63°20.149	55°24.750	7023990	579480	1856
TTR13 AT485D	Canyon Margin A (E)	63°20.240	55°24.579	7024162	579618	1840
		63°20.600	55°24.058	7024842	580036	1562
TTR13 AT486D	Canyon Margin A (E)	63°14.120	55°22.370	7012846	581749	2080
		63°14.114	55°21.300	7012858	582646	1940
TTR13 AT487D	Canyon Margin A (W)	63°18.659	55°27.031	7021177	577644	2105
		63°18.540	55°27.195	7020953	577512	2003
DANA04-04D	Davis Strait High	66°32.985	57°28.702	7381270	478757	584
		66°32.806	57°29.983	7380945	477806	573
DANA04-11D	Seamount C	62°36.816	54°21.079	6945329	635905	2420
		62°37.345	54°21.094	6946310	635852	2382
DANA04-12Gr	Seamount C	62°37.286	54°21.300	6946193	635680	2368
DANA04-20D	Canyon A	63°30.293	55°30.736	7042704	574048	1436
		63°30.269	55°29.182	7042690	575338	1330
DANA04-22D	Canyon A	63°27.077	55°32.495	7036700	572725	1541
		63°26.161	55°31.922	7035010	573240	
DANA04-23D	Canyon A	63°24.041	55°32.676	7031059	572703	1697
		63°23.627	55°32.197	7030300	573119	1730
DANA04-25D	Canyon A	63°22.012	55°29.859	7027346	575136	1836
		63°21.986	55°29.582	7027303	575368	1819
DANA04-27D	Canyon A	63°18.060	55°26.481	7020076	578130	1968
		63°18.044	55°27.371	7020028	577387	1901
DANA04-28D	Canyon A	63°18.043	55°23.648	7020103	580497	2063
		63°18.046	55°23.268	7020116	580814	1963
DANA04-29D	Canyon A	63°17.995	55°19.370	7020105	584073	1306
		63°18.029	55°18.679	7020183	584648	1277
DANA04-32D	Seamount C	62°39.710	54°21.194	6950695	635586	2487
		62°39.320	54°21.084	6949975	635710	2404
DANA04-34D	Canyon A	63°07.447	55°27.748	7000346	577544	2304
		63°07.487	55°28.347	7000408	577038	2215
DANA04-36D	Canyon A	63°09.483	55°18.446	7004323	585262	1893
		63°09.452	55°17.713	7004281	585878	1837
DANA04-37D	Canyon A	63°09.504	55°17.633	7004380	585943	1696
		63°09.465	55°16.740	7004327	586695	1650
DANA04-38D	Seamount H	62°50.505	54°56.075	6969645	605171	2380
		62°50.811	54°56.063	6970213	605163	2307
DANA04-39D	Seamount H	62°50.591	54°55.653	6969816	605524	2225
		62°50.976	54°56.331	6970512	604926	2175

Each dredge is located by its starting point and its ending point. “Depth” is water depth.
Latitude and longitude in degrees and decimal minutes. UTM coordinates for zone 21.

Davis Strait High   66°33′ N, 57°20′ W

The Davis Strait High is a structural high in the central part of the Davis Strait. It is fault-bounded and is associated with the large NNE–SSW-trending Ungava fault zone. It possesses a positive gravity anomaly, and its acoustic basement comes very close to the sea bed. It has been suggested to consist of oceanic crust (Keen & Barrett 1972), a mixture of continental crust and plume-related volcanic rocks similar to those at Cape Dyer on Baffin Island and in West Greenland (Keen et al. 1974), and a sliver of continental crust surrounded by oceanic crust (Srivastava et al. 1982). However, there is no oceanic crust east of the Davis Strait High (Chalmers & Pulvertaft 2001). Basalts have been recovered by shallow core drilling on the exposed hard surface of the high (Srivastava et al. 1982). Some of these drill sites are situated within 6–26 km from the dredge sites.

On the eastern side of the Davis Strait High, seismic profiles show a number of weakly eastward-dipping stratiform units outcropping or very close to the sea floor (Fig. 2). Four dredges which all recovered igneous rocks were made here. A total of 362 rocks were recovered, of which 254 were sediments, mainly Palaeozoic limestones, 25 were igneous rocks, and 83 were Precambrian basement gneisses. The gneisses are considered to be ice-rafted debris. The frequent and large Palaeozoic limestones are considered to be of local derivation from an exposed sedimentary packet.

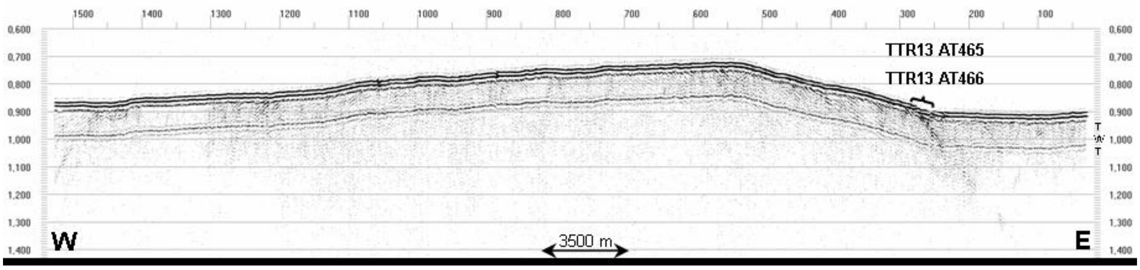

Fig. 2. Single-channel seismic line, PSAT240, across the Davis Strait High. Note the eastward dipping reflectors on the eastern flank coming up very close to the seafloor. The position of the two dredges from 2003 are indicated, with TTR AT465 a few hundred metres offset towards the north.

Canyon A   63°07′–63°30′ N, 55°16′–55°33′ W

Canyon A is a c. 100 km long NNW–SSE trending, deep submarine canyon immediately west of the Fylla Bank, leading southwards from the Hecla High. It is crossed by several seismic lines (Fig. 3). The western canyon side shows outcropping flat-lying strata in which the Selandian–Danian boundary has been located by palynological analysis (H. Nøhr-Hansen, personal communication 2005). The eastern canyon side is interpreted as a fault-controlled crystalline basement high overlain by sedimentary strata.

A total of 19 dredges were placed on both the western and eastern canyon sides and on the canyon floor. Of these, 17 yielded igneous rocks. A total of 630 rocks were recovered, of which 152 were sediments, 99 were igneous rocks, and 379 were Precambrian basement gneisses. Most of the gneisses are considered to be ice-rafted debris, however two dredges on the eastern side yielded what appeared to be local basement rocks (see later).

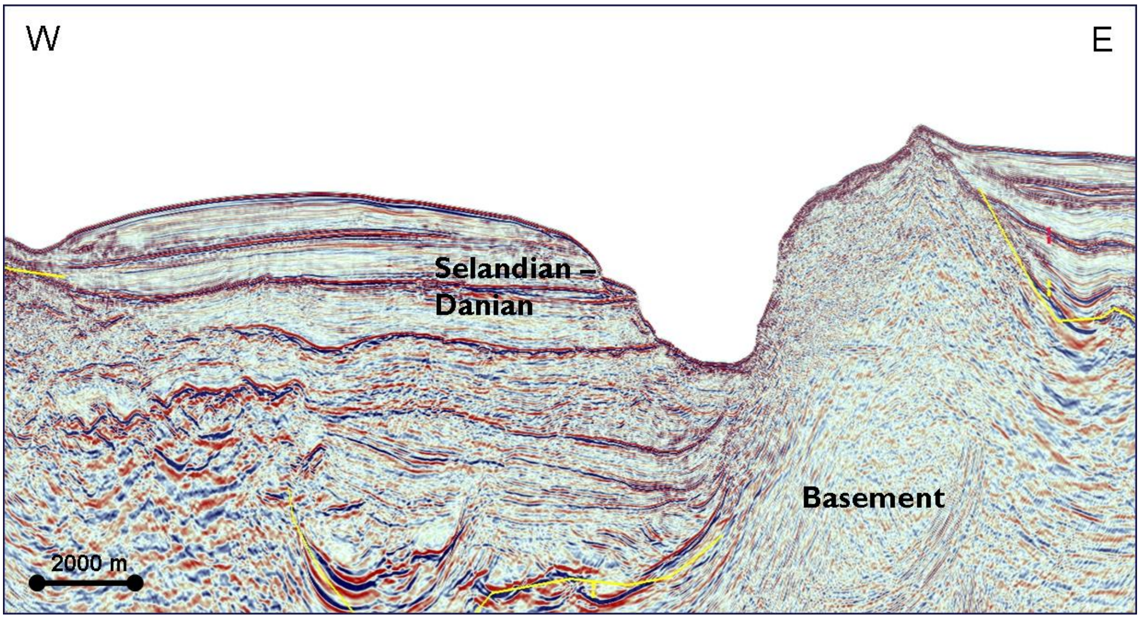

Fig. 3. Seismic line FY01A-11 across Canyon A, showing flat-lying strata on the western side and an interpreted fault-controlled crystalline basement high on the eastern side.

’Canyon’ C   63°00′ N, 52°55′ W

This area is not a deeply incised canyon such as Canyon A but a fault-bounded low area between the Fylla Bank in the west and the higher shelf areas in the east, floored by flat-lying sediments. Two dredges yielded a large number of small transported basement pebbles and some larger basement blocks, all of which are considered to be ice-rafted debris. There were no sediments (except for recent mud) and no igneous rocks.

Seamount H   62°51′ N, 54°56′ W

Seamount H is situated immediately south of Canyon A, on the extension of the eastern side of this canyon. It is a diapiric structure (Fig. 4) rising through possible Paleocene basalts, and it could be either serpentinite, highly extended continental crust, or a sediment diapir.

Two dredges on Seamount H both yielded igneous rocks. A total of 121 rocks were recovered, of which 9 were sediments (limestones and sandstones), 25 were igneous rocks, and 87 were Precambrian basement gneisses. All the gneisses are considered to be ice-rafted debris.

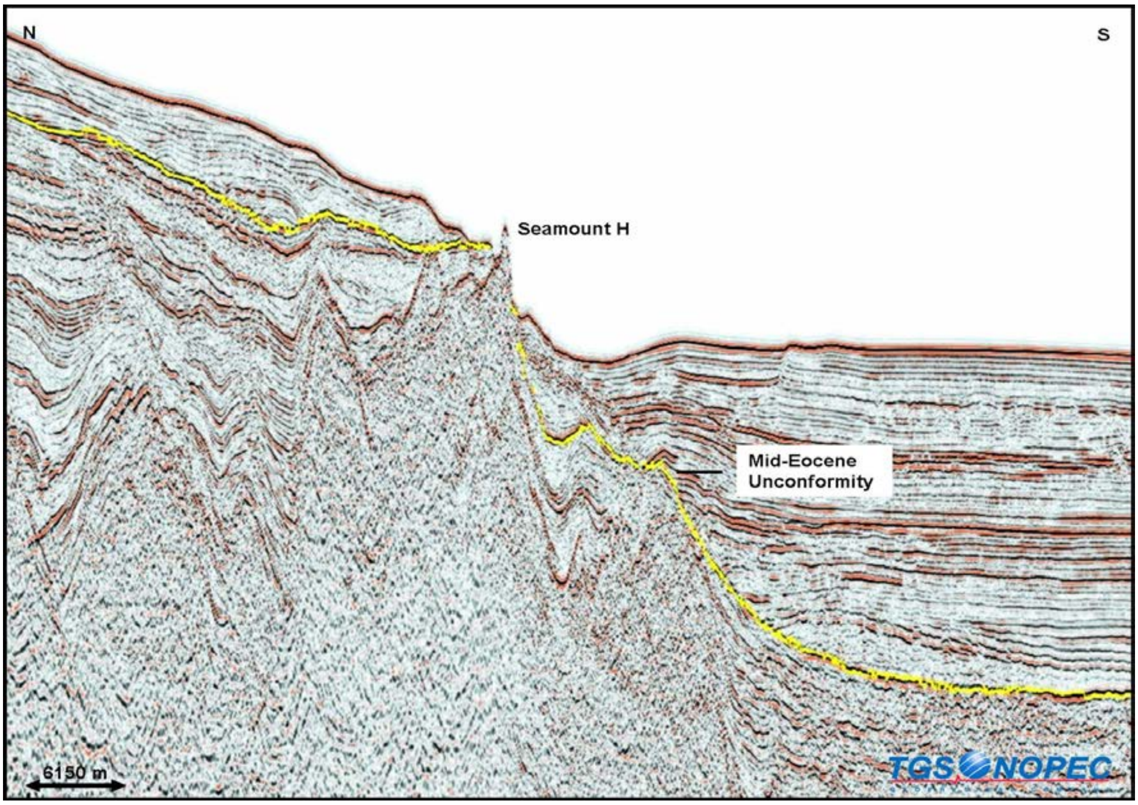

Fig. 4. Seismic line GRC02-9, across Seamount H. The seamount rises from below possible Paleocene basalts, and the seamount could be either serpentinite, faulted basement, or a sediment diapir.

Seamount C   62°38′ N, 54°21′ W

Seamount C is situated south of the Fylla bank, c 30 km south-east of Seamount H. It is separated from Seamount H by sediment subbasins, but it is possible that the two seamounts are part of the same, partly covered structural ridge.

Three dredges on Seamount C all yielded igneous rocks. A total of 138 rocks were recovered, of which 8 were sediments (limestones), 20 were igneous rocks, and 110 were Precambrian basement gneisses. All the gneisses are considered to be ice-rafted debris.

Seamount B   62°27′ N, 56°26′ W

Seamount B is a relatively large structure in the Lady Franklin Basin, situated c. 80 km west of Seamount C. It is considered to be of igneous origin (Sørensen 2005) and has a guyot-like morphology with a flat surface from which several small cone-shaped seamounts rise up to 1000 m above the surface (Fig. 5).

Two dredges on one of the small cones of Seamount B both yielded igneous rocks. A total of 71 rocks were recovered, of which 12 were sediments (sandstones and mudstones), 14 were igneous rocks, and 45 were Precambrian basement gneisses. All the gneisses are considered to be ice-rafted debris. A few of the igneous samples are of local aspect, see later.

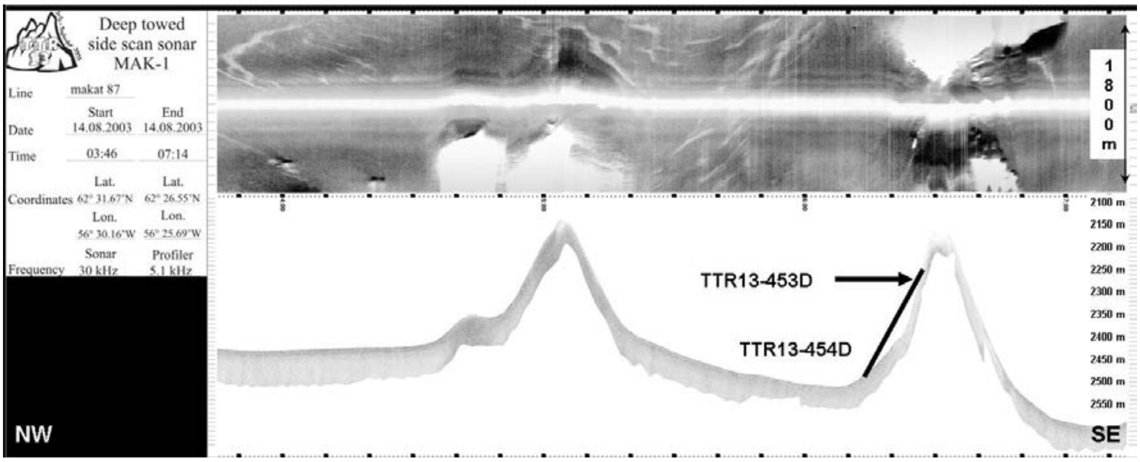

Fig. 5. Deep towed side scan sonar and profile across Seamount B. The location of the two dredges from 2003 is indicated.

Seamount E   59°37′ N, 46°50′ W

Seamount E is a structure rising above the sea floor c. 100 km south of South Greenland. It is faulted, but its detailed origin is not known.

From one dredge on Seamount E, a total of 50 rocks were recovered. Of these, 6 were sediments (sandstones, mudstones and a limestone), 14 were igneous rocks, and 30 were Precambrian basement gneisses. All the gneisses are considered to be ice-rafted debris.

Character and provenance of the dredged material

The recovered clasts were classified into three groups: Precambrian rocks (gneisses, amphibolites, and metasediments), sediments, and igneous rocks. The sampling statistics for each dredged feature are given in the above descriptions of these.

Ice rafting and ice sheet dispersal

It is important to distinguish ice-rafted debris from material of local derivation. Several lines of evidence can be used: lithology of sample populations; sample size, shape and abrasion state; occurrence of lithologies not present in the onshore areas; and the petrography, chemical composition and age of the igneous rocks.

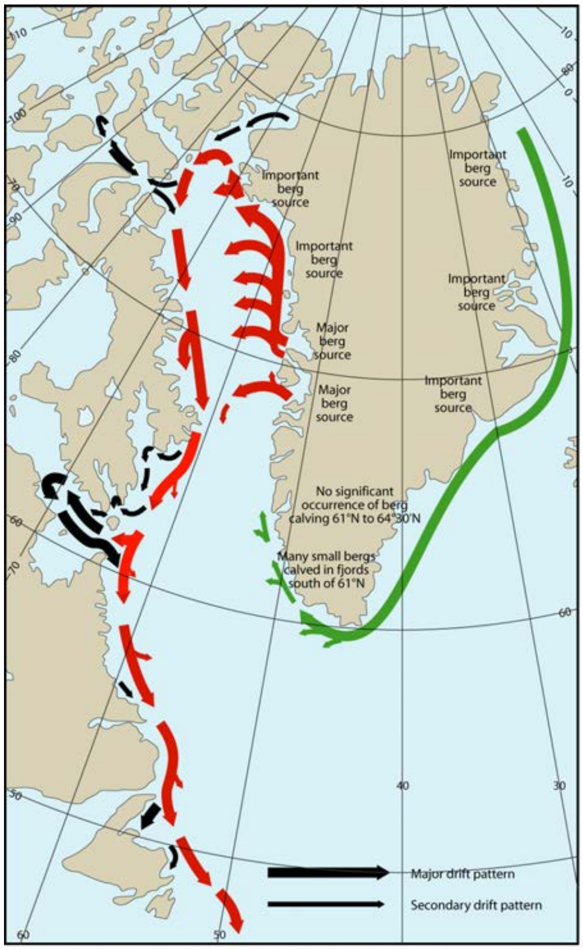

Fig. 6. Iceberg drift pattern around Greenland. Modified from Ghexis 23, 2004.

Ice-rafted debris may be derived not only from the adjacent onshore areas but also from areas farther away in both West and East Greenland. Today, the largest calving areas for glacier ice are central West Greenland with the Jakobshavn Ice Stream, and central to northern East Greenland where large glaciers calve into several fjords. The West Greenland icebergs drift westwards and northwards into the Baffin Bay where they meet the south-flowing Baffin Bay current and drift southwards along the Canadian coast (Fig. 6). The East Greenland icebergs drift southwards along the coast of East Greenland and into the Labrador Sea. A minor amount of icebergs are deflected around the southern tip of Greenland and drift northwestwards along the coast of south-western Greenland to around Paamiut where they swing west across the Labrador Sea and join the south-flowing current on the Canadian side. Iceberg transport around Kap Farvel may have been stronger at an earlier stage (Belan et al. 2004). Linthout et al (2000) recovered ice-rafted debris on the SE Greenland margin at 63°N that was presumably derived from central and northern East Greenland, and thus the possibility that such material is also present in the dredges off-shore West Greenland should be considered.

During the last glacial maximum, the Greenland ice sheet extended to the shelf margin in south-western Greenland (Funder & Hansen 1995; Bennike et al 2002; Fleming & Lambeck 2004). Models for the earlier ice sheets are not available. It is probable that at some stage during the Pleistocene, glaciers covered the Davis Strait High and possibly extended south to cover the Maniitsoq and Hecla Highs, with the seabed being reworked down to at least 800–1000 m water depth. Thus, dispersal of material from the Hecla High via a glacier ice sheet is also possible.

Precambrian rocks

As the onshore areas of Greenland consist predominantly of Precambrian basement, the majority of the ice-rafted debris is expected to consist of Precambrian gneisses with minor metasediments, amphibolites and other metaigneous rocks. Indeed, in most of the dredges more than half of the recovered rocks consist of a variety of different gneisses and a few metasediments and amphibolites, usually of subrounded or subangular shape and with striations and other signs of abrasion. These rocks are considered to be ice-rafted debris. Only two localities yielded Precambrian gneisses of local aspect (see next chapter).

Sediments

Palaeozoic limestone occurs in large quantities in all dredges on the Davis Strait High (Fig. 7). About 70% of the dredged clasts consist of such rocks which form stones, blocks and boulders of which the largest is 50 cm in diameter. The most probable source for these is local outcrops of weakly east-dipping strata on the eastern side of the high. The nearest neighbouring occurrences of Palaeozoic limestone are on the shallow shelf off southern Baffin Island, some 300–400 km SSW of the Davis Strait High (MacLean et al. 1977). While it is perhaps possible that the dredged rocks could be ice-rafted from there it is considered improbable, the more so as similar lithologies are rare in the more southernly situated dredges.

Limestones, calcareous sandstones and sandstones of younger aspect, mainly Tertiary, are found as a minor component and small pebbles and stones in many of the more southernly situated dredges, particularly in Canyon A. They are abraded and transported, but as similar lithologies are not present in the onshore areas they must derive from exposed strata in the offshore areas, most probably in the vicinity of Canyon A (see Fig. 3).

Volcaniclastic sediments were found in two dredges on the western side of Canyon A near its floor. Several pieces of fragile, crumbling tuffaceous rocks up to 10 cm in size, which cannot have withstood long-range transport, were found in dredge AT 487D, and one piece was found in grab sample AT488Gr. In these samples, close-lying rounded clasts are 0.2–2 mm in size, a few up 1 cm. There are three different clast components of which the dominant is dark, very fine-grained plagioclase-phyric basalt. Subordinate components are green fine-grained mudstone, and basement-derived crystals of quartz and feldspar. The basalt and mudstone clasts are well rounded, the crystals less so. Matrix minerals differ between sites and may be either fibrous carbonate or near-isotropic zeolite(?). The clasts indicate that volcanic rocks, mudstones, and basement or basement-derived sandstones were all exposed and available for erosion in the source area of the sediments. The large number of volcanic clasts signals that a substantial part of the source area consisted of basalt. The thin sections contain no microfossils, but in one piece was found a single individual of *Cassidulina reniforme*, suggesting a very young matrix age of Pleistocene to Recent (Sheldon & Rasmussen, unpublished data). Seismic sections across the Hecla High about 100 km to the north show that the top part of the volcanic rocks of the High were exposed and under erosion as late as in Pleistocene time (Fig. 18, see later), and this is the most probable source for the clasts which would subsequently have been deposited and cemented in the canyon where they were dredged.

Fig. 7. Part of the recovery from dredge TTR13-AT-466D, Davis Strait High: Light grey Palaeozoic sediments in the middle and right; dark (coated) gneisses and basalts at left.

Igneous rocks

Igneous rocks constitute 10–20% of the sample population in most of the dredges which is a high proportion, considering that the onshore areas in West Greenland up to 69°N consist almost exclusively of Precambrian gneisses. The rocks form stones and blocks 5–25 cm in size, with a few boulders up to >30 cm across. The majority are grey to black, massive or vesicular, fine-grained aphyric or plagioclase-phyric basalts. There are a few red-oxidised and brecciated samples interpreted as flow tops, a few picrites and gabbros, and two rhyolites.

The major part of the igneous samples are subangular to subrounded, somewhat abraded, and nearly all appear to be somewhat transported (Fig. 7). A notable exception is a few irregular, strongly vesicular and very friable fragments from Diapir B which cannot have withstood long-range transport and must be very local (Fig. 8).

The transported igneous rocks could have originated from local areas with igneous outcrops such as found on the Davis Strait High and Seamount B. Some rocks could also originate in other offshore outcrops, for example on the Hecla High where volcanic rocks have been exposed until recently. Ice-rafted igneous rocks could come from the Paleogene volcanic areas onshore West Greenland and East Greenland, and undeformed Proterozoic dykes could also be present. In a later discussion, chemical compositions and ages are used to distinguish between various sources.

Fig. 8. Samples from dredge TTR13-AT-454D, Seamount B. Upper left: Dredge on deck: coated gneisses and uncoated vesicular volcanic rock. Sample 19: Red-oxidised, brecciated top of subaerial lava flow. Sample 5: Finely vesicular, strongly altered volcanic rock (basanite, analysed sample) with a 5-mm fracture filled with limestone containing Early to Middle Miocene nannofossils (E. Sheldon, unpublished). Sample 22: Angular piece of altered volcanic rock with largely empty vesicles.

Local Archaean basement in Canyon A

Two dredges on the eastern side of Canyon A yielded Precambrian gneisses that are considered to be of local origin. Two features distinguish the local rocks from the ice-rafted debris: firstly, the uniform lithology of many pieces, and secondly the unabraded morphologies very different from those of ice-rafted debris.

The main part of the rocks recovered in dredge TTR-AT-458D comprises several pieces of gneiss of uniform lithology (Fig. 9). A few of the pieces can be fitted onto other pieces. The pieces are up to 20 cm across, angular, sharp-edged, bounded by flat joint planes covered with rusty coatings. When cut, the rocks are very fresh and consist of felsic, weakly foliated grey gneiss.

Fig. 9. Recovery from dredge TTR-AT-458D: Several angular pieces of lithologically uniform gneiss.

Dredge Dana-04-20D included, besides 21 abraded pieces of different types of gneiss considered to be ice-rafted debris, 18 angular, joint-plane-bounded gneiss pieces with identical lithology, consisting of finely foliated red gneiss; the largest piece is 60 cm across.

Close-set jointing and rusty coating is well known from the onshore basement terrains where it occurs close to large fracture zones and faults. The morphology and appearance of the local gneisses in Canyon A therefore support the geophysical interpretation of a large fault along the eastern side of the canyon, exposing an upthrust basement block (Fig. 3).

Dating of a gneiss sample

Dating of a gneiss sample was done by the $^{206}Pb/^{207}Pb$ method. ^{206}Pb and ^{207}Pb are formed by radioactive decay of respectively ^{238}U and ^{235}U. The two uranium isotopes decay at different rates, and the ratio between their daughter isotopes is therefore an unambigous function of the time elapsed since the zircon grain crystallised and U, but not Pb, was entrapped in the crystal. By measuring the $^{206}Pb/^{207}Pb$ ratio of a zircon grain, a simple age determination of the grain is therefore obtained. By measuring the age of 100 grains, an age spectrum for the sample is obtained which may reveal if one or more zircon crystallisation events have taken place in the sample.

A slab of gneiss sample AT 458D-04 was crushed and its zircons separated. Hundred zircon grains (of which a few turned out to be monazite) were mounted on a small plate and their $^{206}Pb/^{207}Pb$ ratios were measured by LA-ICP-MS (laser ablation inductively coupled plasma mass spectrometry) by Thomas V. Rasmussen at GEUS. The resulting age spectrum is shown in Fig. 10. The sample has one simple, well-defined age peak at 2740 Ma, with relative standard deviations on the single grain ages of 2–10%. The sample is therefore clearly Archaean and shows no signs of younger events. The few grains that gave ages younger than 2500 Ma are monazite grains which do not retain U as well as zircon; U loss gives rise to erroneously young ages.

Canyon A is situated offshore of the central part of the Archaean craton in West Greenland, and the Archaean age of the sample is therefore in accordance with the expectation for basement representing the offshore extension of the Archaean craton. This result extends the known occurrences of Archaean basement from the coast and nearly 200 km offshore, well into areas that were previously interpreted as oceanic crust by Srivastava (1978) and Roest & Srivastava (1989).

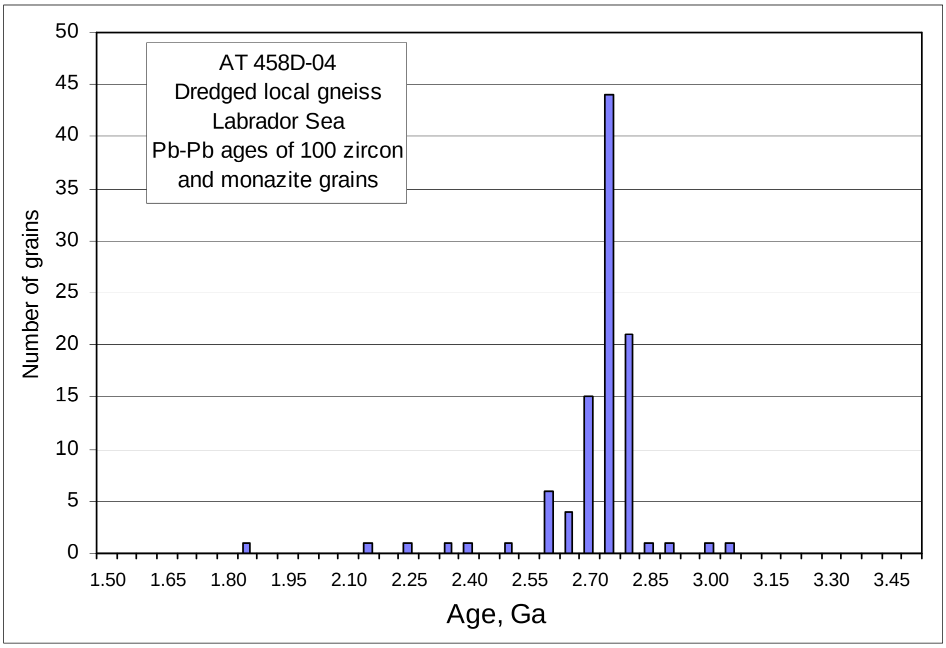

Fig. 10. Pb-Pb ages of 100 zircon grains from a local gneiss sample in Canyon A. The calculated age is 2740 Ma. The few grains with younger ages are monazites, not zircons.

Igneous rocks

From the total of 195 dredged igneous rock samples, 97 samples were analysed by the Rock Geochemical Laboratory at GEUS. Major elements were measured by X-ray fluorescence (XRF) analysis of fused glass discs as described by Kystol & Larsen (1999). Trace elements were measured by ICP-MS analysis using a modified version of the method described by Turner et al. (1999). Reproducibility, based on replicate digestion of samples, varied from 1.5% to 4% for most analyses. All the analyses obtained are included in Appendix 2.

Two samples selected for analysis later turned out, from thin sections and chemistry, to be sediments. Sample Dana04-23D-12 is a fine-grained, dark grey metagreywacke, and sample Dana04-36D-15 is a very fine-grained, dark brown ferrugineous carbonate rock, possibly concretionary. Twelve samples are identified as of Precambrian origin, and thus the total number of presumably younger igneous rocks analysed is 83. These are divided into a number of groups based on their chemical compositions.

Identification of Precambrian igneous rock samples

Unmetamorphosed Precambrian basaltic dykes are known from all the onshore basement areas. Thin sections of such rocks show that the plagioclases are brownish-tinted because of myriads of tiny inclusions, and the mafic minerals are heavily uralitised (altered to green fibrous amphiboles), particularly along the margins. Of the dredged basalts, 10 samples have partly or completely uralitised mafic minerals, and most of these have also brownish-tinted plagioclases. All of these samples have chemical compositions that are different from the main group of analysed basalts; most have low TiO_2 and highish SiO_2 and a distinct Nb-Ta trough in multi-element diagrams, signalling some extent of crustal influence (Fig. 13B). These chemical features are also found in the majority of analysed Precambrian dykes from West Greenland (e.g., Kalsbeek & Taylor 1986; Bridgwater et al. 1995; Cadman et al. 2001; Lassen et al. 2004). Therefore, these 10 samples are considered to be ice-rafted Precambrian igneous rocks, probably mainly dykes. Most of them are coarse-grained, doleritic to gabbroic.

A gabbroic sample (Dana-04-38D-04) with abundant fresh olivine and no signs of such alteration as described above, but with a similar chemistry to the Precambrian rocks, was sent for Ar-Ar dating (see below) and gave a Proterozoic age of 1543+244 Ma.

A single sample, a gabbro from Diapir B (AT 453D-32), is a high-alumina troctolitic alkali gabbro petrographically and geochemically indistinguishable from the gabbros and basalts of the Gardar Province in South Greenland (Upton & Emeleus 1987; Halama et al. 2003). It is therefore considered to be an ice-rafted Gardar gabbro.

The 12 samples considered to be of Precambrian age are all massive, non-vesicular, and do not contain zeolite minerals. They include all the gabbroic rocks. They are not included in the geochemical plots except in Fig. 13B where they are in separate diagrams.

Petrography

The presumably young igneous rocks are, with some exceptions, fairly fresh though groundmass alteration to clay is common. The exceptions include some highly altered and oxidised lava pieces including a few brecciated flow tops, and some samples that have lost alkalies due to leaching.

The hand samples vary from massive to vesicular to highly vesicular to a few brecciated (flow tops). The most common petrographical type is massive to vesicular, aphyric to sparsely plagioclase-phyric, fine-grained basalt with intergranular groundmass. The vesicles are lined or filled with clay or zeolite minerals, and in some samples the vesicles are empty. The second most common type is plagioclase-phyric basalt with microphenocrysts of olivine and clinopyroxene and intergranular to seriate groundmass texture. Five samples are picrites with frequent phenocrysts of olivine with included chromite crystals and fine-grained intergranular to coarse-grained subophitic groundmass textures with frequent interstitial zeolites. Two samples of basanite are highly vesicular and have pseudomorphosed olivine phenocrysts in a very fine-grained to aphanitic, oxidised and severely altered groundmass. Two rhyolite samples, pink and white, are flow-banded and spherulitic, the pink with quartz and feldspar phenocrysts in aphanitic matrix and the white one aphyric, coarse-grained, feldspar-rich, with altered (leached) feldspars.

Geochemistry and outline of compositional groups

Recalculation and plotting of geochemical analyses

Geochemical variation diagrams for the 83 analysed samples of presumably young igneous rocks are presented in Fig. 11 (major elements) and Fig. 12 (trace elements). The main parameter used in these diagrams is the *mg* number (100× atomic $Mg/(Mg+Fe2^{+})$), which is a measure of the degree of evolution of mantle-derived melts. Melts derived directly from the mantle have *mg* numbers around 60–80, and melts with *mg* number <60 are evolved by crystallisation from a more Mg-rich parent melt. Rocks with *mg* number >80 do not represent melts but contain accumulated crystals, mainly of olivine. Rocks with *mg* number <80 can also contain excess olivine accumulated in a melt with lower *mg* number. For the calculation of *mg* numbers, the iron oxidation ratio was adjusted to $Fe_2O_3/FeO=0.15$. Before plotting, all the analyses were recalculated to 100% on a volatile-free basis; this is done to remove the effects of secondary alteration and restore the composition to as close to the original igneous composition as possible.

The incompatible elements, which in general increase in the melt during evolution, are plotted in Fig. 13 in multi-element diagrams. In these diagrams the elements are ordered with decreasing incompatibility from left to right. The right column in Fig. 13 shows a large suite of elements normalised against a primitive mantle composition. The left column shows the geochemically coherent rare earth elements (REE) La to Lu plotted separately and (by convention) normalised against a chondrite composition. All normalisation values are from McDonough & Sun (1995).

Some of the incompatible elements, mainly Rb–Ba–Th–U and K, are mobile during alteration, and therefore altered samples may show irregularities in the left part of the multi-element pattern such as Ba peaks and Rb and K peaks or deeper-than-normal troughs. The most incompatible element that is also immobile is Nb, and therefore the Nb_N/Yb_N ratio (subscript N for normalised) is used as a measure of the slope of the multi-element pattern. For the REE patterns, the heavy REE are not influenced by alteration or crustal contamination (as the light REE are), and therefore the Tb_N/Lu_N or Dy_N/Yb_N ratios are used as measures of the slope of the REE pattern.

The crushing vessel for the samples consists of tungsten carbide which has contaminated some samples with small amounts of Ta, typically around 0.2 ppm which is significant in the geochemically depleted basalts but not in the enriched basalts. Ta is geochemically very similar to Nb, and therefore the mantle-normalised Ta_N and Nb_N should be of the same size. In the multi-element diagrams, Ta has not been plotted for those samples in which $Ta_N > 2Nb_N$.

Based on the geochemical analyses a number of compositional groups can be identified. Some statistics on the occurrence and distribution of samples from each group among the different dredged features are given in Table 1. The compositional groups are distinguished in the geochemical plots and presented in the following.

Table 2. Analysed dredged igneous rocks 2003-2004

Number of samples in each chemical group	**Davis Strait High**	**Canyon A**	**Seamount H**	**Seamount C**	**Seamount B**	**Seamount E**	**Total**
1. Main group of basalts	0	19	3	3	2	4	31
2. Extended main group basalts	0	1	1	1	0	3	6
3. Probably associated main basalts	0	5	1	1	4	1	12
4. Flat-patterned basalts	0	6	1	0	1	0	8
5. Contam. enriched or normal basalts	0	0	1	0	0	1	2
6. Rhyolites	0	1	1	0	0	0	2
7. Highly depleted basalts	4	0	0	1	0	1	6
8. Depleted basalts	4	0	0	0	0	0	4
9. Contaminated depleted basalts	4	0	0	0	0	0	4
10. Enriched basalts	0	3	0	1	1	1	6
11. Basanites	0	0	0	0	2	0	2
12. Precambrian basalts	0	3	4	0	3	2	12
Sum	12	38	12	7	13	13	95
Main group + extended + associated	0	25	5	5	6	8	49

In per cent of young rocks	**%**	**%**	**%**	**%**	**%**	**%**	**%**
1. Main group of basalts	0	54	38	43	20	36	37
2. Extended main group basalts	0	3	13	14	0	27	7
3. Probably associated main basalts	0	14	13	14	40	9	14
4. Flat-patterned basalts	0	17	13	0	10	0	10
5. Contam. enriched or normal basalts	0	0	13	0	0	9	2
6. Rhyolites	0	3	13	0	0	0	2
7. Highly depleted basalts	33	0	0	14	0	9	7
8. Depleted basalts	33	0	0	0	0	0	5
9. Contaminated depleted basalts	33	0	0	0	0	0	5
10. Enriched basalts	0	9	0	14	10	9	7
11. Basanites	0	0	0	0	20	0	2
Main group + extended + associated	0	71	63	71	60	73	59

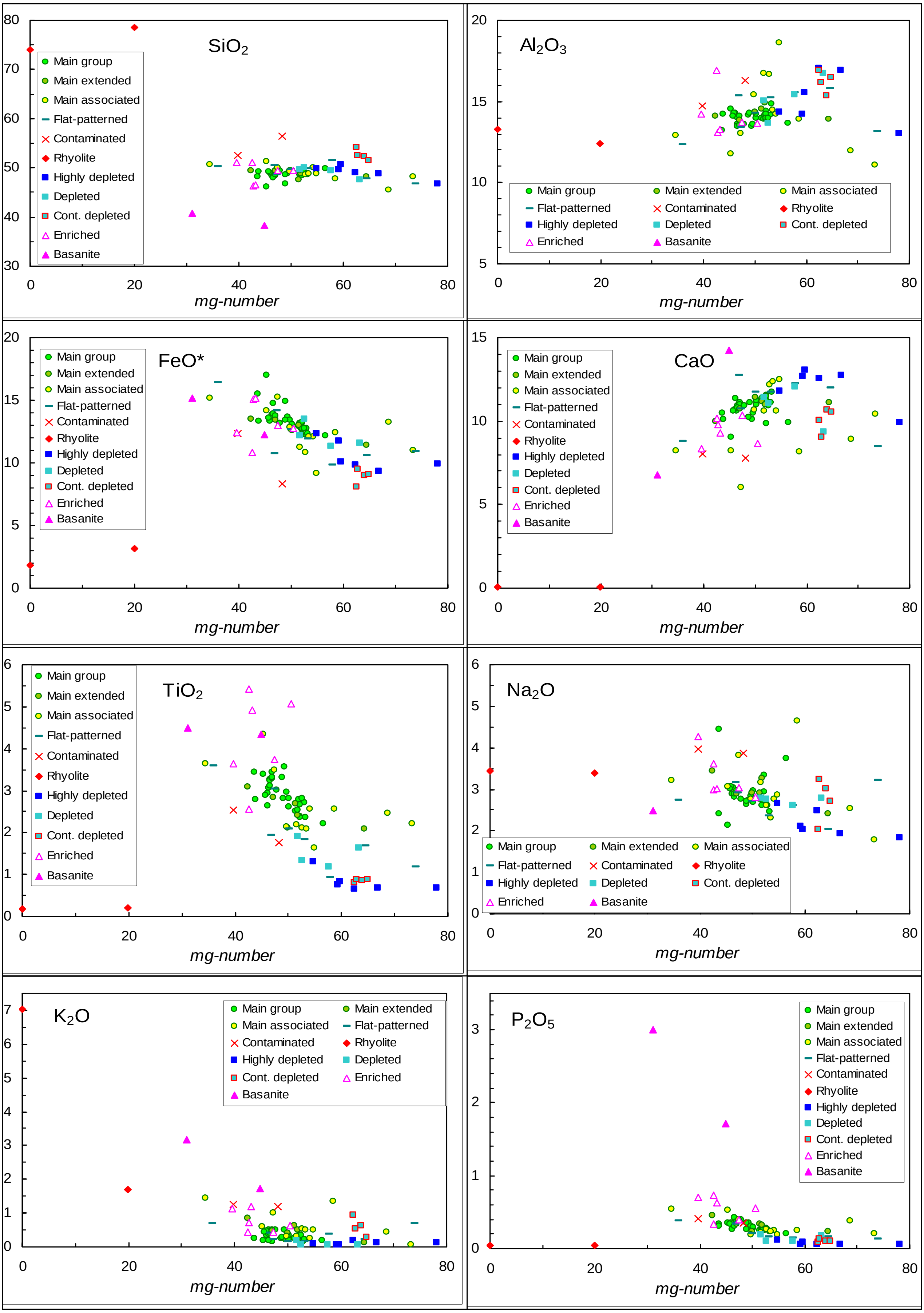
SiO2
Al2O3
FeO*
CaO
TiO2
Na2O
K2O
P2O5
Main group
Main extended
Main associated
Flat-patterned
Contaminated
Rhyolite
Highly depleted
Depleted
Cont. depleted
Enriched
Basanite
mg-number

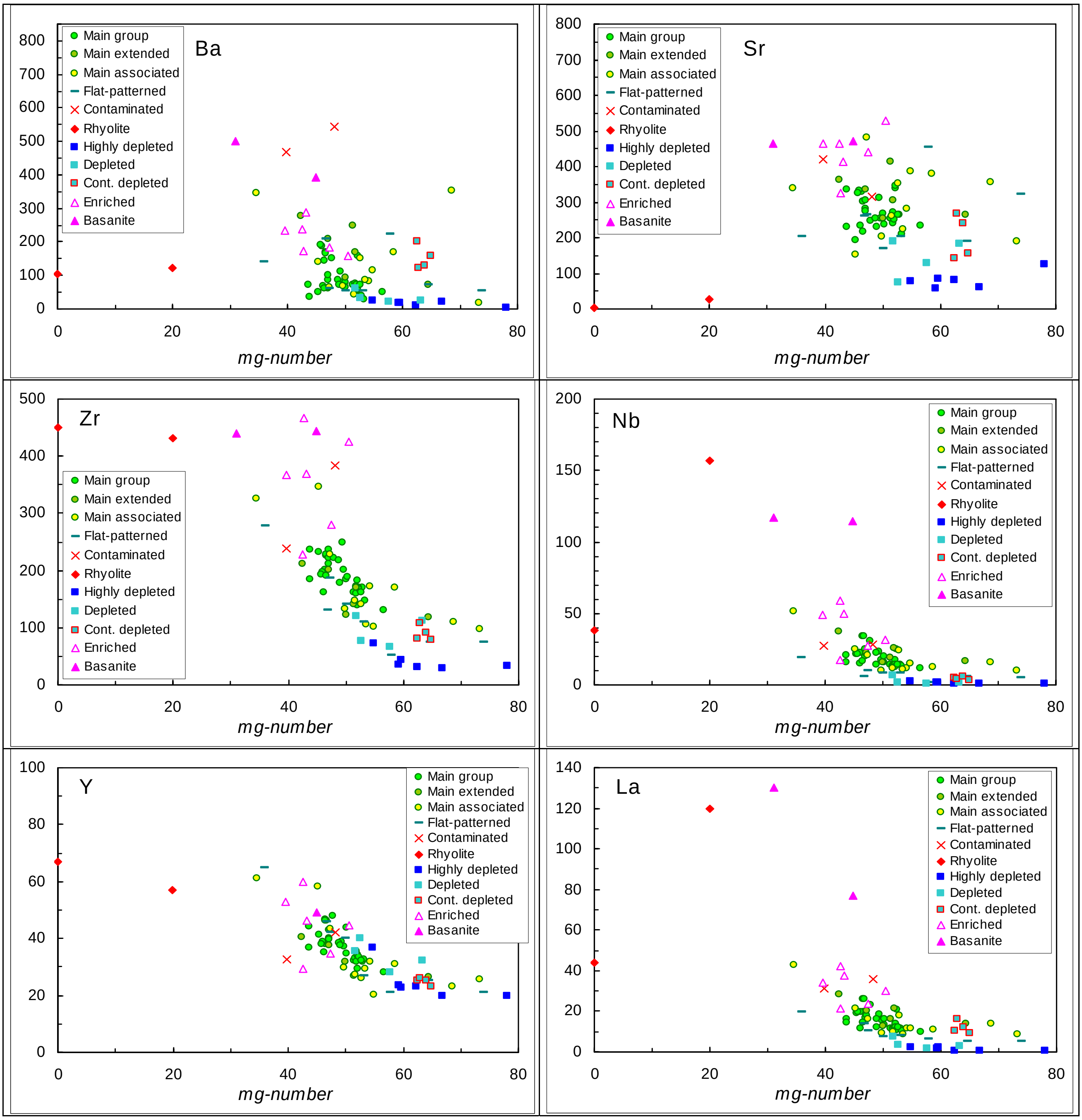

Fig. 12A. Strongly incompatible elements *vs mg-number.* Element concentrations in ppm.

Previous page: Fig. 11. Major elements *vs mg-number*. Element concentrations in ppm

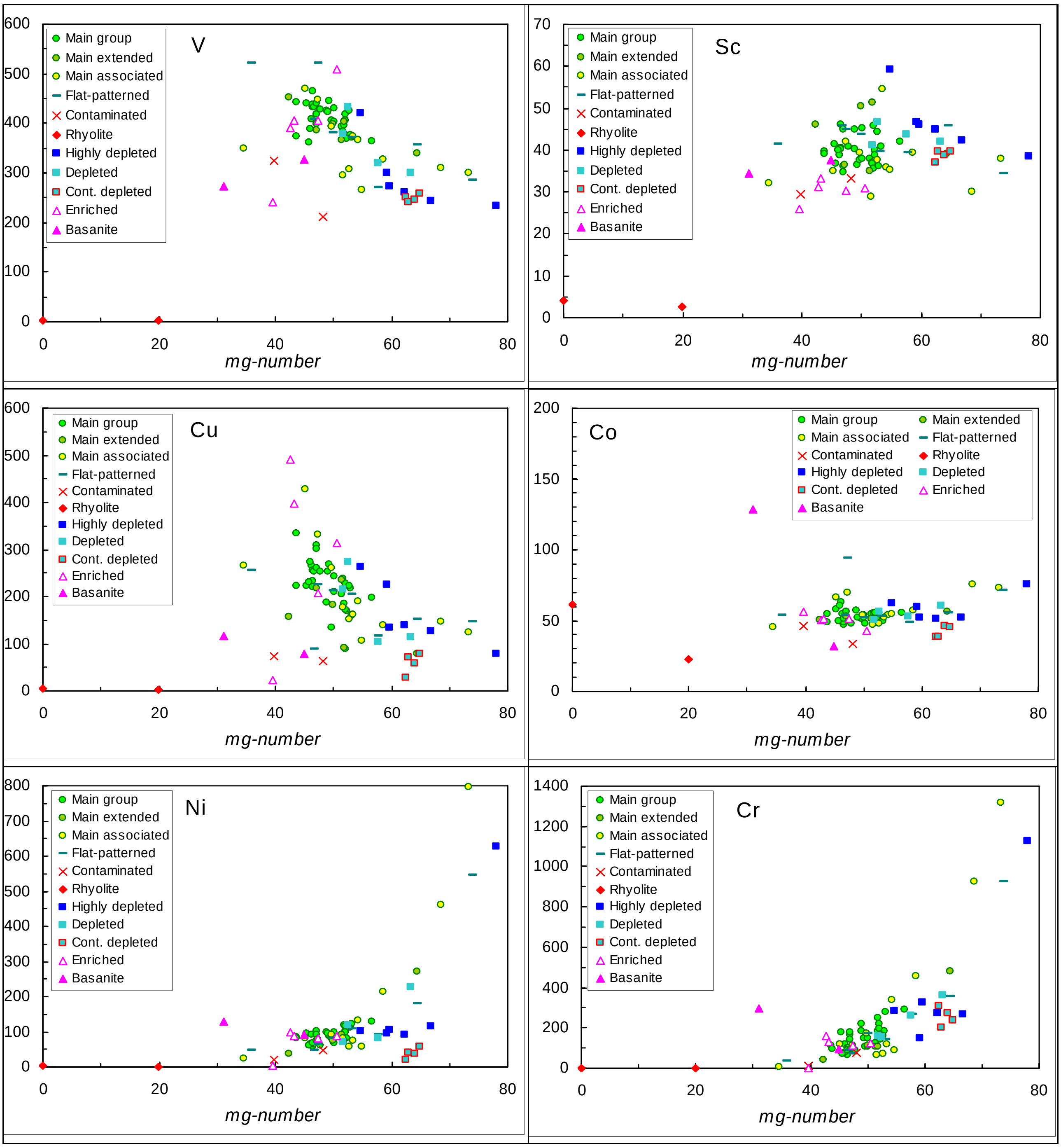

Fig. 12B. Moderately incompatible and compatible trace elements *vs mg-number.* Element concentrations in ppm.

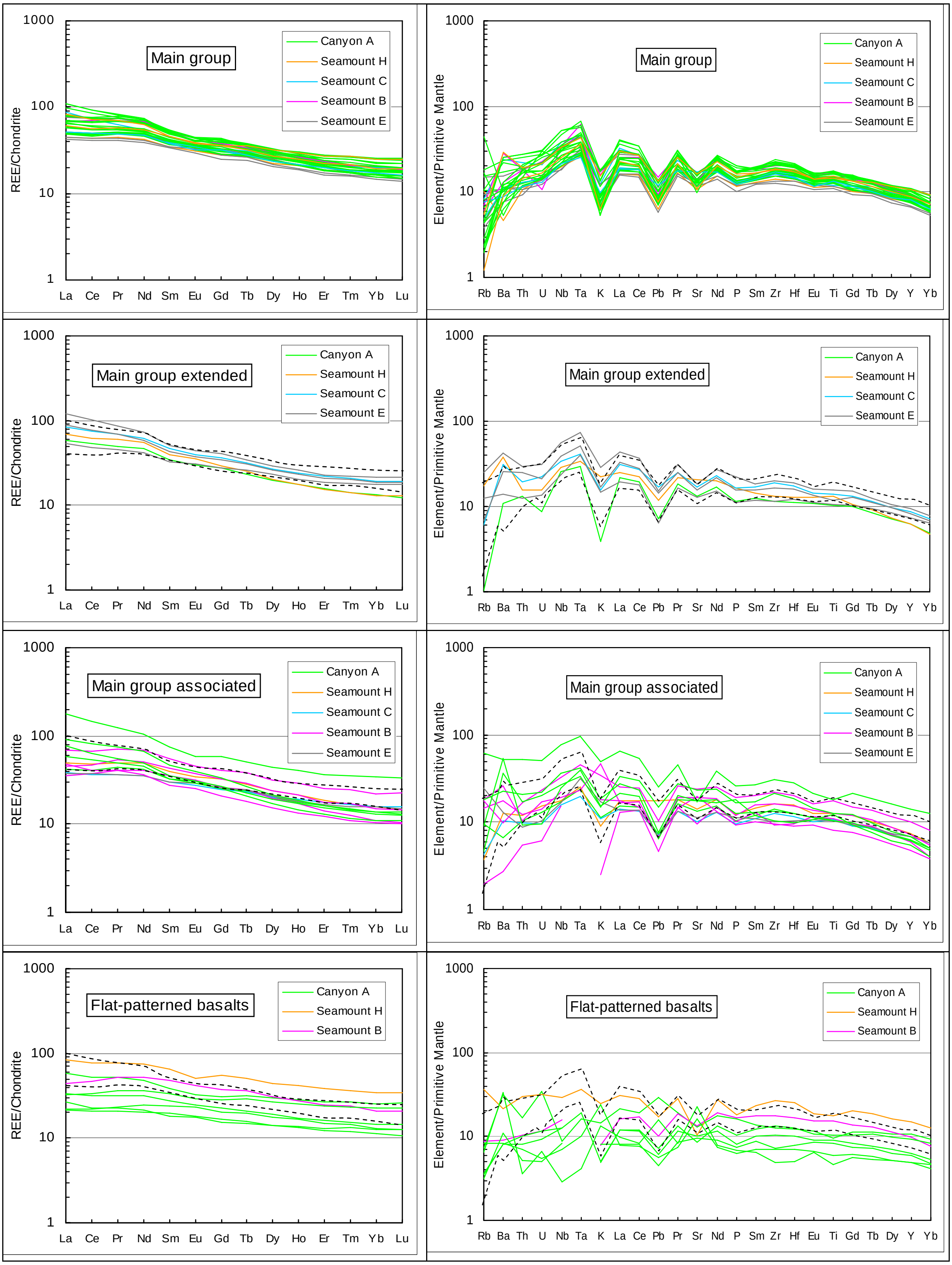

Fig. 13A REE and multi-element patterns. The dotted curves delineate the variation range of the main group *ss*.

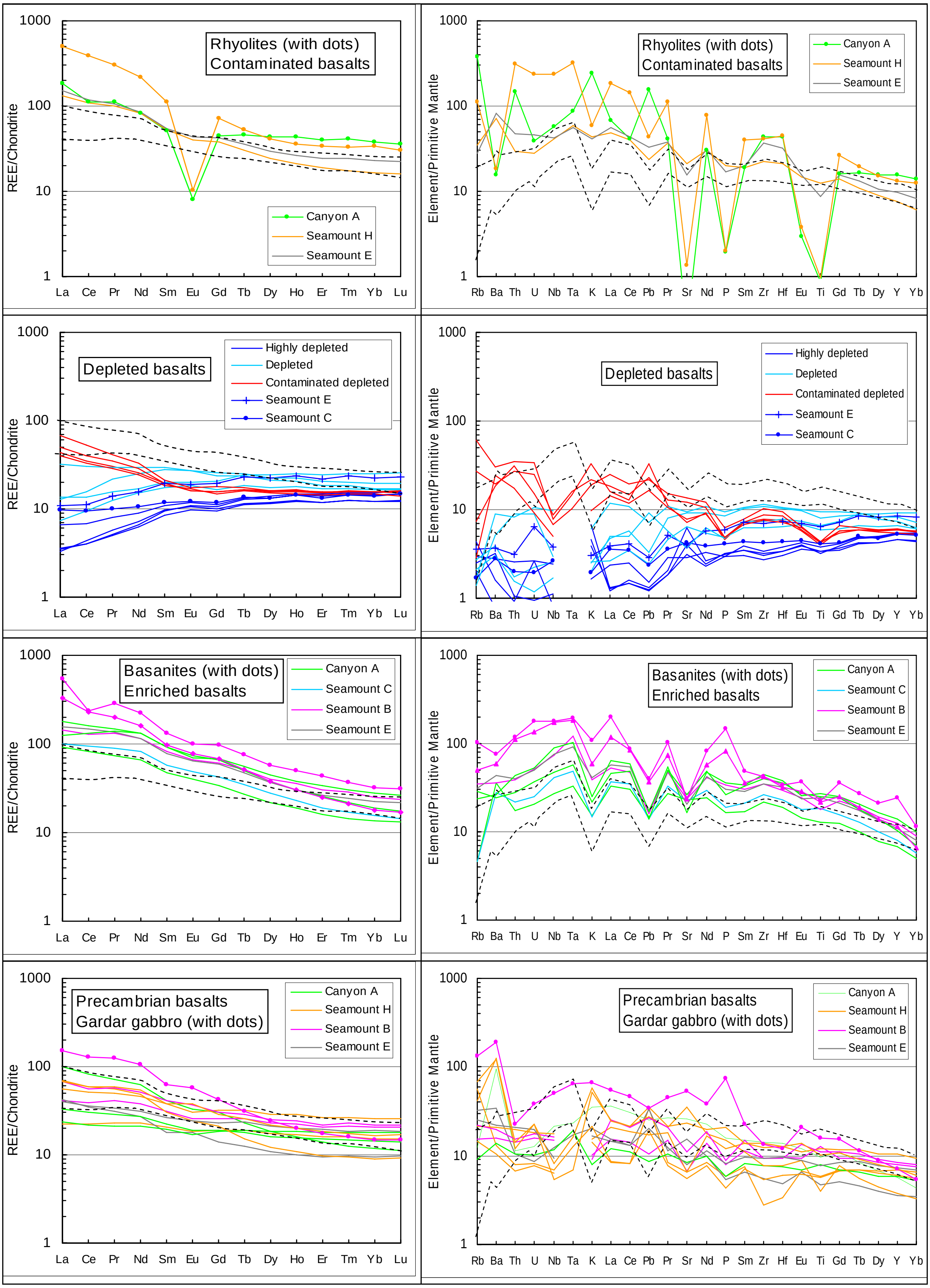

Fig. 13B. REE and multi-element patterns. The dotted curves delineate the variation range of the main group *ss*.

Main group of basalts

Of the 83 presumably young samples, 31 are closely geochemically related to each other; they form tight clusters in geochemical variation diagrams (Figs 11–12) and have closely parallel REE and multi-element patterns (Fig. 13A). This *main group* can be *extended* with six samples showing some more variation, but still quite similar to the main group. If still more variation is allowed, a further 12 samples, which are more similar to the main group than to any other groups, can be considered *associated* with the main + extended group of basalts. Together, these 49 samples constitute 59% of the total young sample set. No samples of this group were found on the Davis Strait High; in strong contrast, the main group basalts constitute 60–73% of the young samples from *all* of the southern stations south of 64°N (Table 2). Petrographically, aphyric fine-grained basalts dominate in this group; fewer are plagioclase-phyric basalts, and two are picrites.

The 'central' main group of 31 samples comprises tholeiitic basalts with *mg* numbers = 43.7–56.6, MgO = 5.1–7.8 wt%, TiO_2 = 2.1–3.5 wt%, and parallel REE and multi-element patterns (excepting some alteration in the Rb–U parts). The REE patterns slope smoothly from La to Lu, and Tb_N/Lu_N (chondrite normalised) ratios are in the range 1.4–2.0. The multi-element patterns are convex-upward with Nb_N/Yb_N (mantle normalised) ratios in the range 2.7–5.9. There are distinct troughs for K and Pb and lesser troughs for Sr and P. This shape characterizes many Tertiary North Atlantic magmas that are derived from a mantle that is depleted in the most incompatible elements Rb-to-U and K.

If the whole group of 49 samples is considered, the ranges are extended to *mg* numbers = 34.6–73.4, MgO = 3.9–14.9 wt%, and TiO_2 = 1.6–4.3 wt%; trace element ratios are slightly extended to higher values, with Tb_N/Lu_N ratios of 1.4–2.3, and Nb_N/Yb_N ratios of 2.7–7.7.

Flat-patterned basalts

This group comprises eight samples mainly from Canyon A (Table 2). They are tholeiitic basalts and one picrite with widely spaced *mg* numbers (35.9–73.8), MgO = 4.6–15.2 and TiO_2 = 0.9–3.5 wt%. The common feature of this group is relatively flat REE and multi-element patterns, with Tb_N/Lu_N = 1.1–1.7 and Nb_N/Yb_N = 1.0–2.4. One sample is siliceous and has a multi-element pattern with a Nb–Ta trough and Ba, K and Pb peaks, signalling contamination with continental crust. Also the picrite has high Pb and K and appears to be contaminated. The group shows some internal variation, for example Zr–Hf and Ti form troughs in some samples and peaks in others. The samples in this group may not be genetically related. The siliceous sample has similarities to the Precambrian rocks; but as it is distinctly vesicular with vesicles filled with fresh zeolites it is most probably fairly young.

Crustally contaminated basalts

This group consists of only two samples (from Seamounts H and E) of quite evolved rocks with *mg* numbers of 40–48; they have recalculated SiO_2 = 52–56 wt% and are basaltic andesites after Le Maitre (2002). They have high Rb, Ba, K, and Pb, but no significant Nb–Ta trough. They are probably basaltic magmas contaminated with continental crust, but their parental magmas cannot be identified with certainty. They have Tb_N/Lu_N = 1.5–1.9, similar to the main group of basalts to which the parental magma may belong.

Rhyolites

Two samples, one from Canyon A and one from Seamount H, are rhyolites with 74–78.5 wt% SiO_2. Both show signs of extended fractionation of feldspar (Ba, Sr, Eu troughs), apatite (P trough) and oxide (Ti trough). They have very different K_2O contents (1.7 and 7.0 wt%). The low-K sample has heavily clouded feldspar and contains 5.5 % normative corundum, and the low K is considered to be caused by alteration (leaching). Excepting Rb, Ba, and K (Fig. 13B) this rhyolite has very high contents of highly incompatible elements and was most probably originally peralkaline; if it had as much K as the other rhyolite sample it would indeed have been acmite normative. The high-K rhyolite is much less enriched in the most incompatible elements and has a much flatter REE pattern. Its multi-element pattern has a Nb–Ta trough and a Pb peak, indicating a component of crustal contamination. Thus, the two rhyolite samples are strongly different and apparently unrelated.

Depleted basalts

This group of 14 samples comprises three subgroups (groups 7, 8, 9 in Table 2): strongly depleted (6), depleted (4), and crustally contaminated (4) basalts. The major part of the samples (12) come from the Davis Strait High where it is the only basalt type found (Table 2). One strongly depleted sample is from Seamount C and another is from Seamount E. The basalts, and one picrite, are fairly magnesian, with *mg* numbers = 52–78, high MgO (6.5–17.4 wt%) and low iron.

The group is characterised by depletion in most of the incompatible elements. The REE and multi-element patterns slope from right to left of the diagrams or are near-horizontal, with Tb_N/Lu_N = 0.83–1.01 (strongly depleted) and 0.95–1.41 (depleted) and Nb_N/Yb_N = 0.16–0.52 (strongly depleted) and 0.28–1.38 (depleted) . The very low contents of the mobile elements Rb–Ba–Th–U and K are easily disturbed by small degrees of alteration, and three of the six strongly depleted basalts have multi-element patterns with Rb and K peaks that are considered due to secondary alteration; these samples are vesicular with zeolite-filled vesicles, and the increase in K_2O required to produce the peaks is only from c. 0.05 to 0.15 wt%.

Four samples bear the distinct hallmarks of crustal contamination: they have increased SiO_2 (51–54 wt%) and K_2O and decreased CaO (Fig. 11), and the multi-element patterns show increased Rb-to-U, La-to-Gd, Pb, and Zr-Hf, and decreased Nb, P, and Ti (Fig. 13B). On the other hand, their low Tb_N/Lu_N (1.06–1.16) and Nb_N/Yb_N (0.94–1.5) testify to their origin as depleted basalts.

Petrographically, the depleted samples comprise both massive and vesicular rocks. All are olivine-phyric or -microphyric, and the more evolved rocks also contain plagioclase phenocrysts. Groundmasses are mainly fine-grained, intergranular. The vesicles are filled with zeolites. In several samples the olivine is replaced by clay.

Enriched basalts

This group comprises six samples that are in many ways akin to the main group of basalts; they have similar *mg* numbers and major elements but higher contents of incompatible elements and steeper REE and multi-element patterns, with Tb_N/Lu_N = 2.1–2.9 and Nb_N/Yb_N = 5.4–9.4. They are found in four of the five southern dredged areas. Petrographically, they are similar to the main basalts, either aphyric or plagioclase-phyric.

Basanites

Two samples from Seamount B are basanites. They are strongly altered and their alkali contents are corrupted; one sample is nepheline normative and the other is corundum normative. However, their high Nb contents (100 ppm volatile-free) and steep REE and multi-element patterns with Tb_N/Lu_N = 2.4–3.1 and Nb_N/Yb_N = 15–27 are indicative. They are highly vesicular and have pseudomorphosed olivine phenocrysts in a very fine-grained to aphanitic, oxidised and severely altered groundmass.

$^{40}Ar/^{39}Ar$ dating of igneous rocks

A total of 14 igneous samples were selected for radiometric dating by the $^{40}Ar/^{39}Ar$ step-heating method. The samples represent the different geochemical groups and locations as far as possible; however the strongly depleted basalts are too K-poor, and the basanites are, unfortunately, too altered to be datable by this method with any confidence.

The samples were dated at Oregon State University, the Noble Gas Mass Spectrometry Laboratory led by professor Robert Duncan. The laboratory and method is described at http://www.coas.oregonstate.edu/research/mg/chronology.html. One sample failed to give an age; one sample was Proterozoic, one sample was Cretaceous, and 11 samples were Palaeogene. The results are shown in summary form in Tables 3 and 4, and plateau and isochron plots are shown in Appendix 1.

Table 3. $^{40}Ar/^{39}Ar$ radiometric age determinations on igneous rocks from the Labrador Sea and the Davis Strait

		Total Fusion (Ma)	Plateau (Ma)				Inverse Isochron (Ma)	
Sample	Material	Age ± 2 σ	Age ± 2 σ	Steps[1]	% ^{39}Ar[1]	MSWD	Age ± 2 σ	$^{40}Ar/^{36}Ar$ ± 2 σ
AT453D-27	plagioclase	55.22 ± 0.57	**52.48 ± 0.56**	6/7	96.9	0.16	52.49 ± 0.63	293.7 ± 31.0
AT453D-40	plagioclase	48.36 ± 0.88	**48.13 ± 0.87**	4/7	76.3	0.19	47.82 ± 1.22	299.8 ± 11.9
AT465D-39	plagioclase	59.96 ± 0.68	**62.97 ± 0.74**	3/8	44.4	0.10	62.88 ± 0.85	298.2 ± 13.4
AT484D-05	groundmass	53.47 ± 1.00	**53.96 ± 0.85**	4/7	88.6	1.41	53.71 ± 0.85	300.1 ± 4.9
AT484D-10	groundmass	56.42 ± 0.79	**56.11 ± 0.97**	3/7	73.2	4.09	56.75 ± 1.41	269.8 ± 42.4
Dana-04-11D-11	groundmass	53.65 ± 0.40	**51.69 ± 0.48**	5/8	46.0	1.64	51.88 ± 0.67	287.2 ± 20.3
Dana-04-20D-25	sanidine	58.98 ± 0.38	**58.94 ± 0.37**	7/10	95.0	0.46	58.84 ± 0.47	335.9 ± 109.0
Dana-04-22D-16	plagioclase	86.77 ± 1.75	56.60 ± 0.80	3/7	49.8	1.56	**55.35 ± 0.85**	330.7 ± 11.5
Dana-04-23D-16	groundmass	56.53 ± 0.40	**54.80 ± 0.45**	5/8	62.3	3.02	54.66 ± 0.56	308.1 ± 29.1
Dana-04-27D-16	plagioclase	55.54 ± 0.77	**55.52 ± 0.72**	7/7	100.0	0.58	55.13 ± 0.88	302.2 ± 8.3
Dana-04-36D-18	groundmass	50.48 ± 0.43	**50.13 ± 0.41**	6/8	88.4	0.62	50.10 ± 0.42	297.8 ± 7.1
Dana-04-37D-12	plagioclase	625.0 ± 4.7	662.8 ± 7.5	2/7	41.1	1.37	None	None
Dana-04-38D-02	plagioclase	124.9 ± 1.1	119.4 ± 1.1	3/8	73.0	1.87	**118.8 ± 1.2**	464.2 ± 41.9
Dana-04-38D-04	plagioclase	2227 ± 18	None				**1543 ± 244**	15917 ± 3869

Samples irradiated at Oregon State University TRIGA reactor for 6 hours at 1MW power. Neutron flux measured using FCT-3 biotite monitor (FCT age 28.03 Ma, Renne *et al.* 1994). Data reduced by ArArCALC software (Koppers 2002).

Preferred age in **BOLD TEXT.** Age in **GREY** not meaningful.

1. Plateau age data includes number of steps in the plateau (steps in plateau / total steps) and % ^{39}Ar in plateau.

Table 4. Dated samples arranged according to chemical group

Group	Age ± 2 σ	Location	Sample
1. Main basalt	50.13 ± 0.41	Canyon A	Dana-04-36D-18
1. Main basalt	52.48 ± 0.56	Seamount B	AT453D-27
1. Main basalt	55.52 ± 0.72	Canyon A	Dana-04-27D-16
1. Main basalt	56.11 ± 0.97	Canyon A	AT484D-10
2. Main basalt extended	51.69 ± 0.48	Seamount C	Dana-04-11D-11
3. Main basalt associated	48.13 ± 0.87	Seamount B	AT453D-40
4. Flat-patterned	53.96 ± 0.85	Canyon A	AT484D-05
10. Enriched	54.80 ± 0.45	Canyon A	Dana-04-23D-16
10. Enriched	55.35 ± 0.85	Canyon A	Dana-04-22D-16
6. Rhyolite	58.94 ± 0.37	Canyon A	Dana-04-20D-25
9. Depleted high-Si	62.97 ± 0.74	Davis Strait High	AT465D-39
4. Flat-patterned	118.8 ± 1.2	Seamount H	Dana-04-38D-02
5 (to 12). Contaminated	1543 ± 244	Seamount H	Dana-04-38D-04

Proterozoic basalt

Sample Dana-04-38D-04, a 6 cm irregular pebble, was originally classed in Group 5, contaminated. It was chosen for dating because it is gabbroic and petrographically very fresh, with abundant fresh olivine, but with a chemistry similar to the Precambrian rocks. It gave no age plateau; the total fusion age is 2227 Ma and a poor three-point isochron age is 1543 ± 244 Ma. its true age lies between these figures. The result shows that Precambrian samples may not always be discernible by their petrography, but chemistry is a good indication. Moreover, all the gabbroic samples have now turned out to be Precambrian.

Cretaceous basalt

Sample Dana-04-38D-02 gave an age of 118.8 ± 1.2 Ma. The dated feldspar contains excess argon, but the three-step plateau and isochron ages, comprising 73% of the released argon, are concordant and eliminate the excess argon effect. The age is Early Cretaceous, Aptian. The sample is from chemical group 4, samples with relatively flat multi-element patterns. As this group is heterogeneous (another sample is Eocene, Table 4), it is not possible to conclude anything about the age of the other samples in group 4. The Cretaceous sample shows some geochemical and petrographic similarities to one or two other samples which could also be Cretaceous.

Palaeogene basalts and rhyolite

The 11 Paleogene samples have ages in the range 48–63 Ma, with a concentration of ages in the interval 54–56 Ma (Fig. 14). Eight of the ages are good to excellent, being based on 62–100% of the released argon, and with no excess argon. Three ages are based on 44–50% of the released argon, and one sample has excess argon. These ages are still reasonable and reliable (Table 3–4, Appendix 1).

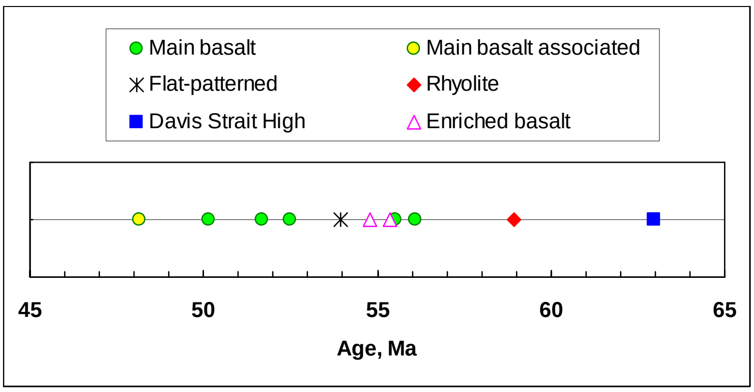

Fig. 14. Age distribution of 11 Paleogene samples, divided into chemical groups.

Davis Strait High

A sample of Si-enriched depleted basalt from the Davis Strait High gave a reasonable plateau age of 62.97 ± 0.74 Ma. In comparison, the oldest onshore volcanic rocks on Disko and Nuussuaq, which are normally magnetised, have been referred to Chron 27n (Storey *et al.* 1998); the most recent age interval for Chron 27n is 61.98–61.65 Ma (Ogg & Smith 2004). The volcanic rocks on Baffin Island are also normally magnetised and have by analogy been inferred to be from Chron 27n (Pedersen *et al.* 2002). Thus, the dredged lavas appear to be slightly older than the oldest onshore volcanics.

Paleocene rhyolite

Sanidine phenocrysts from a rhyolite sample from Canyon A gave an excellent age of 58.94 ± 0.37 Ma. The rhyolite is clearly the oldest sample from the southern area. Similar rhyolites are not known from the Paleocene onshore lava succession in central West Greenland which is near-contemporaneous but probably slightly older (Storey *et al.* 1998). In East Greenland, the very few acid rocks are post-basaltic dykes and sheets younger than about 55 Ma (e.g. Brooks & Rucklidge 1976; Upton *et al*. 1984).

Paleocene–Eocene basalts

The volcanism of the ‘main basalt’ type spans the interval 56–48 Ma, a period of seven million years, crossing the Paleocene–Eocene boundary. The enriched and flat-patterned basalts are contemporaneous with the main basalts. There is a concentration of ages in the period 56–54 Ma; this is the same age as that of the major Paleocene–Eocene volcanic successions on Nuussuaq, Ubekendt Ejland and Svartenhuk Halvø and several dykes within the same region (Larsen (2006) and unpublished data), and also of the major lava plateaus In East Greenland which are dated at c. 57 to c. 55 Ma (Upton et al. 1995; Storey *et al.* 1996, see below).

Discussion

General character of the magmas

Compositional differences between basalt groups are most easily seen in plots of incompatible trace elements such as Th, Nb, Zr, and REE. In particular, ratios of such elements eliminate differences in fractionation states and highlight primary differences that are caused by differences in mantle materials and melting processes. Four such ratio diagrams are shown here in Fig. 15.

Fig. 15A is another way of showing the slopes of the REE patterns in Fig. 13. Rocks with left-to-right sloping REE patterns have $La_N/Sm_N > 1$ and $Gd_N/Lu_N > 1$ and plot in the first quadrant. Flat-patterned rocks plot near values around 1 for these ratios, and depleted rocks with right-to-left sloping REE patterns have have $La_N/Sm_N < 1$ and $Gd_N/Lu_N < 1$ and plot in the third quadrant. The figure distinguishes well between the depleted rocks of the Davis Strait High and the non-depleted to enriched to alkaline rocks of the southern areas. Crustally contaminated rocks have increased La_N/Sm_N relative to their uncontaminated parents.

Ratios between Nb, Th and La are sensitive to crustal contamination because this process increases Th and La and usually lowers Nb. The contamination effect is seen in Fig.15B where the contaminated rocks, including the contaminated rhyolite, plot in the third quadrant. This diagram also distinguishes the depleted rocks from the others, but not the enriched basalts and basanites from the main basalts.

Excellent discrimination between the various geochemical groups is achieved in Fig. 15C, where Nb_N/Yb_N represents the overall slope of the multi-element pattern. The depleted basalts have very low Nb_N/Yb_N, and this ratio increases in the succession flat-patterned basalts – main basalts – enriched basalts – basanites and one rhyolite. Concomitantly, the Nb_N/La_N ratio also increases. The contaminated depleted and flat-patterned basalts are assembled in a small area with low Nb_N/La_N and Nb_N/Yb_N around 1; the two contaminated samples with no certain parent and the rhyolite have lowered La_N/Nb_N relative to the main basalts, supporting that these may represent their parental magmas.

Fig. 15D shows a plot of Nb/Y vs Zr/Y that was originally designed by Fitton *et al.* (1997). It highlights the difference between the volcanic rocks of Iceland, which all plot between the two parallel lines, and mid-ocean-ridge basalts (MORB) generated away from the influence of the Iceland mantle plume; MORB plot below the Iceland field. The dredged rocks straddle the boundary between the Iceland and MORB fields; however nearly all the main basalts plot within the Iceland field.

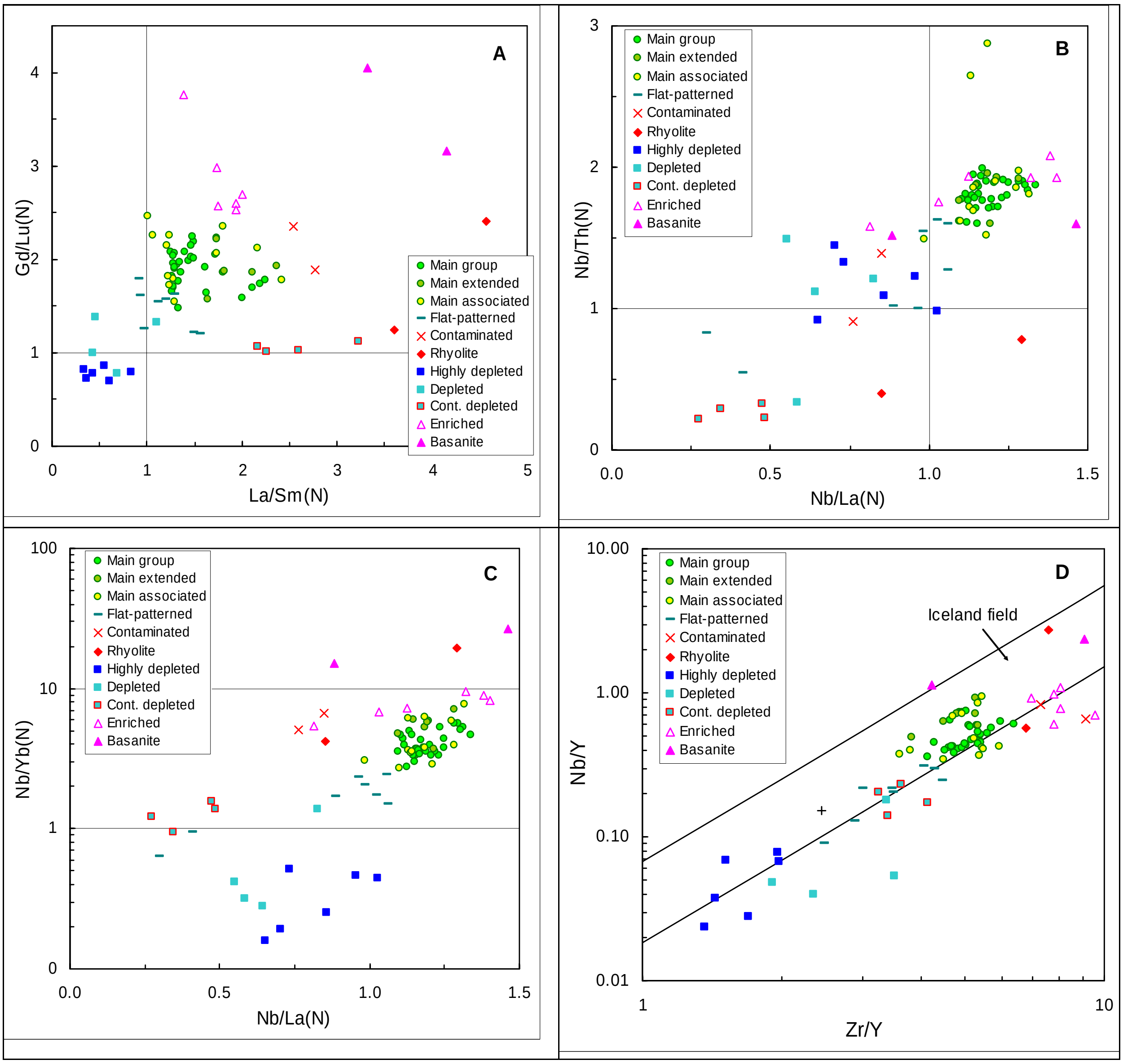

Fig. 15. Cross plots of trace element ratios. Note the excellent discrimination between the geochemical groups in C.

Comparison with other igneous rocks

Offshore and onshore West Greenland and Canada

The plots in Fig. 15 are useful for a comparison with other igneous rocks. Fig. 16 shows the same four plots as in Fig. 15, with analyses of a large number of other rocks from the offshore areas and onshore West Greenland and Canada. The following observations can be made.

The Paleocene basalts of the Maligât Formation on Disko and Nuussuaq are different from any of the dredged basalts and cannot be the source for these. In particular, the La_N/Sm_N, Nb_N/La_N and Nb/Y ratios are too low.

The Paleocene–Eocene basalts of the Kanissut Formation (Previously the Kanísut Member of the Maligât Formation, Hald 1976) in western Nuussuaq are similar to the dredged group of main basalts in all aspects revealed by the four diagrams, and also in other aspects such as major element compositions. Thus the Kanissut Formation is a possible source for the main basalts (but see below).

Dykes in southeastern Nuussuaq are akin to the dredged enriched basalts but have higher Nb/Y and lower Zr/Y ratios.

The Hareøen Formation and rare late alkaline intrusions on Disko and Nuussuaq are off-scale in La_N/Sm_N in Fig. 16A and have no counterparts in the dredged material.

Lavas on Baffin Island comprise two geochemical groups: depleted (N-type) and non-depleted (E-type) lavas (Francis 1985; Robillard et al. 1992; Kent et al. 2004; Lass-Evans 2004). The E-type lavas do not resemble any dredged material; the N-type lavas show some similarities to the depleted lavas dredged from the Davis Strait High, but they have Gd_N/Lu_N >1 in contrast to the dredged lavas.

The closest similarity to the lavas dredged from the Davis Strait High is found in the composition of lavas drilled on the Davis Strait High itself, where lava flows are exposed on the sea floor (Srivastava et al. 1982; Williamson et al. 2003).

Fig. 16 also shows data for basalts from wells drilled in the Labrador Sea and the Davis Strait. (In all three wells, the lavas are deep-seated and as such could not have delivered material to the dredges.) The lavas of the Hellefisk, Hekja, and Gjoa Wells are all more or less depleted, with the Hekja lavas the most depleted and most similar to the lavas from the Davis Strait High. The Nukik-2 well presents a large range of compositions. The data from the wells will be presented in a separate report by M.-C. Williamson and L.M. Larsen.

In the central southern Davis Strait, ocean floor basalts were drilled at ODP Site 647A (Clarke *et al.* 1989). Analyses of these basalts are not included in Fig. 16 because Gd was not analysed and the Nb analyses are not accurate enough. With La_N/Sm_N around 0.5 and Tb_N/Lu_N around 0.8–0.9, these basalts are close in composition to those of the Davis Strait High.

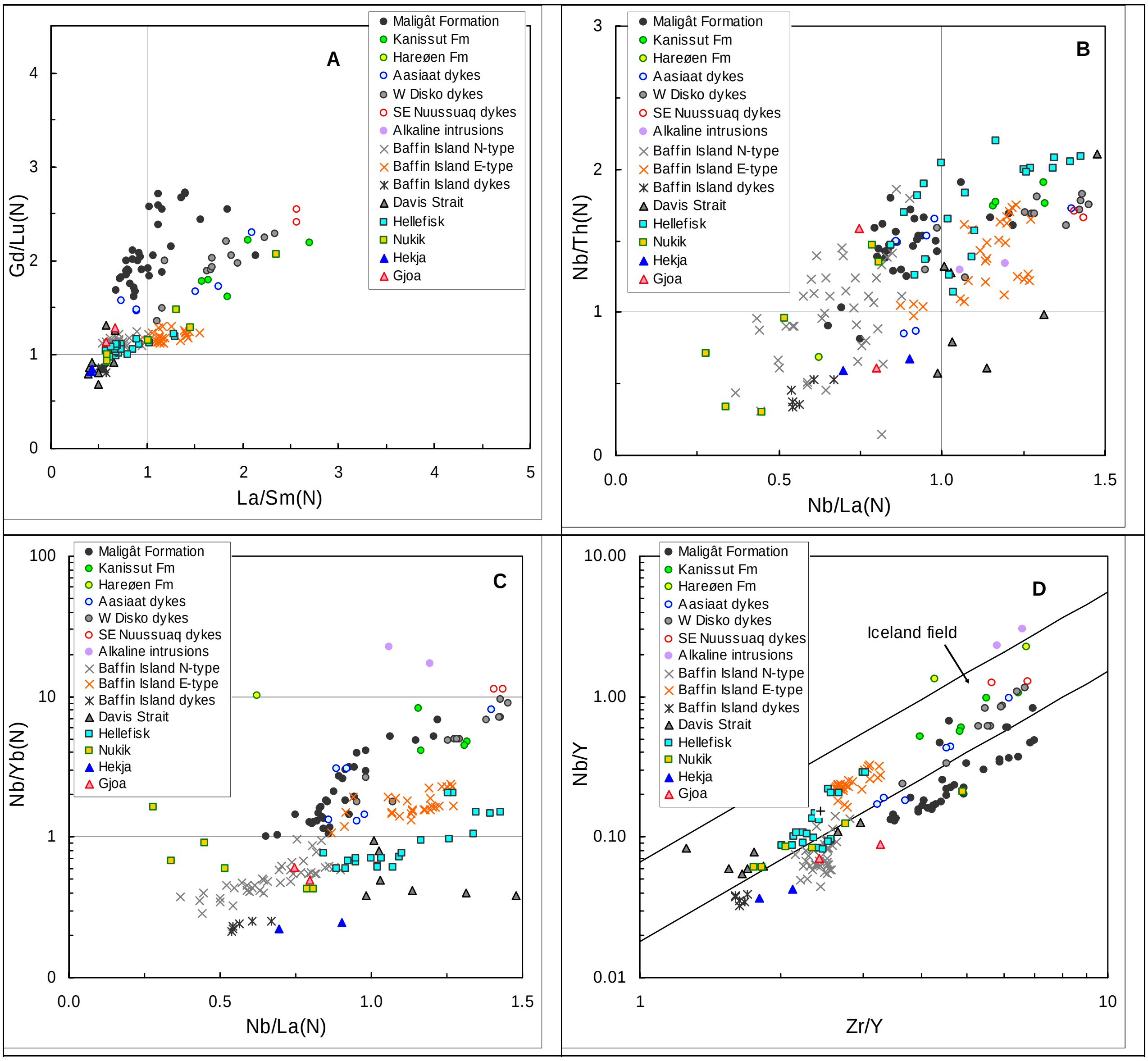

Fig. 16. Cross plots of trace element ratios for other igneous rocks from the offshore areas and onshore West Greenland and Canada. All analyses are by ICP-MS. Data sources: Onshore West Greenland localities: GEUS data, unpublished; Baffin Island: Lass-Evans (2004); Davis Strait, Hekja and Gjoa: Williamson et al. (2003) and unpublished data; Hellefisk and Nukik-2: GEUS data, unpublished.

East Greenland

Fig. 17 shows the same four plots as in Fig. 15, with analyses of a large number of rocks from East Greenland. The following observations can be made.

The voluminous plateau basalts on the Blosseville Kyst between Kangerlussuaq and Scoresby Sund, comprising the Magga Dan, Milne Land, Geikie Plateau, Rømer Fjord, and Skrænterne Formations, cover a compositional range that is generally similar to that of the dredged samples. In detail, the Magga Dan and Milne Land Formations have different ratios, e.g. Nb/Y, Zr/Y, and Nb/La. But even when critical screens are applied to the data, the Geikie Plateau, Rømer Fjord, and Skrænterne Formations comprise rocks that are very similar to the main group of rocks in the dredges. The Geikie Plateau and Skrænterne Formations also comprise rocks with a character similar to the flat-patterned group of the dredged samples, and these rocks appear to be a part of the general continuum of compositions. The Rømer Fjord Formation also comprises enriched rocks similar to those in the dredges. There are also geochemically very depleted rocks in some of the formations. The age of the plateau basalts is 56.2–54.8 Ma (Storey *et al*. 1996, here recalculated with the FCT tuff standard =28.03 Ma).

Several rock groups in East Greenland have no counterparts among the dredged rocks. These are all late: the lavas above the Skrænterne Formation, the Igtertivâ Formation, the Prinsen af Wales Bjerge Formation, and the Vindtop Formation. A sill drilled in ODP Hole 918 on the SE Greenland margin, dated to 52.8 Ma (Sinton & Duncan 1998, recalculated), is similar in character to the late lavas.

Of the lavas in northern East Greenland, the data of Thirlwall *et al.* (1994) fall in two distinct groups (not shown here). The Upper Lava Series on Hold With Hope is very similar to the dredged main group rocks, whereas the Lower Lava Series on Hold With Hope and the Wollaston Forland basalts are very similar to the dredged flat-patterned group. The age of these basalts is around 56–57 Ma (Upton *et al.* 1995).

In all, the voluminous lava plateaus in central and northern East Greenland with ages of 57–55 Ma cannot be rejected as possible source areas for some of the dredged rocks. The younger lavas in East Greenland are not represented in the dredged material.

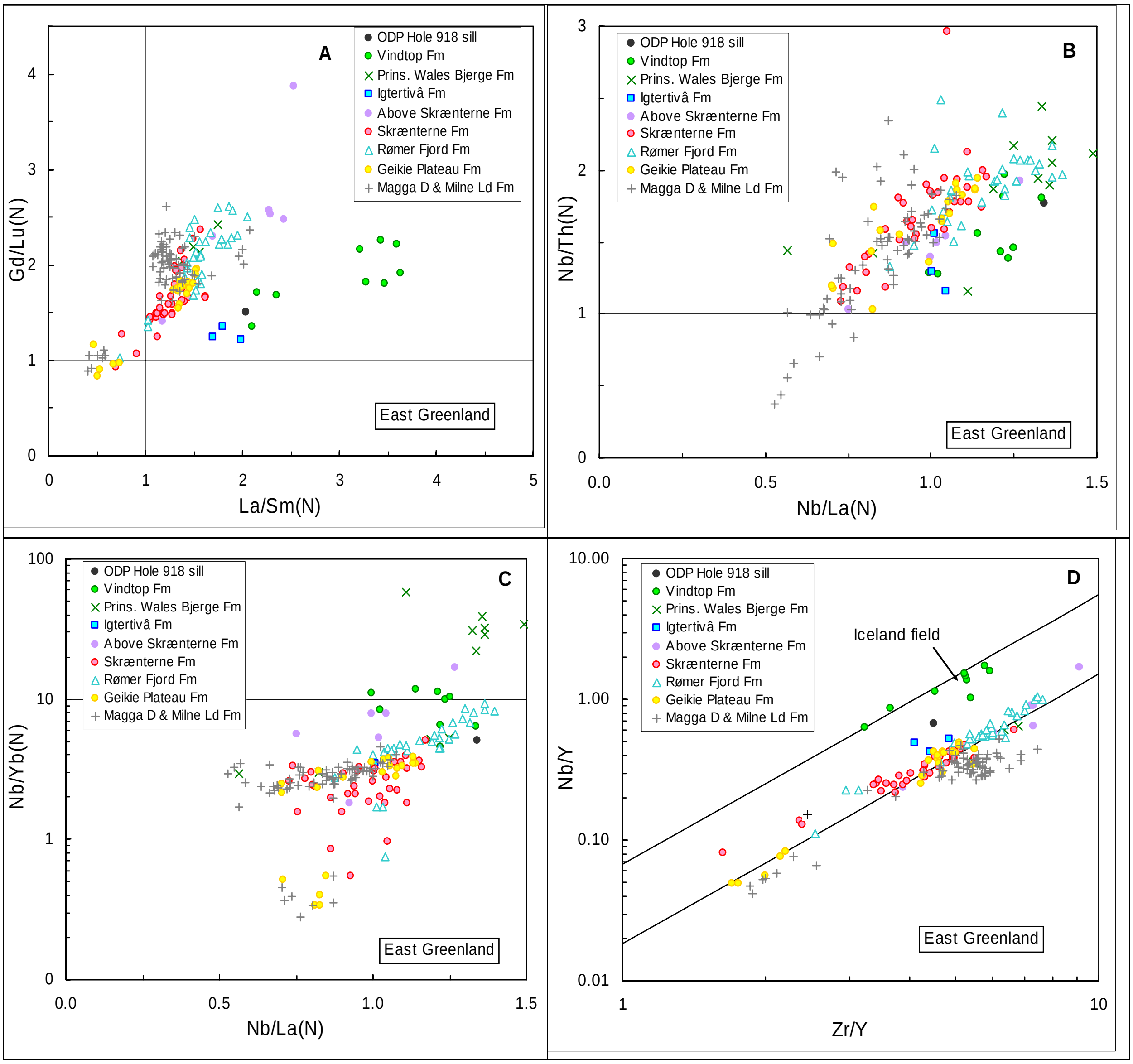

Fig. 17. Cross plots of trace element ratios for igneous rocks from East Greenland. Data source: Danish Lithosphere Centre, unpublished ICP-MS analyses by C. Tegner, see Tegner *et al.* 1998.

Source areas for the dredged igneous rocks

Based on the combined evidence presented in the foregoing, the following conclusions and suggestions can be made.

Davis Strait High

The basalts dredged on the eastern flank of the Davis Strait High are all geochemically depleted. They are dissimilar to any onshore occurrences of volcanic rocks on Baffin Island and West Greenland. They are closely similar to lavas drilled on the Davis Strait High itself. These drill sites are situated between 5.6 and 30 km from the dredge stations. In conclusion, the lavas dredged on the Davis Strait High represent local, almost untransported lavas, just as the Palaeozoic limestones dredged there are considered to be of local origin.

The southern areas south of 64°N

The geochemical 'main group' of basalts (including the extended and associated groups) constitute 70% of the dredged igneous rocks in the southern areas (Table 2). They are geochemically similar to the volcanic rocks of the Paleocene–Eocene Kanissut Formation in western Nuussuaq and dykes in the Aasiaat–Disko area. They are also geochemically similar to some of the plateau basalts in East Greenland.

The complete absence of all types but depleted basalts in the dredges on the Davis Strait High, closest to Nuussuaq, is in accordance with the iceberg drift pattern (Fig. 6) and strongly argues against ice rafting from north of the Davis Strait High to the southern areas.

Ice-rafting from East Greenland is a possibility. In favour of this source speak the geochemistry of rocks from nearly all the groups (Figs 15 and 17), the ocean current pattern now and earlier (Fig. 6), and the similar distribution of the various chemical groups in all the dredged southern localities (Table 2). It is a simple explanation for the two depleted samples found on Seamounts C and E.

However, several of the dredged rocks have no counterparts in East Greenland and at least these must have a different source. Whereas the relevant East Greenland basalts have ages in the narrow interval 57-55 Ma (see above), at least five, and possibly six, of the 10 dated dredged Paleogene samples from the southern areas have ages outside of this interval (Table 4, Fig. 14). These are four main group basalts of age 48.1-52.5 Ma and one 58.9 Ma rhyolite. Thus, statistically, *at least* half of the dredged basalts in the southern offshore areas have another source than in East Greenland.

Hecla High as a source area

The dredge locations south of 64°N are situated immediately south of the large volcanic complexes of the Hecla and Maniitsoq Highs (Fig. 1). The lava succession of the Hecla High is dated stratigraphically as Eocene and possibly older, and seismic sections show that an eroded and tilted cuesta landscape of lava flows has been exposed subaerially until some time during the Pleistocene (Fig. 18). It is therefore considered most likely that a large part of the dredged rocks from south of 64°N originate from the Hecla High volcanic area. They could have been eroded off the Hecla High by subaerial erosion and transported south by large rivers such as that which must have flowed through Canyon A. As the dredged localities in Canyon A are situated only 5–30 km from the seismically mapped volcanic areas, it is also possible that some lava flows erupted from the Hecla High area extend farther south and are exposed in the walls of Canyon A. The strong reflector and shoulder on the western side of the canyon (Fig. 3) was tested by piston coring, however no lava flows were found.

Alternatively, as described earlier, a local ice cap on the high could have dispersed material from the high and into the surroundings; this would explain the similar distribution of the various basalt types on all the dredged features in the south.

The origin of the volcaniclastic sediments encountered in two stations near the floor of Canyon A is understandable in the context of transport from the Hecla High area. The volcanic clasts would be the fine fraction of erosion material derived from the exposed basalts, deposited together with eroded mudstones and sandstones in valley fill in Canyon A and cemented during Pleistocene to Recent time (see earlier description), more or less in the place where they were dredged and grabbed.

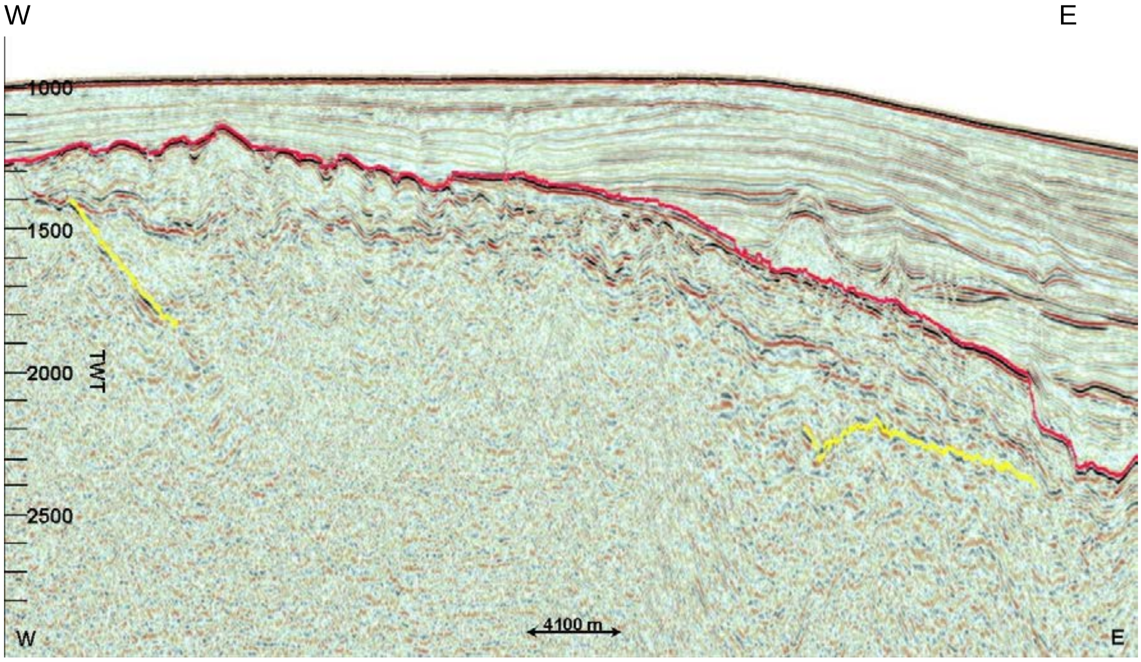

Fig. 18. Seismic section GR2000-117 across the Hecla High (W–E). The red line indicates the top of the basalts. Note the eroded basalt cuestas in the left part of the section. The volcanic succession is 300–500 m thick. The overlying 200–300 m thick sediments in the left half of the section are of Pleistocene to Holocene age. The yellow line is interpreted top Santonian sandstone.

If these inferences are correct, the major part of the Hecla High volcanic succession consists of Paleocene–Eocene basalts with chemical compositions similar to contemporaneous basalts elsewhere in West and East Greenland. It is probable that the Hecla High volcanic succession comprises all the basalt types found except the depleted types and the basanites. In addition, other volcanic areas and local volcanic centres such as Seamount B could also have produced similar magmas. The main type basalt appears to have been very widespread during the Eocene.

Seamount B

Seamount B is a local physiographic high and is inferred to be of volcanic origin. The dredges were made on one of the highest parts, on the side of an alleged small volcanic cone (Fig. 5). The main basalt types found there could be local eruption products rather than transported from the Hecla High or ice-rafted. Certainly the basanites dredged there are local products, probably from the small volcanic cone. The two dated basalts from Seamount B are some of the youngest dated rocks (52.5–48.1 Ma, Table 4).

Seamounts C, H, and E

These three seamounts are supposed to be structural ridges. One of the reasons for dredging Seamount H was to test for serpentinites, and therefore some coarse-grained to gabbroic samples were analysed; however these turned out to be Precambrian basement rocks, probably ice-rafted dykes. Apart from these, the three seamounts yielded a range of different basalt types, including two highly depleted samples. This could be taken to suggest that the dredged rocks on these seamounts are ice rafted from East Greenland; indeed some of them are are probably so, particularly those from Seamount E in South Greenland. But the dated sample from Seamount C (51.7 Ma, Table 4) is outside the age range for East Greenland and could rather come from the Hecla High. There could also be volcanic centres associated with the seamounts themselves, and as long as this is not known no definite conclusions can be made.

Canyon C

Two dredges in Canyon C yielded no igneous rocks at all, only ice-rafted basement debris and a few small sediment clasts. This fact illustrates that ice-rafting alone does not explain the widespread occurrence and abundance of igneous rocks in dredges elsewhere.

Cretaceous rocks

The origin of the 119 Ma old Cretaceous sample from Seamount H is open for discussion. It is a 20 cm subrounded block of massive, coarse-grained basalt. It is improbable that the Hecla High volcanic area should comprise so old, recently exposed, basalts, because the Cretaceous strata underlying the basalts are interpreted to be Santonian and younger (Fig. 18). Other occurrences of Cretaceous igneous rocks are very rare in Greenland. Two recently dated onshore intrusions have given Cretaceous ages (Larsen 2006): a 20 km long, 20 m wide coast-parallel phonolite dyke from the Ravn Storø area has an age of 105.4 ± 1.5 Ma, i.e. Albian. A camptonite sill on Tuttutooq in South Greenland has an age of 114.7 ± 4.7 Ma, very close to the age of the dredged sample. Both these two samples are chemically very different from the dredged basalt sample. The dredged Cretaceous sample could well come from an intrusion such as a dyke, either in the sea-covered areas or undiscovered onshore.

Geodynamic implications

Basalt compositions, mantle sources, and depths of melting

All the basalt compositions encountered among the dredged rocks can in principle be generated by melting of the same mantle material to different extents and at a range of depths. It is, however, probable that there are also different mantle components involved, such as MORB mantle and plume mantle, but identification of such differences relies on isotopic data which are not available. The composition of both MORB mantle and plume mantle will be depleted relative to a primitive mantle composition, most for MORB mantle and less for plume mantle.

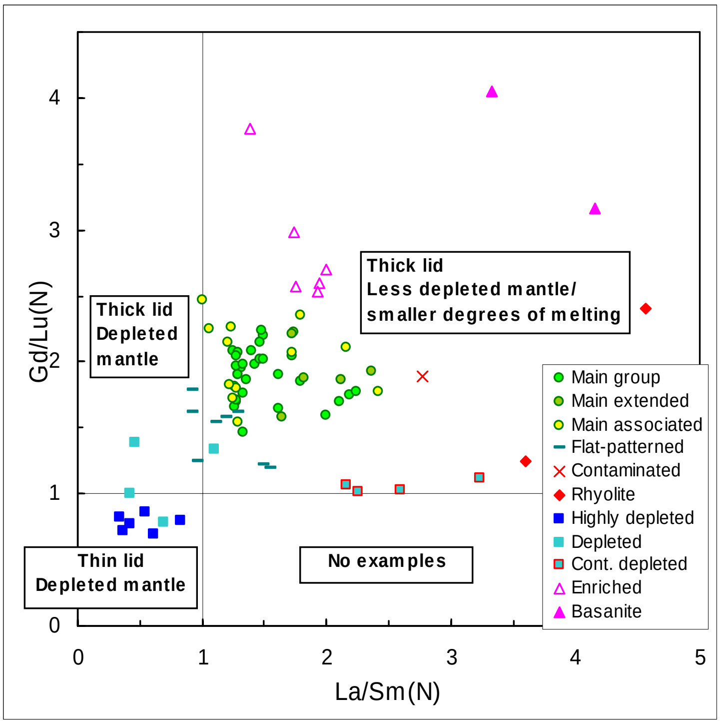

Fig. 19. Cross plot of REE ratios (as in Fig. 15A), indicating the effects of melting beneath lithospheric lids of varying thickness and varying degrees of melting and mantle depletion.

The REE may be used to distinguish between melts generated deeper or shallower than about 80 km depth, i.e., beneath a thicker or a thinner lithospheric lid. This is because at about 80 km depth (somewhat dependent on the temperature), an important phase transition takes place in the mantle. Deeper than this, garnet is the stable Al-rich phase, and shallower than this, spinel is the stable Al-rich phase. These two minerals have strongly different behaviour towards the REE, and therefore melts generated above and below this level have different REE patterns. Mantle melts generated in the presence of garnet will have REE patterns with the right half sloping to the right (Gd_N/Lu_N >1). Mantle melts generated in the presence of spinel and absence of garnet will have REE patterns with the right half sloping to the left (Gd_N/Lu_N <1). The left halves of the REE patterns (La_N/Sm_N ratios) are more dependent on compositions and degrees of melting, with melts from more depleted (MORB-like) mantle having La_N/Sm_N <1 and melts from less depleted mantle, or small-degree melts, have La_N/Sm_N <1. This is the basis for the usefulness of Figs 15A and 16A, as shown in principle in Fig. 19 where the three relevant quadrants have been labelled.

Davis Strait High: thin continental lithosphere

As noted in an earlier chapter, the structure of the Davis Strait High is contentious. It has been suggested to consist of oceanic crust (Keen & Barrett 1972), a mixture of continental crust and plume-related volcanic rocks similar to those at Cape Dyer on Baffin Island and in West Greenland (Keen et al. 1974), and a sliver of continental crust surrounded by oceanic crust (Srivastava et al. 1982). Chalmers & Pulvertaft (2001) concluded that there is no oceanic crust east of the Davis Strait High. The compositions of the dredged basalts are significant with regard to two aspects of the geodynamic setting of the Davis Strait High.

The existence on the Davis Strait High of basalts that show clear signatures of contamination with siliceous continental crustal material shows without doubt that such material is present in the high. It is not possible to distinguish between contaminants such as crystalline basement and sandstones derived from basement.

Comparison of Figs 15A and 19 shows that the basalts from the Davis Strait High, with $Gd_N/Lu/_N$ <1, are generated in the spinel stability field and thus at depths shallower than about 80 km. As the basalts are asthenospheric melts, the lithosphere would have been thinner than about 80 km, but the thickness cannot be specified further. This thickness should be compared with the thickness of the continental margins on both sides. On the Greenland side, the basalts from the Maligât Formation on Disko, with $Gd_N/Lu/_N$ = 1.6–2.7 (Fig. 16A), are generated in the garnet stability field deeper than 80 km. The thickness of the lithospheric lid in West Greenland has been calculated to around 100 km by Herzberg & O'Hara (1998). On the Baffin Island side, the basalts have $Gd_N/Lu/_N$ = 1.0–1.3 (Fig. 16A) and must be generated close to the transition zone between garnet and spinel around 80 km depth. Thus, around 63–60 Ma the lithospheric lid in the Davis Strait was distinctly thinner than beneath the continental margins on both sides.

The composition of the asthenospheric mantle was quite depleted beneath all three areas. La_N/Sm_N ratios are low (less than 1) in basalts from all three areas, the exception being that the Baffin Island mantle consisted of two discrete components, both a depleted (N-type) and an enriched (E-type) component. The depleted mantle component is geochemically very similar to oceanic mantle from which oceanic basalts (MORB) are generated. This appears to be an intrinsic feature of the initial Proto-Icelandic mantle plume (Holm *et al.* 1993, Fitton *et al*. 1997). It is therefore not possible to make a clear distinction between oceanic and plume mantle sources.

Hecla High: continental margin

The Hecla High is a structural high capped by volcanic rocks underlain by Mesozoic to Paleocene sediments and crystalline basement (Chalmers et al. 1993; Chalmers & Pulvertaft 2001). The 300–500 m thick volcanic succession appears to be subaerially emplaced and terminates to the east in an escarpment that suggests transformation into hyaloclastite facies (Fig. 18). As judged from the dredged and dated material, the volcanics are Paleocene–Eocene (59–48 Ma) and of compositions very similar to rocks emplaced extensively and near-contemporaneously onto the continental margins of West and East Greenland, largely in similar sedimentary basin environments with thinned lithosphere. This confirms the nature of the Hecla High as part of the West Greenland continental margin.

Seamount B: continental edge?

Seamount B forms part of a more widespread volcanic succession with a stratigraphic age of Paleocene–Early Eocene (Sørensen 2005). It is thus contemporaneous with the volcanic successions in the neighbouring Hecla and Maniitsoq Highs. If the dredged rocks (apart from the basanites) are indeed representative of the local major eruption products, their similarity to those of the Hecla High indicate similar melting material and melting conditions, including comparable lithospheric thicknesses >80 km. The lithosphere at Seamount B could be abnormally thick oceanic lithosphere as suggested by Gerlings (2005) based on refraction and reflection seismic data, but it could as well be continental. The basanites would represent late, small-volume melting at relatively deep levels, comfirming the existence of relatively thick lithosphere. Similar basanites have been described from Bathurst Island in Canada (Mitchell & Platt 1983; 1984); they were suggested to be associated with rifting in the Canadian Arctic around 47 Ma.

Seamounts C, H, and E: structural ridges

These seamounts are confirmed as structural ridges; the occurrence of local volcanic rocks is contentious. No serpentinites were found on any of them.

Summary and conclusions

During the summers of 2003 and 2004, seabed sampling was carried out by dredging and grabbing at a number of submarine features in the Davis Strait and Labrador Sea. These features include the Davis Strait High at 66°32′–66°34′ N, a large submarine canyon at 63°07′–63°31′ N along the western side of the Fylla platform (Canyon A), a low area on the eastern side of the Fylla platform (Canyon C), three physiographic highs at 62°27′–62°51′ N (seamounts B, C, and H), and a high area off South Greenland at 59°38′ (Seamount E). The only feature that did not yield any igneous rocks was Canyon C. At the other features, igneous rocks constituted 7–20% of the recovered clasts, the remaining being sediments (6–70%) and Precambrian basement lithologies (23–80%).

The recovered rocks are either rafted with icebergs, dispersed by an earlier ice sheet on the shelf, or derived from local outcrops. Most, but not all, of the Precambrian rocks have very variable lithologies and are considered to be ice-rafted debris. Most of the sediments are considered to be local or short-distance transported. The igneous rocks may be either local, short-distance transported, or long-distance ice-rafted.

Precambrian basement

In situ Precambrian basement was recovered at two dredge stations on the eastern side of Canyon A, confirming the existence of exposed, upthrust basement as inferred from seismic sections. Zircons from a basement sample gave an Archaean $^{206}Pb/^{207}Pb$ age of 2740 Ma; thus it is demonstrated that the Archaean basement in West Greenland extends for nearly 200 km offshore, well into areas that have earlier been interpreted as oceanic crust.

Chemical analyses

A total of 95 igneous rock samples were chemically analysed by XRF and ICP-MS. Of these, 12 are Precambrian and must represent ice-rafted material, probably large Proterozoic dykes. All the analysed coarse-grained gabbroic to doleritic samples are Precambrian. The 83 samples considered to be young are divided into 11 compositional groups. On the Davis Strait High, the only basalt type found is geochemically depleted basalt. In contrast, very different compositional groups are found in the southern area. Here, the ‘main group’ is the most frequently encountered, and together with two related groups (‘extended main group’ and ‘associated basalts’) these rocks constitute 70% of the igneous rocks dredged south of 64°N. Other groups in the southern area such as ‘flat-patterned basalts’, contaminated basalts, rhyolites, enriched basalts and basanites may be genetically related to the main group of basalts and form part of the same volcanic succession.

Age determinations

Fourteen samples were sent for dating by the $^{40}Ar/^{39}Ar$ step-heating method. Of these, one failed to yield an age, one was Proterozoic, and one was Cretaceous, 119 Ma. Eleven samples were Palaeogene, 63–48 Ma.

Davis Strait High

The geochemically depleted basalts from the Davis Strait High are dated at 63.0 ±0.7 Ma. They are compositionally different from contemporaneous depleted basalts onshore West Greenland and Canada but similar to basalts drilled on the High itself, and they must be locally derived. Their REE patterns indicate mantle melting in spinel facies, i.e. beneath a lithospheric lid thinner than about 80 km. However, the presence of siliceous, crustally contaminated depleted basalts clearly shows that the Davis Strait High contains continental crystalline basement.

Areas south of 64°N

In the areas south of 64°N, 10 samples have ages in the range 59–48 Ma. The dredged basalts are geochemically similar to basalts from both central West Greenland and central and northern East Greenland. Ice rafting is therefore a serious concern. The ocean current pattern does not favour ice rafting from central West Greenland, and the lack of these geochemical types on the Davis Strait High speaks strongly against it. On the other hand, there may well be a component of ice rafted material from East Greenland. The similar East Greenland basalts have a narrow eruption interval of 57–55 Ma, and five of the 10 dated dredged samples are outside of this age interval. Therefore, at least half of the dredged material must have another source. The **Hecla High** is suggested as a local source for the basalts in the southern areas, where the rocks could have been dispersed by a former ice sheet on the shelf, and by river transport. The REE patterns of the basalts indicate mantle melting in garnet facies, i.e. beneath a lithospheric lid thicker than about 80 km. The Hecla High, with its Paleocene–Early Eocene volcanic succession similar to the onshore successions in both West and East Greenland, clearly forms part of the West Greenland continental margin.

Seamount B, of volcanic origin, yielded rocks geochemically very similar to those assumed to be derived from the Hecla High. If these rocks originated on Seamount B, they indicate a lithosphere of similar thickness as at Hecla High; it could be of continental character or it could be abnormally thick oceanic lithosphere. Two basanite samples from Seamount B are of indisputable local origin. They represent late, small-volume deep melts and confirm the existence of relatively thick lithosphere beneath Seamount B.

Seamounts C, H, and E are structural highs. No serpentinites were found on them.

Acknowledgements

The work was funded by the Bureau of Minerals and Petroleum, Nuuk. Bob Duncan and John Huard at the Noble Gas Mass Spectrometry Lab, Oregon State University, are thanked for exerting their analytical skills to get good ages out of small amounts of sample.

References

Balkwill, H.R., Mcmillan, N.J., Maclean, B., Williams, G.L. & Srivastava, S.P. 1990: Geology of the Labrador Shelf, Baffin Bay, and Davis Strait. In: Keen, M.J. & Williams, G.L. (eds): Geology of the Continental Margin of Eastern Canada. Geological Survey of Canada, Geology of Canada **2**, 293–348.

Belan, A.B., Abbuehl, L. & Kuijpers, A. 2004: Relict iceberg ploughmarks on the western Greenland margin. In: North Atlantic and Labrador Sea margin architecture and sedimentary processes. Intergovernmental Oceanographic Commission Workshop Report **191**, 9–11.

Bennike, O., Björck, S. & Lambeck, K. 2002: Estimates of South Greenland late-glacial ice limits from a new relative sea level curve. Earth and Planetary Science Letters **197**, 171–186.

Bridgwater, D., Mengel, F., Fryer, B., Wagner, P. and Hansen, S.C. 1995: Early Proterozoic mafic dykes in the North Atlantic and Baltic cratons: field setting and chemistry of distinctive dyke swarms. In: Coward, M.P. & Ries, A.C. (eds): Early Precambrian Processes. Geological Society Special Publication **95**, 193–210.

Brooks, C.K. & Rucklidge, J.C. 1976: Tertiary peralkaline rhyolite dikes from the Skærgaard area, Kangerdlugssuaq, East Greenland. Meddelelser om Grønland **197 (3),** 27 pp.

Cadman, A.C., Tarney, J., Bridgwater, D., Mengel, F., Whitehouse, M.J. & Windley, B.F. 2001: The petrogenesis of the Kangâmiut dyke swarm, W. Greenland. Precambrian Research **105**, 183–203.

Chalmers, J.A. 1991: New evidence on the structure of the Labrador Sea/ Greenland continental margin. Journal of the Geological Society, London **148**, 899–908.

Chalmers, J.A. & Laursen, K.H. 1995: Labrador Sea: The extent of continental crust and the timing of the start of sea-floor spreading. Marine and Petroleum Geology **12**, 205–217.

Chalmers, J.A. & Pulvertaft, T.C.R. 2001: Development of the continental margins of the Labrador Sea: a review. In: Wilson, R.C.L. et al. (eds): Non-volcanic rifting of continental margins: a comparison of evidence from land and sea. Special Publication, Geological Society, London **187**, 77–105.

Chalmers, J.A., Pulvertaft, T.C.R., Christiansen, F.G., Larsen, H.C., Laursen, K.H. & Ottesen, T.G. 1993: The southern West Greenland continental margin: rifting history, basin development, and petroleum potential. In: Parker, J.R. (ed) Petroleum Geology of Northwest Europe: Proceedings of the 4th Conference. The Geological Society, London, 915–931.

Christiansen, F.G., Bojesen-Koefoed, J., Chalmers, J.A., Dalhoff, F., Mathiesen, A., Sønderholm, M., Dam, G., Gregersen, U., Marcussen, C., Nøhr-Hansen, H., Piasecki, S., Preuss, T., Pulvertaft, T.C.R., Rasmussen, J.A. & Sheldon, E. 2001: Petroleum geological activitites in West Greenland in 2000. Geology of Greenland Survey Bulletin **189**, 24–33.

Clarke, D.B., Cameron, B.I., Muecke, G.K. & Bates, J.L. 1989: Early Tertiary basalts from the Labrador Sea and the Davis Strait region. Canadian Journal of Earth Sciences **26**, 956–968.

Dalhoff, F., Nielsen, T., Kuijpers, A. & Poulsen, N.E. 2003: Togtrapport, havbundsprøveind-samling offshoreVestgrønland 2003. GEUS-notat nr. 08-EN-03-10, 9 pp + appendices.

Dalhoff, F., Kuijpers, A., Nielsen, T., Lassen, S., Boserup, J., Hansen, E. & the crew on H/F DANA 2004: Togtrapport. Havbundsprøveindsamling ud for Vestgrønland, H/F DANA 17/09-04/10 2004. Danmarks og Grønlands Geologiske Undersøgelse Rapport **2005/1**, 44 pp.

Fitton, J.G., Saunders, A.D., Norry, M.J., Hardarson, B.S. & Taylor, R.N. 1997: Thermal and chemical structure of the Iceland plume. Earth and Planetary Science Letters **153**, 197–208.

Fleming, K. & Lambeck, K. 2004: Constraints on the Greenland Ice Sheet since the Last Glacial Maximum from sea-level observations and glacial-rebound models. Quaternary Science Reviews **23**, 1053–1077.

Francis, D. 1985: The Baffin Bay lavas and the value of picrites as analogues of primary magmas. Contributions to Mineralogy and Petrology **89**, 144–154.

Funder, S. & Hansen, L. 1995: The Greenland ice sheet – a model for its culmination and decay during and after the last glacial maximum. Bulletin of the Geological Society of Denmark **42**, 137–152.

Gerlings, J. 2005: The crustal structure of the Davis Strait transform-rifted margin derived from refraction/wide-angle reflection seismic data. Master thesis, Niels Bohr Institute, University of Copenhagen, 100 pp.

Halama, R., Wenzel, T., Upton, B.G.J. & Markl, G. 2003: A geochemical and Sr-Nd-O isotopic study of the Proterozoic Eriksfjord Basalts, Gardar Province, South Greenland: Reconstruction of an OIB signature in crustally contaminated rift-related basalts. Mineralogical Magazine **67**, 831–853.

Hald, N. 1976: Early Tertiary flood basalts from Hareøen and western Nûgssuaq, West Greenland. Bulletin Grønlands Geologiske Undersøgelse **120**, 36 pp.

Henderson, G., Schiener, E.J., Risum, J.B., Croxton, C.A. & Andersen, B.B. 1981: The west Greenland Basin. In: Kerr, J. W. (ed) Geology of the North Atlantic Borderlands. Memoir, Canadian Society of Petroleum Geologists **7**, 399–428.

Herzberg, C. & O’Hara, M.J. 1998: Phase equilibrium constraints on the origin of basalts, picrites, and komatiites. Earth-Science Reviews **44**, 39–79.

Holm, P.M., Gill, R.C.O., Pedersen, A.K., Larsen, J.G., Hald, N., Nielsen, T.F.D. & Thirlwall, M.F. 1993: The Tertiary picrites of West Greenland: contributions from 'Icelandic' and other sources. Earth and Planetary Science Letters **115**, 227–244.

Kalsbeek, F. & Taylor, P.N. 1986: Chemical and isotopic homogeneity of a 400 km long basic dyke in central West Greenland. Contributions to Mineralogy and Petrology **93**, 439–448.

Keen, C.E., Keen, M.J., Ross, D.I. & Lack, M. 1974: Baffin Bay: small ocean basin formed by seafloor spreading. Bulletin American Association of Petroleum Geologists **58**, 1098–1108.

Keen C.E., Loncarevic, B.D., Reid, I., Woodside, J., Haworth, R.T. and Williams, H. 1990: Tectonic and geophysical overview. In: Geology of the Continental Margin of Eastern Canada. Edited by M. J. Keen and G.L. Williams. Geological Survey of Canada, Geology of Canada **2**, 31–85.

Kent, A.J.R., Stolper, E.M., Francis, D., Woodhead, J., Frei, R. & Eiler, J. 2004: Mantle heterogeneity during the formation of the North Atlantic Igneous Province: Constraints from trace element and Sr-Nd-Os-O isotope systematics of Baffin Island picrites. Geochemistry, Geophysics, Geosystems **5**, doi:10.1029/2004GC000743, 26 pp.

Koppers. A.A.P. 2002: ArArCALC; software for 40Ar/39Ar age calciulations. Computers and Geosciences **28**, 605–619.

Kystol, J. & Larsen, L.M. 1999: Analytical procedures in the Rock Geochemical Laboratory of the Geological Survey of Denmark and Greenland. Geology of Greenland Survey Bulletin **184**, 59–62.

Larsen, L.M. 2006: Mesozoic to Palaeogene dyke swarms in West Greenland and their significance for the formation of the Labrador Sea and the Davis Strait. Danmarks og Grønlands Geologiske Undersøgelse Rapport **2006/34**, 69 pp + appendices.

Lass-Evans, S. 2004: The anatomy of the ancestral Iceland plume: a chemical and isotopic study of the Tertiary basalts and picrites from Baffin Island. PhD thesis, University of Edinburgh, 200 pp + appendices.

Lassen, B., Bridgwater, D., Bernstein, S. & Rosing, M. 2004: Assimilation and high-pressure fractional crystallization (AFC) recorded by Paleo-proterozoic mafic dykes, South-east Greenland. Lithos **72**, 1–18.

Le Maitre, R.W. (ed) 2002: Igneous Rocks, A classification and glossary of terms. 2nd edition. Recommendations of the IUGS subcommission on the systematics of igneous rocks. Cambridge: Cambridge University Press, 236 pp.

Linthout, K., Troelstra, S.R. & Kuijpers, A. 2000: Provenance of coarse ice-rafted detritus near the SE Greenland margin. Geologie en Mijnbouw **79**, 109–121.

MacLean, B., Jansa, L.F., Falconer, R.K.H. & Srivastava, S. P. 1997: Ordovician strata on the southeastern Baffin Island shelf revealed by shallow drilling. Canadian Journal of Earth Sciences **14**, 1925–1939.

McDonough, W.F. & Sun, S.-S. 1995: The composition of the Earth. Chemical Geology **120**, 223–253.

Mitchell, R.H. & Platt, R.G. 1983: Primitive nephelinitic volcanism associated with rifting and uplift in the Canadian Arctic. Nature **303**, 609–612.

Mitchell, R.H. & Platt, R.G. 1984: The Freemans Cove volcanic suite: field relations, petrochemistry, and tectonic setting of nephelinite-basanite volcanism associated with rifting in the Canadian Arctic Archipelago. Canadian Journal of Earth Sciences **21**, 428–436.

Ogg, J.G. & Smith, A.G. 2004: The geomagnetic polarity time scale. In: Gradstein, F.M., Ogg, J.G. & Smith, A.G. (eds), A geologic time scale 2004, 63–86. Cambridge: Cambridge University Press.

Pedersen, A.K., Larsen, L.M., Riisager, P. & Dueholm, K.S. 2002: Rates of volcanic deposition, facies changes and movements in a dynamic basin: the Nuussuaq Basin, West Greenland, around the C27n–C26r transition. In: Jolley, D.W. & Bell, B.R. (eds), The North Atlantic Igneous Province: stratigraphy, tectonics, volcanic and magmatic processes. Special Publication, Geological Society, London **197**, 157–181.

Renne, P.R., Deino, A.L., Walter, R.C., Turrin, B.D., Swisher, C.C., Becker, T.A., Curtis, G.H., Jaouni, A.R. 1994: Intercalibration of astronomical and radioisotopic time. Geology **22**, 783–786.

Robillard, I., Francis, D. & Ludden, J.N., 1992: The relationship between E- and N-type magmas in the Baffin Bay lavas. Contributions to Mineralogy and Petrology **112**, 230–241.

Roest, W.R. & Srivastava, S.P. 1989: Sea-floor spreading in the Labrador Sea: A new reconstruction. Geology **17**, 1000–1003.

Sinton, C.W. & Duncan, R.A. 1998: $^{40}Ar/^{39}Ar$ ages of lavas from the Southeast Greenland margin, ODP Leg 152, and the Rockall Plateau, DSDP Leg 81. In: Saunders, A.D., Larsen, H.C. & Wise, S.H. (eds), Proceedings ODP, Scientific Results **152**: College Station, TX (Ocean Drilling Program), 387–402.

Sørensen, A.B. 2005: Structural development and exploration potential of the Lady Franklin and Maniitsoq Basins, Southwest Greenland. Halifax 2005, Halifax, Nova Scotia, Canada, 15–18 May, 2005, Abstracts, 184 only.

Srivastava, S.P. 1978: Evolution of the Labrador Sea and its bearing on the early evolution of the North Atlantic. Royal Astronomical Society, Geophysical Journal **52**, 313–357.

Srivastava, S.P., Maclean, B., Macnab, R.F. & Jackson, H.R. 1982: Davis Strait: Structure and Evolution as Obtained from a Systematic Geophysical Survey. In Embry, A.F. & Balkwill, H.R. (eds) Arctic Geology and Geophysics. Canadian Society of Petroleum Geologists, Memoir, 8, 267–278.Turner, S.P., Platt, J.P., George, R.M.M., Kelly, S.P., Pearson, D.G. & Nowell, G.M. 1999: Magmatism associated with orogenic collapse of the Beltic–Alboran domain, SE Spain. Journal of Petrology **40**, 1011–1036.

Storey, M., Duncan, R.A., Larsen, H.C., Waagstein, R., Larsen, L.M., Tegner, C. & Lesher, C.E. 1996: Impact and rapid flow of the Iceland plume beneath Greenland at 61 Ma. Eos, Transactions, American Geophysical Union **77** (46), 839 only.

Storey, M., Duncan, R.A., Pedersen, A.K., Larsen, L.M. & Larsen, H.C. 1998: $^{40}Ar/^{39}Ar$ geochronology of the West Greenland Tertiary volcanic province. Earth andPlanetary Science Letters **160**, 569–586.

Tegner, C., Lesher, C.E., Larsen, L.M. & Watt, W.S. 1998: Evidence from the rare-earth element record of mantle melting for cooling of the Tertiary Iceland plume. Nature **395**, 591–594.

Thirlwall, M.F., Upton, B.G.J. & Jenkins, C. 1994: Interaction between continental lithosphere and the Iceland Plume – Sr-Nd-Pb isotope geochemistry of Tertiary basalts, NE Greenland. Journal of Petrology **35**, 839–879.

Upton, B.G.J. & Emeleus, C.H. 1987: Mid-Proterozoic alkaline magmatism in southern Greenland: the Gardar Province. In: Fitton, J.G. & Upton, B.G.J. (eds): Alkaline igneous rocks. Special Publication Geological Society, London **30**, 449–471.

Upton, B.G.J., Emeleus, C.H., Rex, D.C. & Thirlwall, M.F. 1995: Early Tertiary magmatism in NE Greenland. Journal of the Geological Society, London **152**, 959–964.

Upton, B.G.J., Emeleus, C.H., Beckinsale, R.D. & Macintyre, R.M. 1984: Myggbukta and Kap Broer Ruys: the most northerly of the East Greenland Tertiary igneous centres(?). Mineralogical Magazine **48**, 323–343.

Williamson, M-C., Larsen, L.M., Jackson, H.R.& Oakey, G.N. 2003: Evolution of the Baffin Island–West Greenland Tertiary Volcanic Province: Evidence from basaltic rocks on the conjugate margins. EGS–AGU–EUG Joint Assembly, Nice, France, April 2003. Geophysical Research Abstracts **5**, abstract no. 06113. CD-ROM only.

Appendix 1

$^{40}Ar/^{39}Ar$ dating of igneous rocks

Fourteen samples were dated by the Ar-Ar step-heating method at Oregon State University, the Noble Gas Mass Spectrometry Laboratory led by professor Robert Duncan. The laboratory and the method are described at
http://www.coas.oregonstate.edu/research/mg/chronology.html.
This appendix shows three plots for each sample, a plateau, a normal isochron, and a reverse isochron.

Summary table. $^{40}Ar/^{39}Ar$ radiometric age determinations on igneous rocks from the Labrador Sea and the Davis Strait

		Total Fusion (Ma)	Plateau (Ma)				Inverse Isochron (Ma)	
Sample	Material	Age ± 2 σ	Age ± 2 σ	Steps[1]	%^{39}Ar[1]	MSWD	Age ± 2 σ	$^{40}Ar/^{36}Ar$ ± 2 σ
AT453D-40	plagioclase	48.36 ± 0.88	**48.13 ± 0.87**	4/7	76.3	0.19	47.82 ± 1.22	299.8 ± 11.9
Dana-04-36D-18	groundmass	50.48 ± 0.43	**50.13 ± 0.41**	6/8	88.4	0.62	50.10 ± 0.42	297.8 ± 7.1
Dana-04-11D-11	groundmass	53.65 ± 0.40	**51.69 ± 0.48**	5/8	46.0	1.64	51.88 ± 0.67	287.2 ± 20.3
AT453D-27	plagioclase	55.22 ± 0.57	**52.48 ± 0.56**	6/7	96.9	0.16	52.49 ± 0.63	293.7 ± 31.0
AT484D-05	groundmass	53.47 ± 1.00	**53.96 ± 0.85**	4/7	88.6	1.41	53.71 ± 0.85	300.1 ± 4.9
Dana-04-23D-16	groundmass	56.53 ± 0.40	**54.80 ± 0.45**	5/8	62.3	3.02	54.66 ± 0.56	308.1 ± 29.1
Dana-04-27D-16	plagioclase	55.54 ± 0.77	**55.52 ± 0.72**	7/7	100.0	0.58	55.13 ± 0.88	302.2 ± 8.3
Dana-04-22D-16	plagioclase	86.77 ± 1.75	56.60 ± 0.80	3/7	49.8	1.56	**55.35 ± 0.85**	330.7 ± 11.5
AT484D-10	groundmass	56.42 ± 0.79	**56.11 ± 0.97**	3/7	73.2	4.09	56.75 ± 1.41	269.8 ± 42.4
Dana-04-20D-25	sanidine	58.98 ± 0.38	**58.94 ± 0.37**	7/10	95.0	0.46	58.84 ± 0.47	335.9 ± 109.0
AT465D-39	plagioclase	59.96 ± 0.68	**62.97 ± 0.74**	3/8	44.4	0.10	62.88 ± 0.85	298.2 ± 13.4
Dana-04-38D-02	plagioclase	124.9 ± 1.1	119.4 ± 1.1	3/8	73.0	1.87	**118.8 ± 1.2**	464.2 ± 41.9
Dana-04-37D-12	plagioclase	625.0 ± 4.7	662.8 ± 7.5	2/7	41.1	1.37	None	None
Dana-04-38D-04	plagioclase	2227 ± 18	None				**1543 ± 244**	15917 ± 3869

Samples irradiated at Oregon State University TRIGA reactor for 6 hours at 1MW power. Neutron flux measured using FCT-3 biotite monitor (FCT age 28.03 Ma, Renne *et al.* 1998). Data reduced by ArArCALC software (Koppers 2002).

Preferred age in **BOLD TEXT.** Age in **GREY** not meaningful.

1. Plateau age data includes number of steps in the plateau (steps in plateau / total steps) and % ^{39}Ar in plateau.

Sample AT 453D-40: Type 3, Main basalt (associated), Seamount B

04C2190.AGE >>> AT 453D-40 >>> Greenland

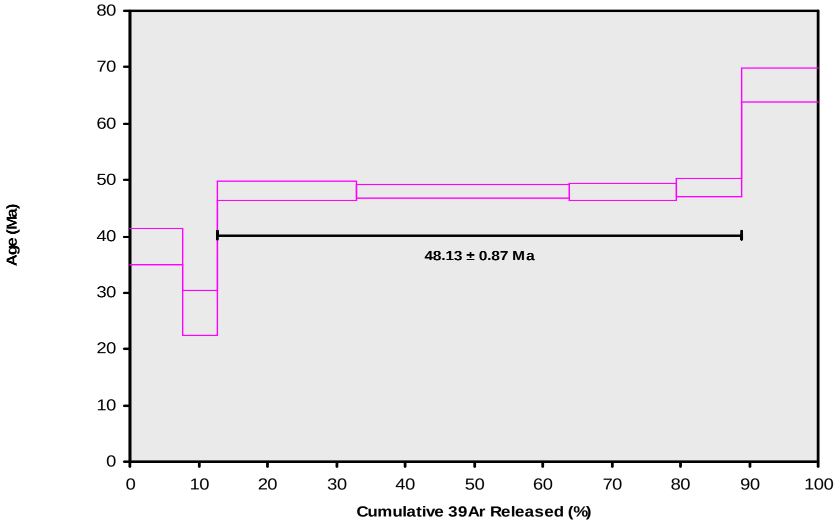

Ar-Ages in Ma

Weighted Plateau
48.13 ± 0.87
Total Fusion
48.36 ± 0.88
Normal Isochron
47.82 ± 1.22
Inverse Isochron
47.82 ± 1.22

MSWD
0.19

Sample Info

plagioclase
N. Atlantic
jh
OSU2F04
0.001517 (J)

04C2190.AGE >>> AT 453D-40 >>> Greenland

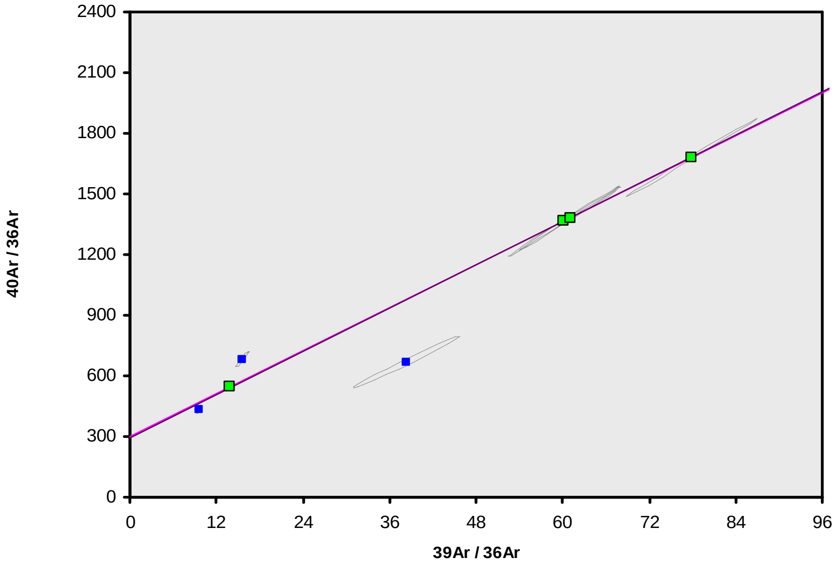

Ar-Ages in Ma

Weighted Plateau
48.13 ± 0.87
Total Fusion
48.36 ± 0.88
Normal Isochron
47.82 ± 1.22
Inverse Isochron
47.82 ± 1.22

MSWD
0.01

Sample Info

plagioclase
N. Atlantic
jh
OSU2F04
0.001517 (J)

04C2190.AGE >>> AT 453D-40 >>> Greenland

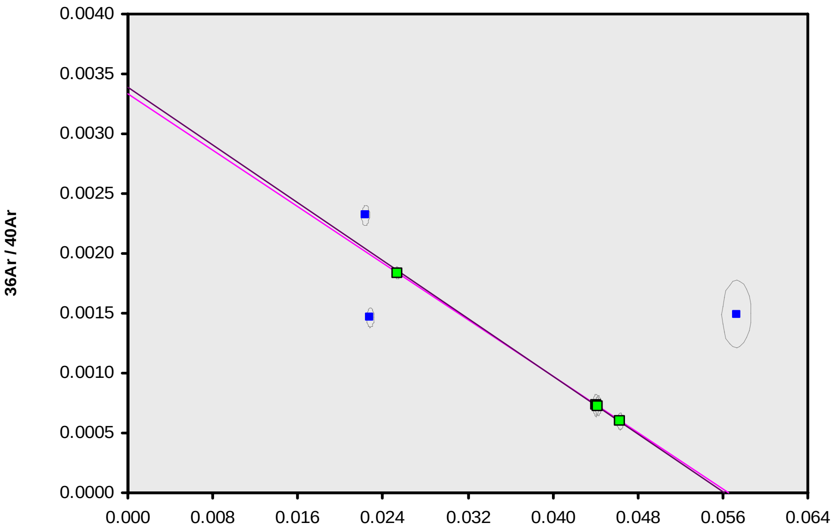

Ar-Ages in Ma

Weighted Plateau
48.13 ± 0.87
Total Fusion
48.36 ± 0.88
Normal Isochron
47.82 ± 1.22
Inverse Isochron
47.82 ± 1.22

MSWD
0.01

Sample Info

plagioclase
N. Atlantic
jh
OSU2F04
0.001517 (J)

Sample Dana-04-36D-18: Type 1, Main basalt, Canyon A

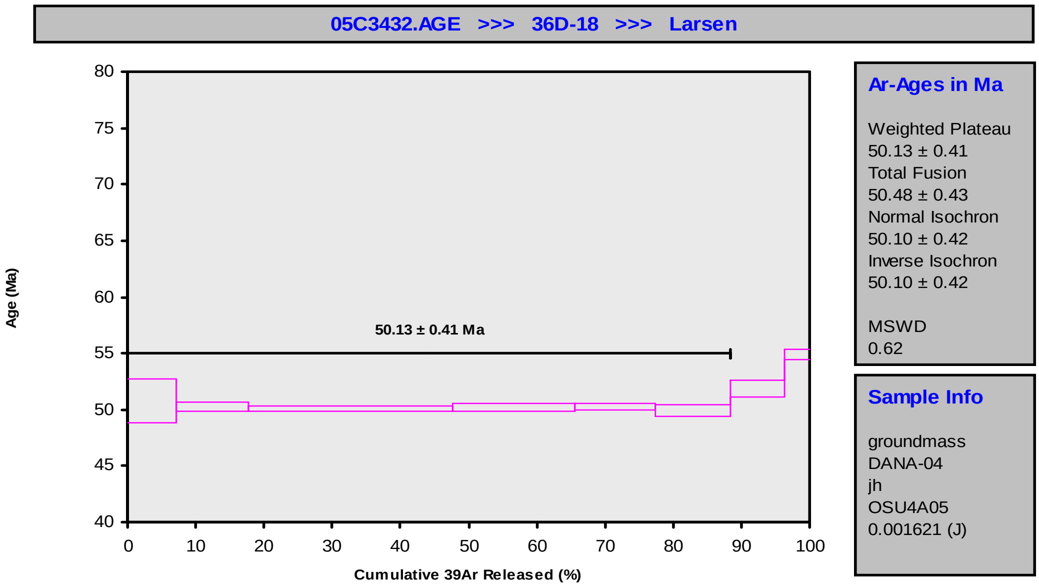

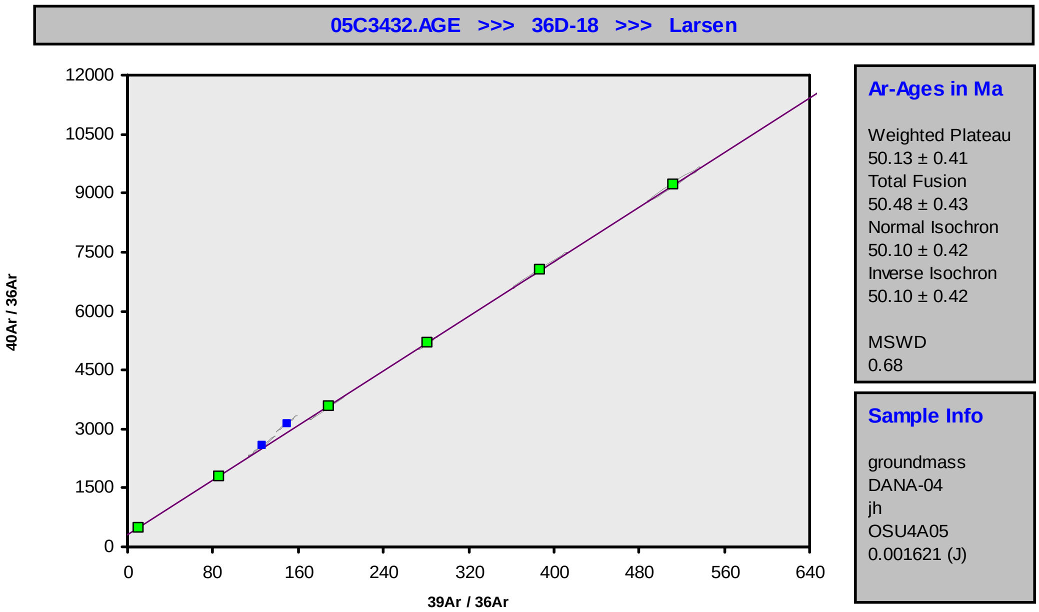

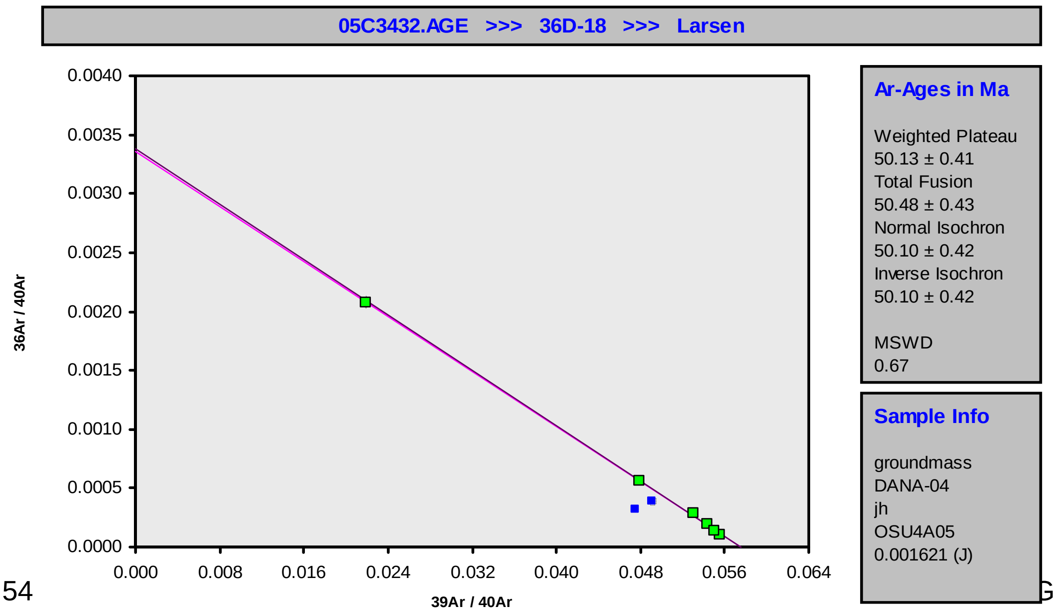

Sample Dana-04-11D-11: Type 2, Main basalt (extended), Seamount C

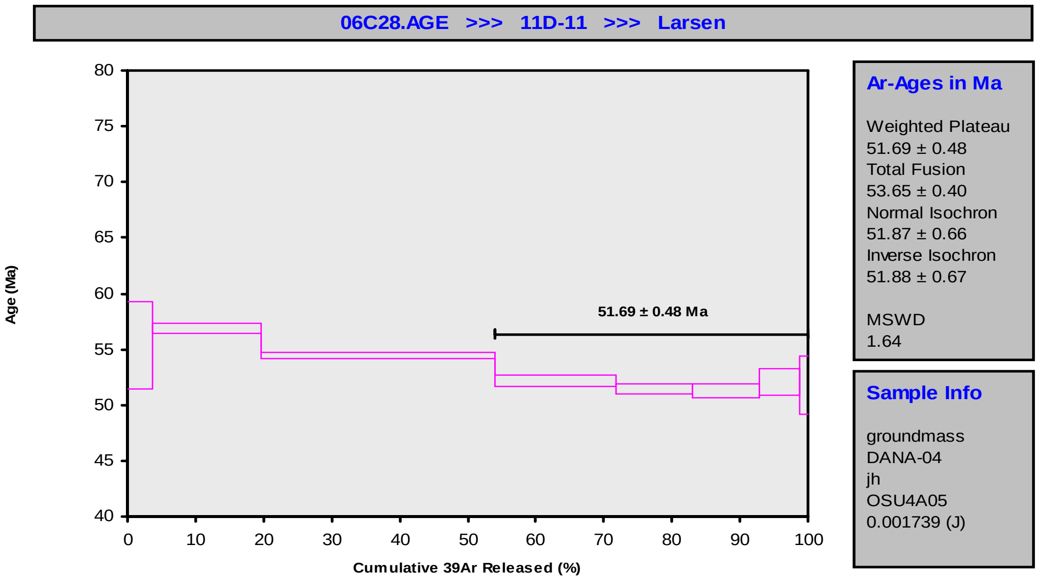

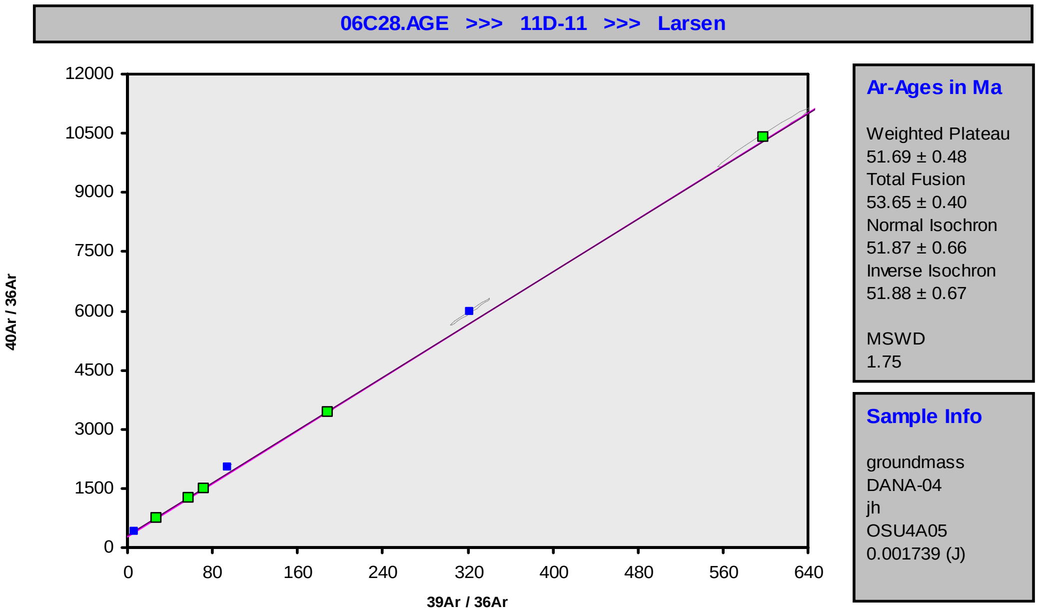

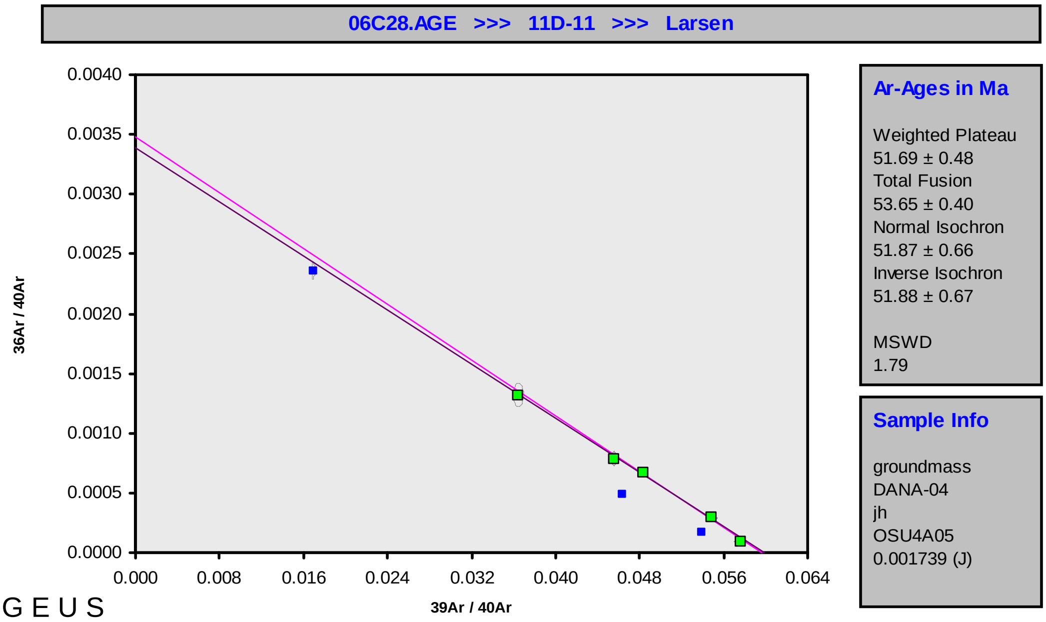

Sample AT453D-27: Type 1, Main basalt, Diapir B

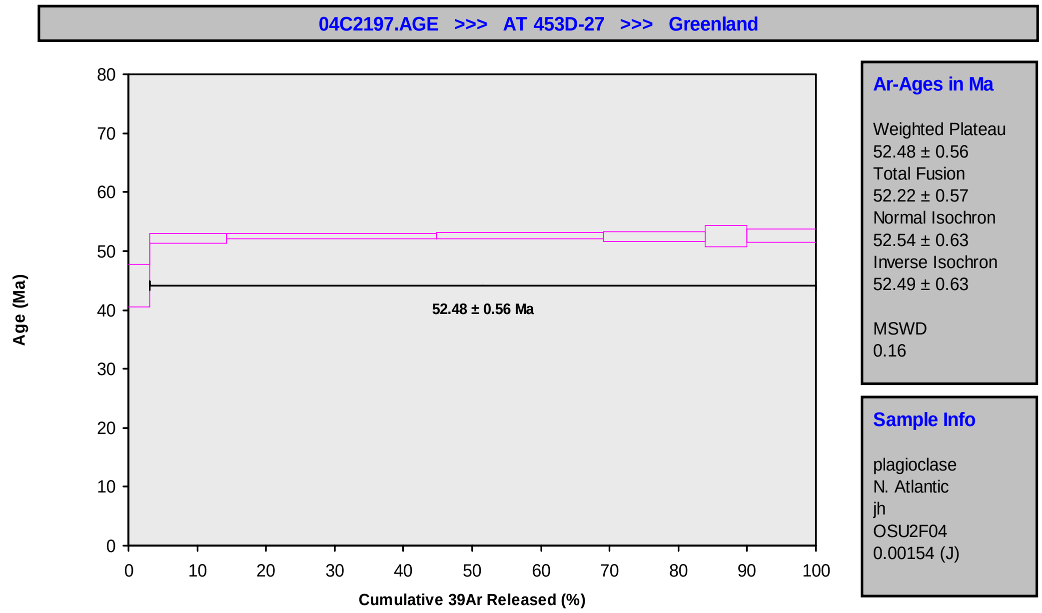

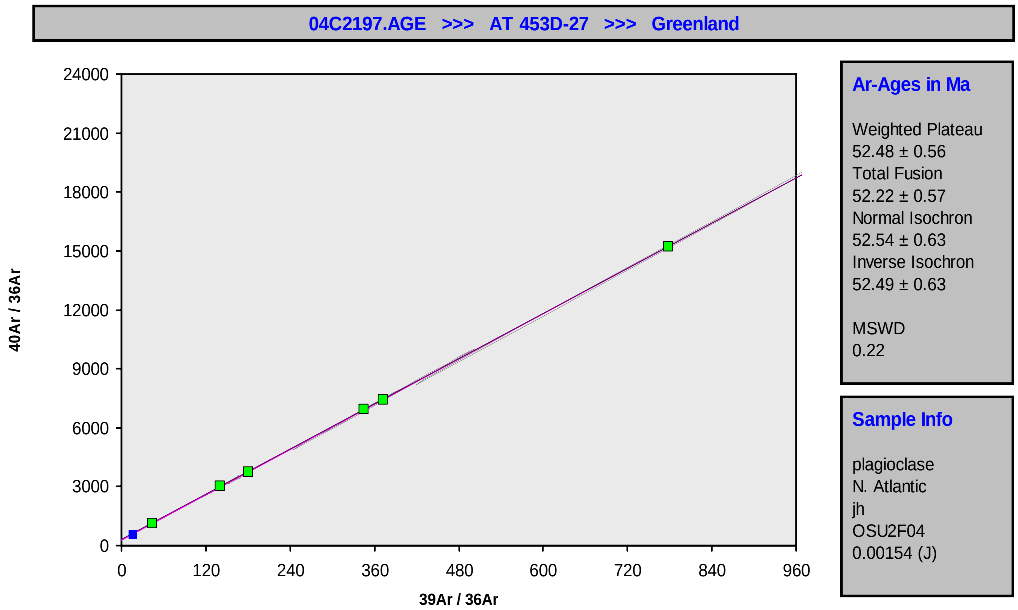

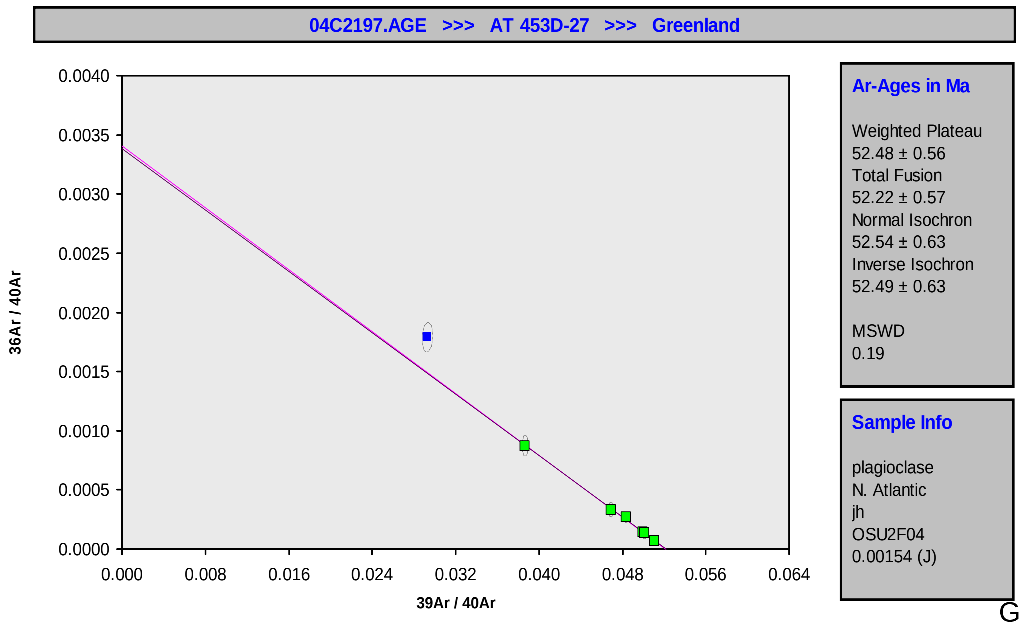

Sample AT 484D-05: Type 4, Flat-patterned basalt, Canyon A

04C2824.AGE >>> AT 484D-05 >>> Greenland

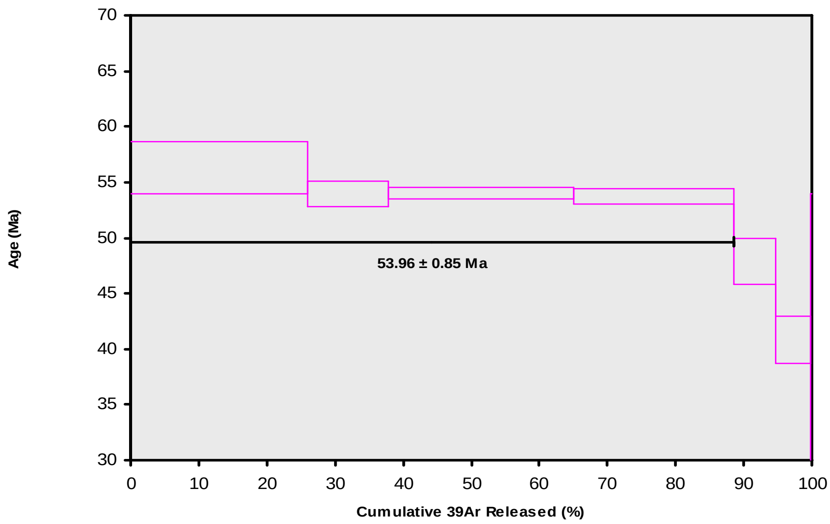

Ar-Ages in Ma

Weighted Plateau
53.96 ± 0.85
Total Fusion
53.47 ± 1.00
Normal Isochron
53.71 ± 0.85
Inverse Isochron
53.71 ± 0.85

MSWD
1.41

Sample Info

groundmass
N. Atlantic
jh
OSU2C04
0.001431 (J)

04C2824.AGE >>> AT 484D-05 >>> Greenland

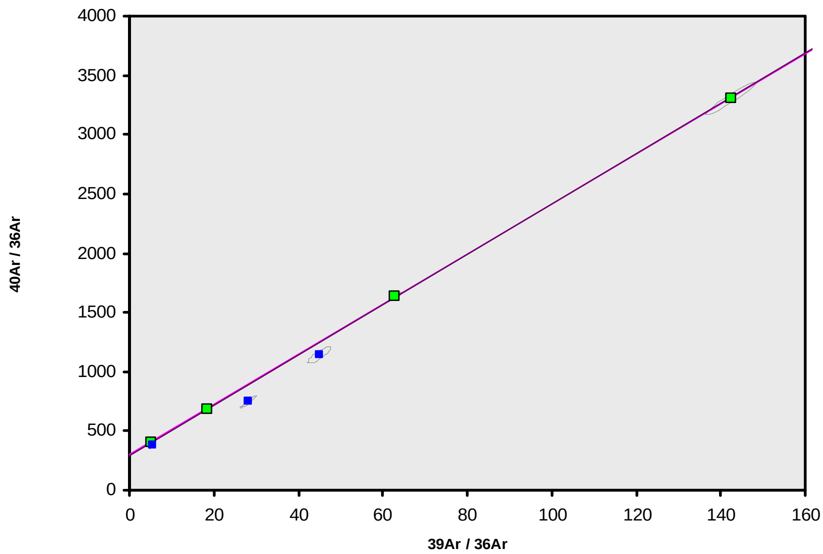

Ar-Ages in Ma

Weighted Plateau
53.96 ± 0.85
Total Fusion
53.47 ± 1.00
Normal Isochron
53.71 ± 0.85
Inverse Isochron
53.71 ± 0.85

MSWD
0.30

Sample Info

groundmass
N. Atlantic
jh
OSU2C04
0.001431 (J)

04C2824.AGE >>> AT 484D-05 >>> Greenland

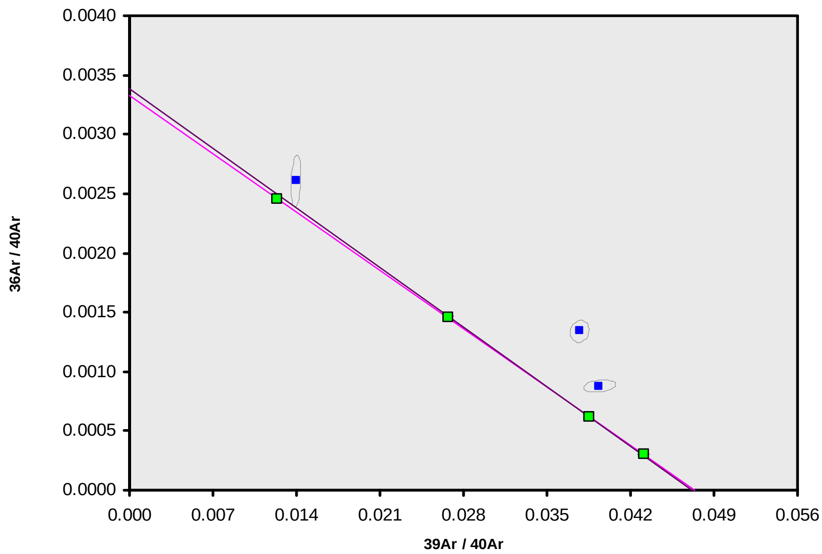

Ar-Ages in Ma

Weighted Plateau
53.96 ± 0.85
Total Fusion
53.47 ± 1.00
Normal Isochron
53.71 ± 0.85
Inverse Isochron
53.71 ± 0.85

MSWD
0.30

Sample Info

groundmass
N. Atlantic
jh
OSU2C04
0.001431 (J)

Sample Dana-04-23D-16: Type 10, Enriched basalt, Canyon A

05C3440.AGE >>> 23D-16 >>> Larsen

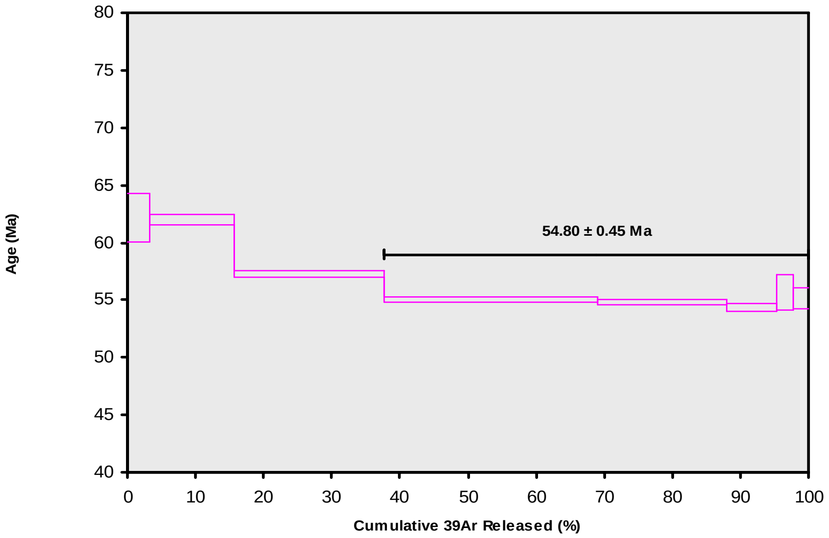

Ar-Ages in Ma

Weighted Plateau
54.80 ± 0.45
Total Fusion
56.53 ± 0.40
Normal Isochron
54.66 ± 0.57
Inverse Isochron
54.66 ± 0.56

MSWD
3.02

Sample Info

groundmass
DANA-04
jh
OSU4A05
0.001681 (J)

05C3440.AGE >>> 23D-16 >>> Larsen

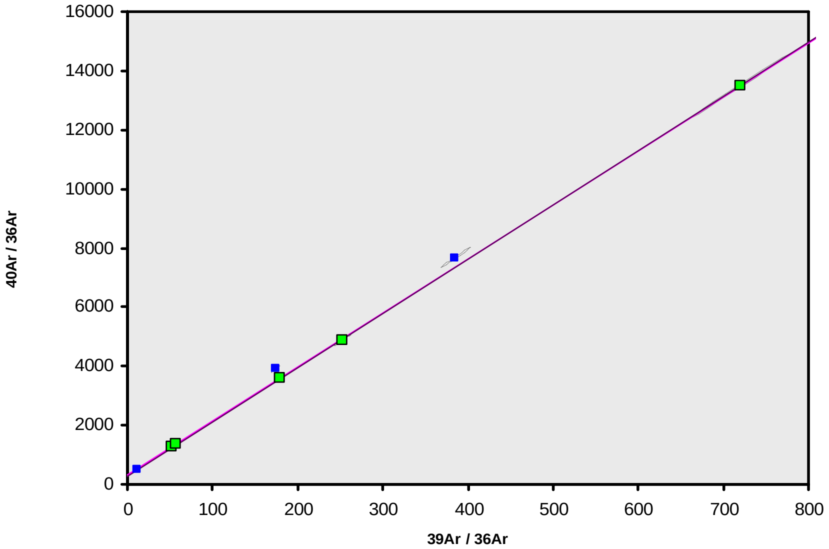

Ar-Ages in Ma

Weighted Plateau
54.80 ± 0.45
Total Fusion
56.53 ± 0.40
Normal Isochron
54.66 ± 0.57
Inverse Isochron
54.66 ± 0.56

MSWD
3.26

Sample Info

groundmass
DANA-04
jh
OSU4A05
0.001681 (J)

05C3440.AGE >>> 23D-16 >>> Larsen

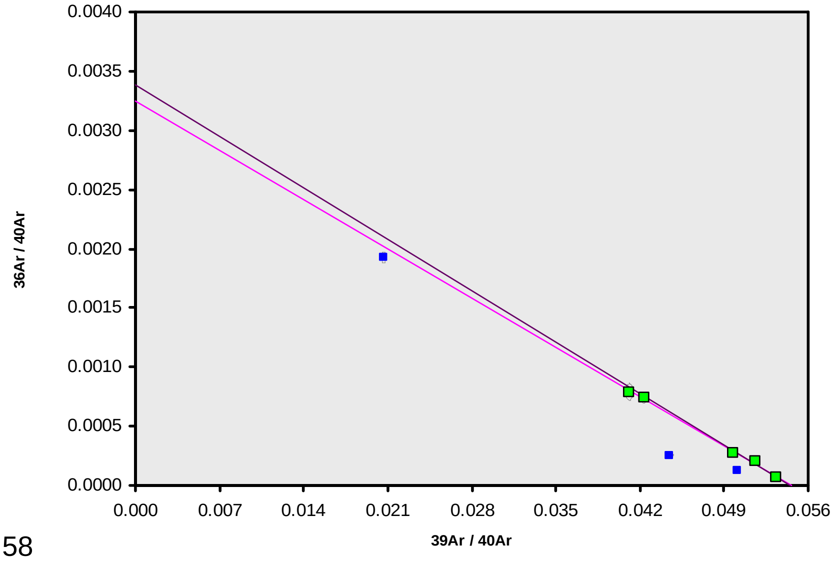

Ar-Ages in Ma

Weighted Plateau
54.80 ± 0.45
Total Fusion
56.53 ± 0.40
Normal Isochron
54.66 ± 0.57
Inverse Isochron
54.66 ± 0.56

MSWD
3.17

Sample Info

groundmass
DANA-04
jh
OSU4A05
0.001681 (J)

Sample Dana-04-27D-16: Type 1, Main basalt, Canyon A

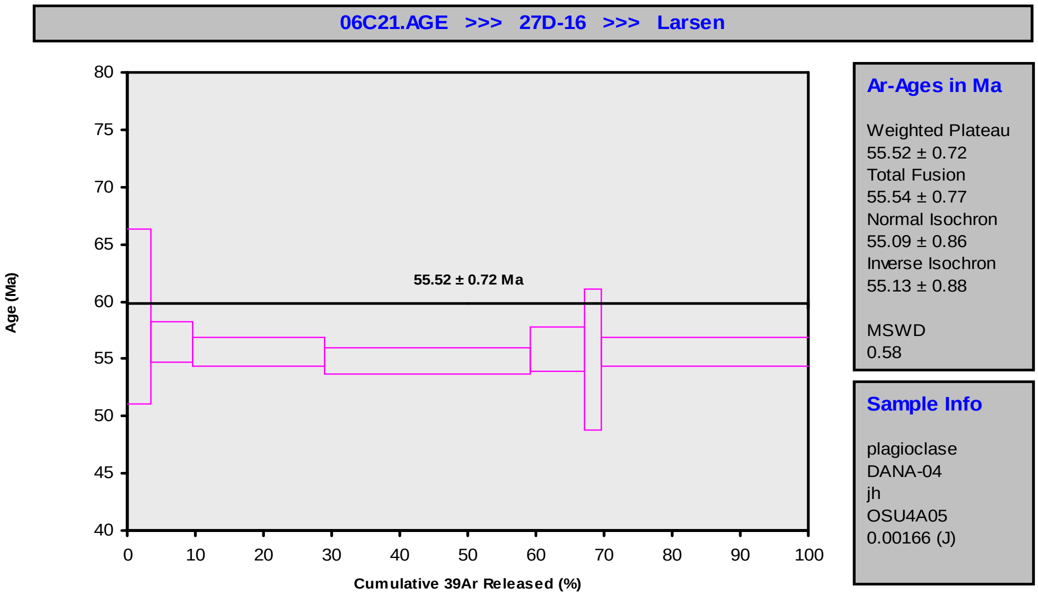

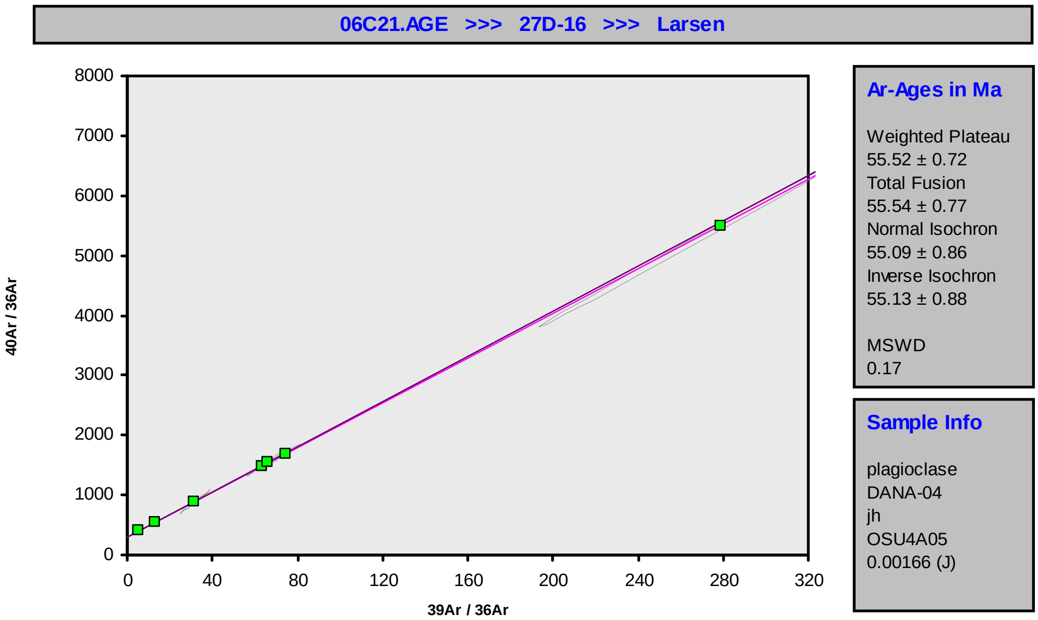

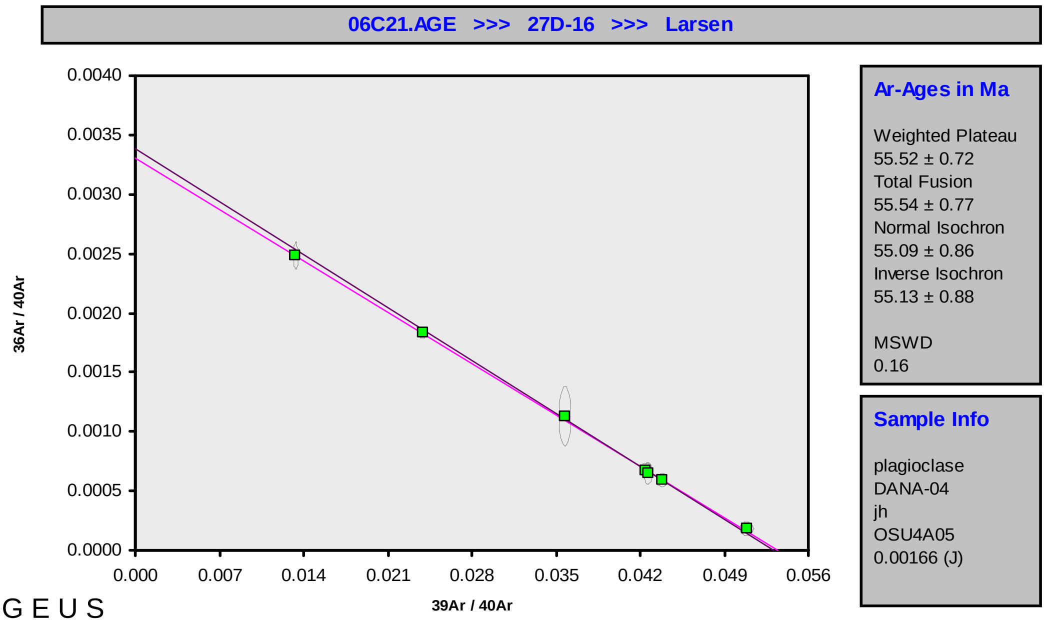

Sample Dana-04-22D-16: Type 10, Enriched basalt, Canyon A

05C3460.AGE >>> 22D-16 >>> Larsen

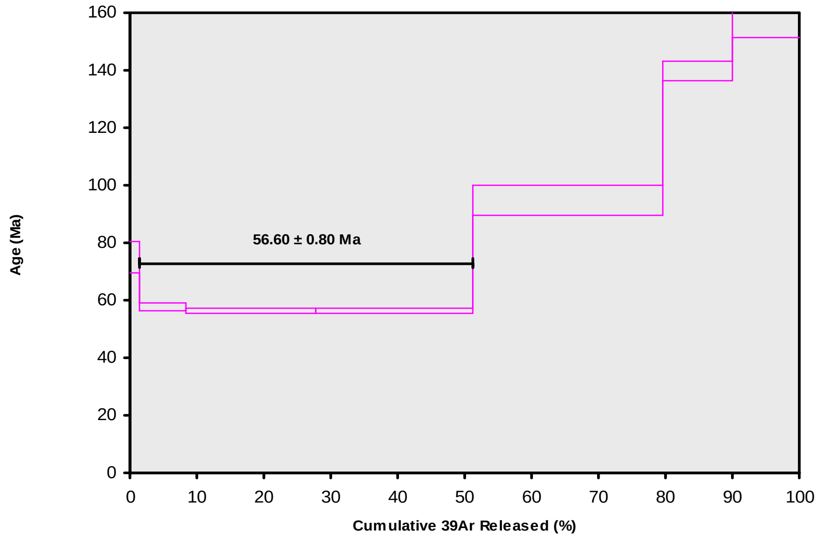

Ar-Ages in Ma

Weighted Plateau
56.60 ± 0.80
Total Fusion
86.77 ± 1.75
Normal Isochron
55.54 ± 1.51
Inverse Isochron
55.55 ± 1.50

MSWD
1.56

Sample Info

plagioclase
DANA-04
jh
OSU4A05
0.0017 (J)

05C3460.AGE >>> 22D-16 >>> Larsen

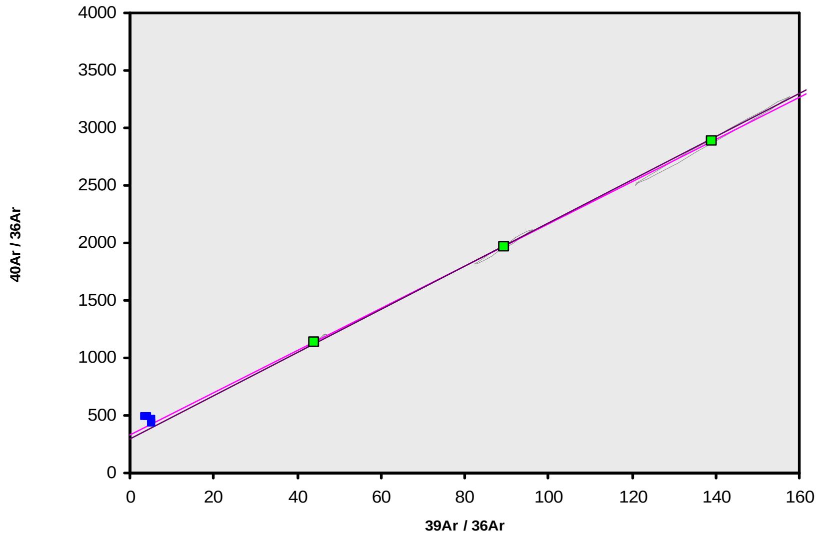

Ar-Ages in Ma

Weighted Plateau
56.60 ± 0.80
Total Fusion
86.77 ± 1.75
Normal Isochron
55.54 ± 1.51
Inverse Isochron
55.55 ± 1.50

MSWD
0.10

Sample Info

plagioclase
DANA-04
jh
OSU4A05
0.0017 (J)

05C3460.AGE >>> 22D-16 >>> Larsen

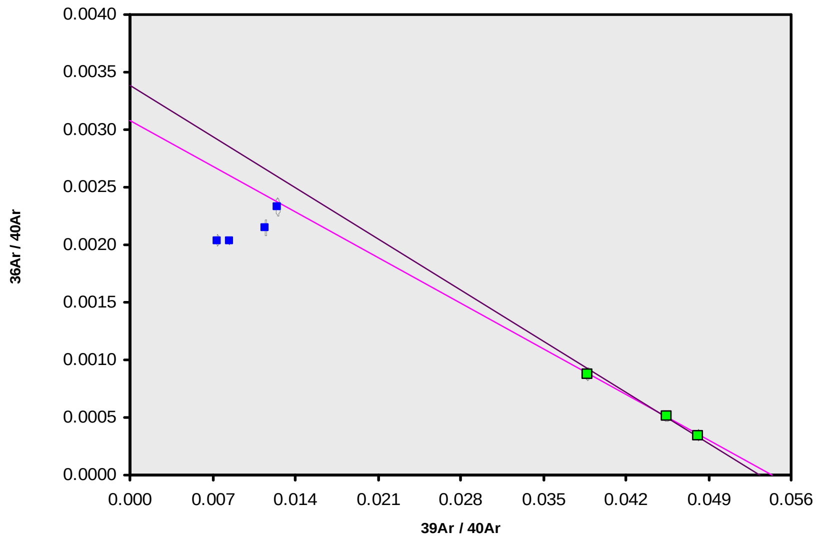

Ar-Ages in Ma

Weighted Plateau
56.60 ± 0.80
Total Fusion
86.77 ± 1.75
Normal Isochron
55.54 ± 1.51
Inverse Isochron
55.55 ± 1.50

MSWD
0.10

Sample Info

plagioclase
DANA-04
jh
OSU4A05
0.0017 (J)

Sample AT 484D-10: Type 1, Main basalt, Canyon A

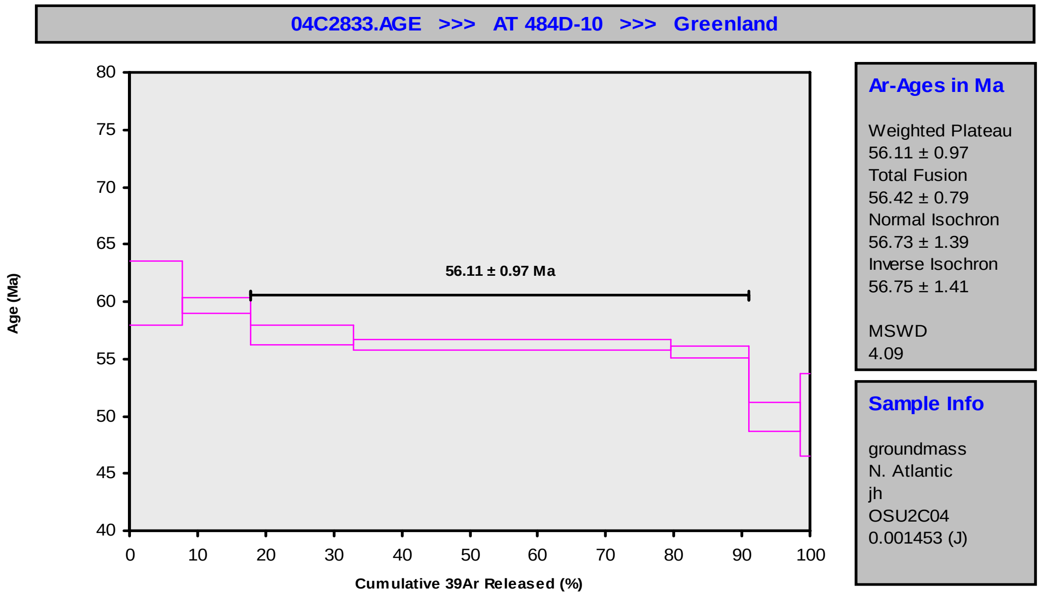

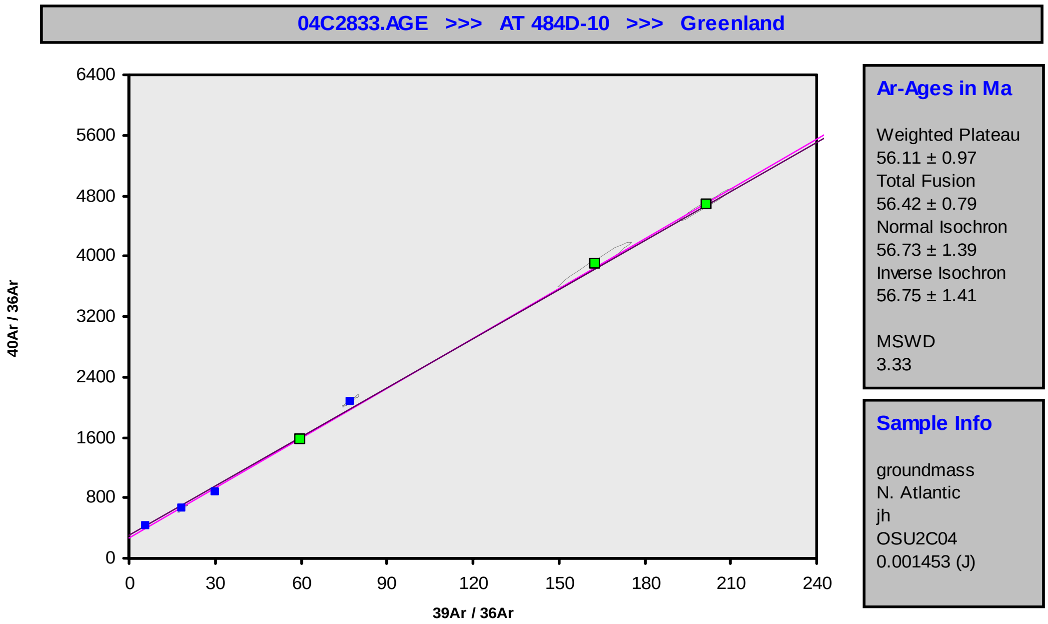

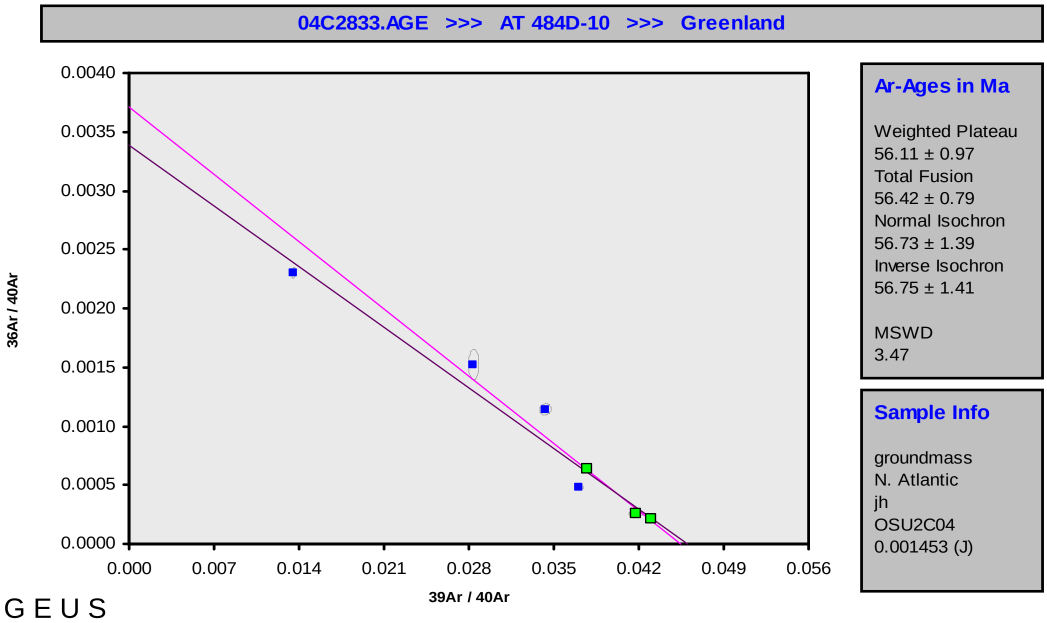

Sample Dana-04-20D-25: Type 6, Rhyolite, Canyon A

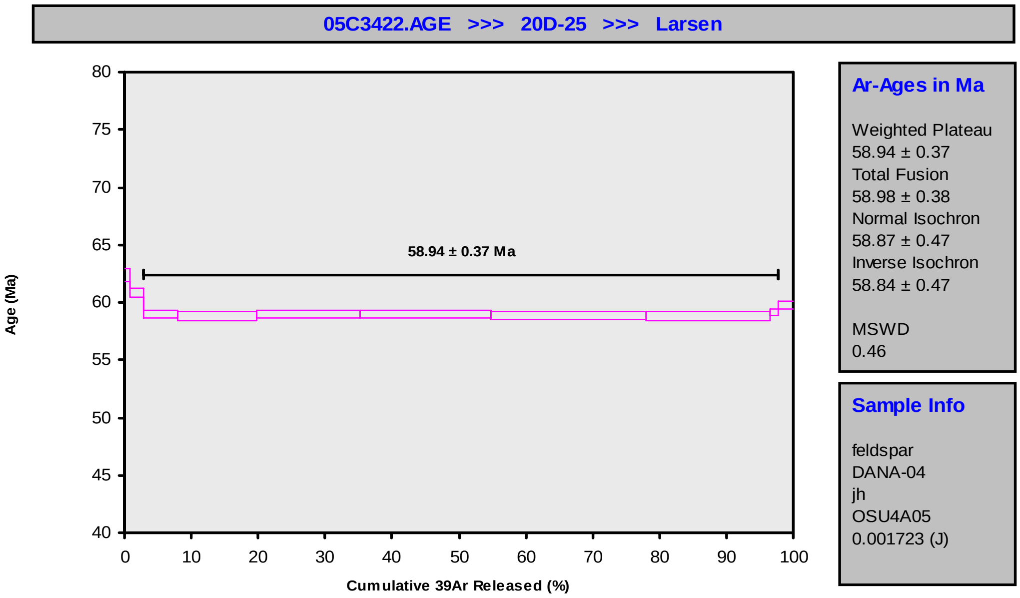

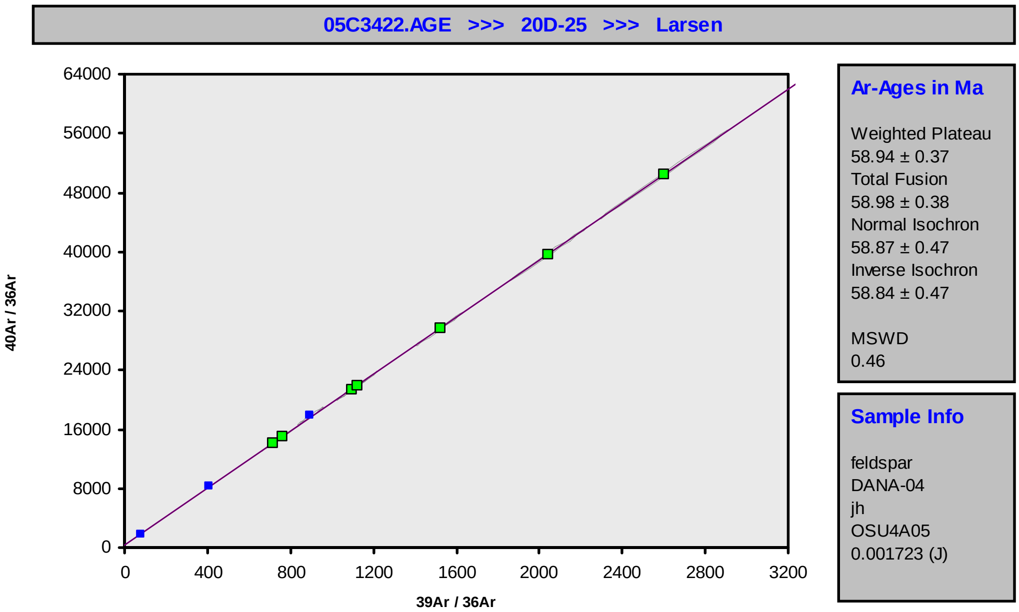

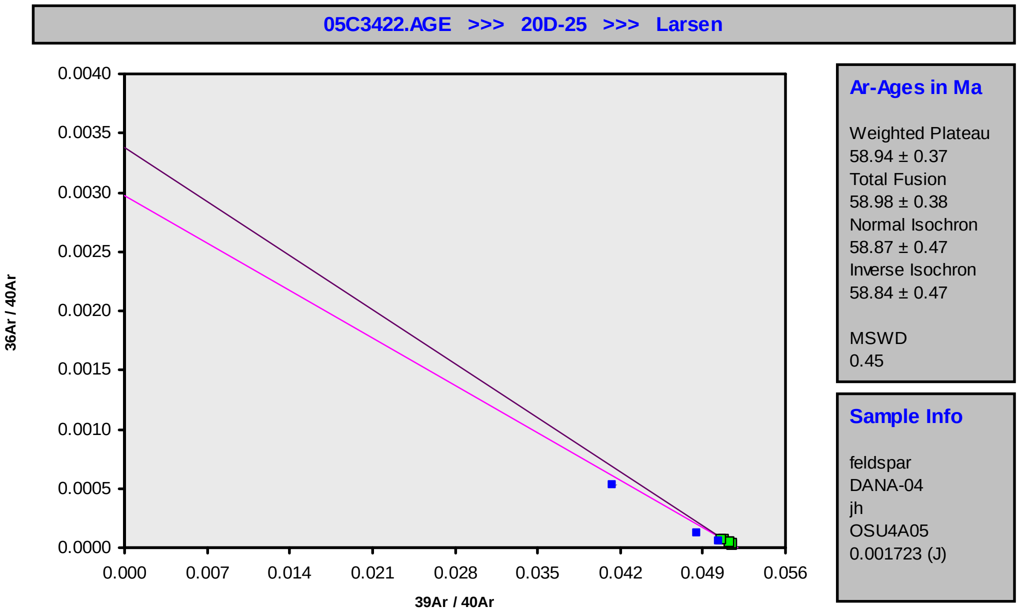

Sample AT 465D-39: Type 9, Depleted high-Si, Davis Strait High

04C2182.AGE >>> AT 465D-39 >>> Greenland

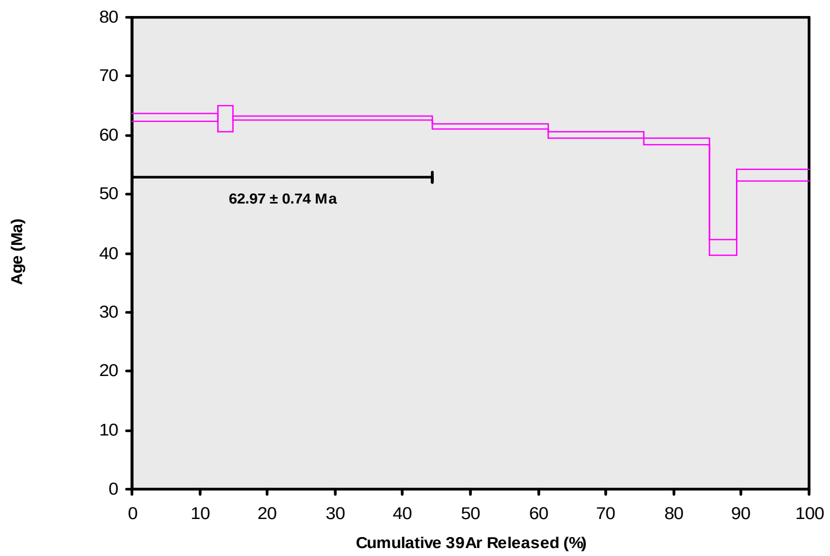

Ar-Ages in Ma

Weighted Plateau
62.97 ± 0.74
Total Fusion
59.96 ± 0.68
Normal Isochron
62.88 ± 0.85
Inverse Isochron
62.88 ± 0.85

MSWD
0.10

Sample Info

plagioclase
N. Atlantic
jh
OSU2F04
0.001496 (J)

04C2182.AGE >>> AT 465D-39 >>> Greenland

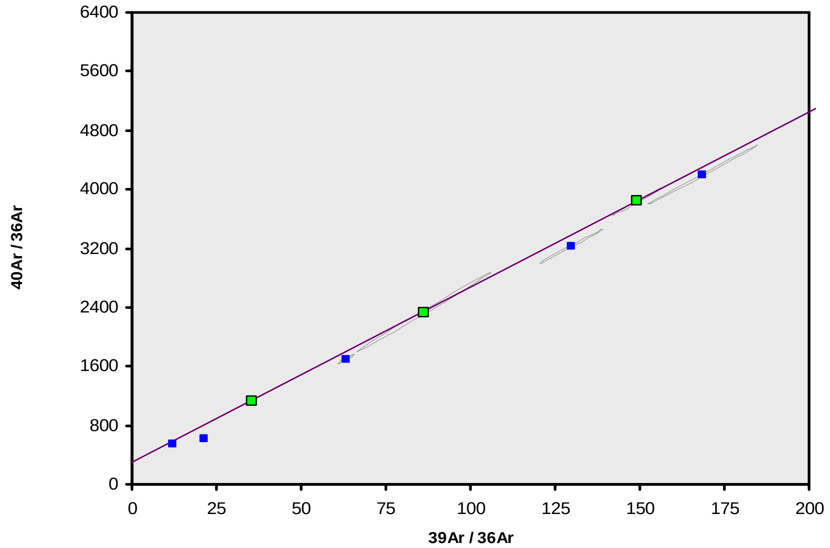

Ar-Ages in Ma

Weighted Plateau
62.97 ± 0.74
Total Fusion
59.96 ± 0.68
Normal Isochron
62.88 ± 0.85
Inverse Isochron
62.88 ± 0.85

MSWD
0.03

Sample Info

plagioclase
N. Atlantic
jh
OSU2F04
0.001496 (J)

04C2182.AGE >>> AT 465D-39 >>> Greenland

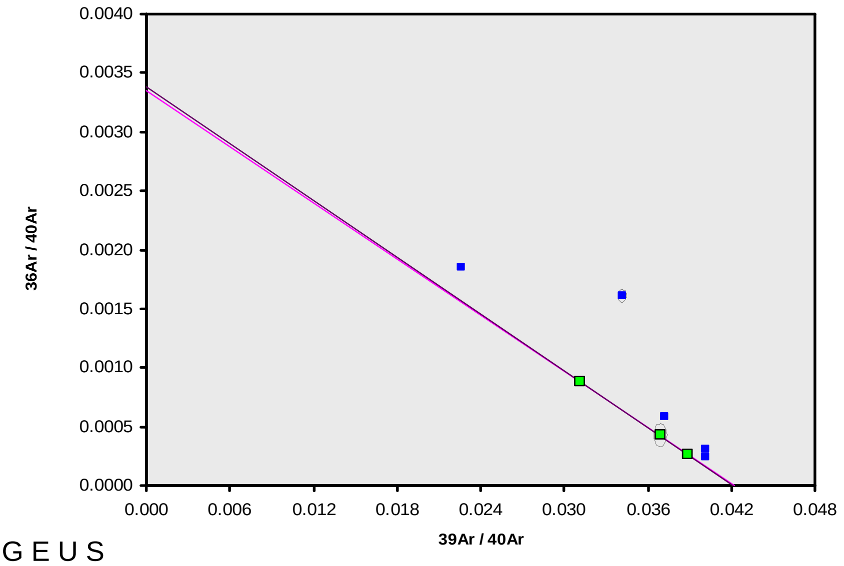

Ar-Ages in Ma

Weighted Plateau
62.97 ± 0.74
Total Fusion
59.96 ± 0.68
Normal Isochron
62.88 ± 0.85
Inverse Isochron
62.88 ± 0.85

MSWD
0.03

Sample Info

plagioclase
N. Atlantic
jh
OSU2F04
0.001496 (J)

Sample Dana-04-38D-02: Type 4, Flat-patterned basalt, Seamount H

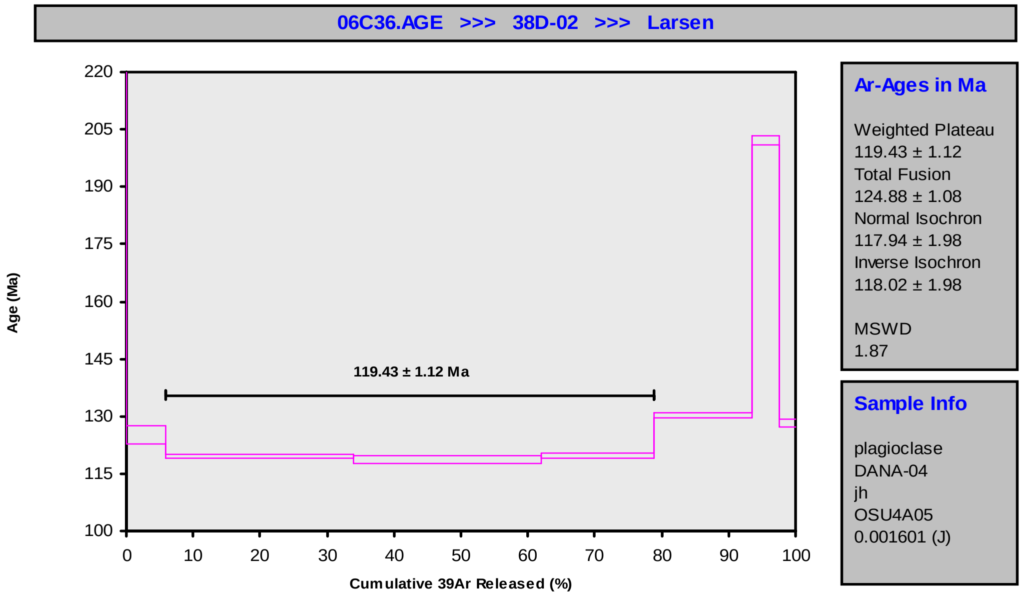

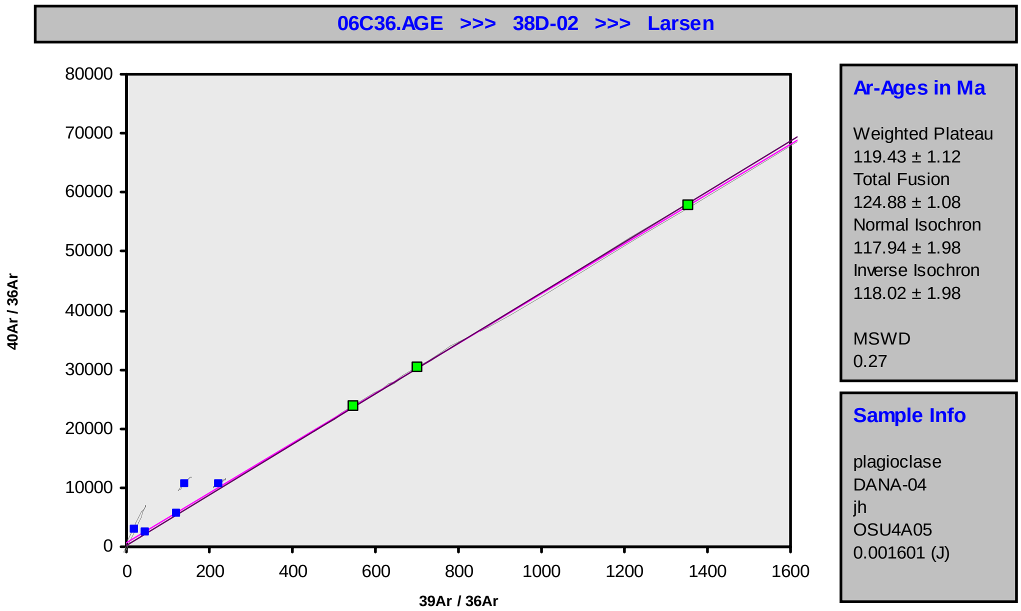

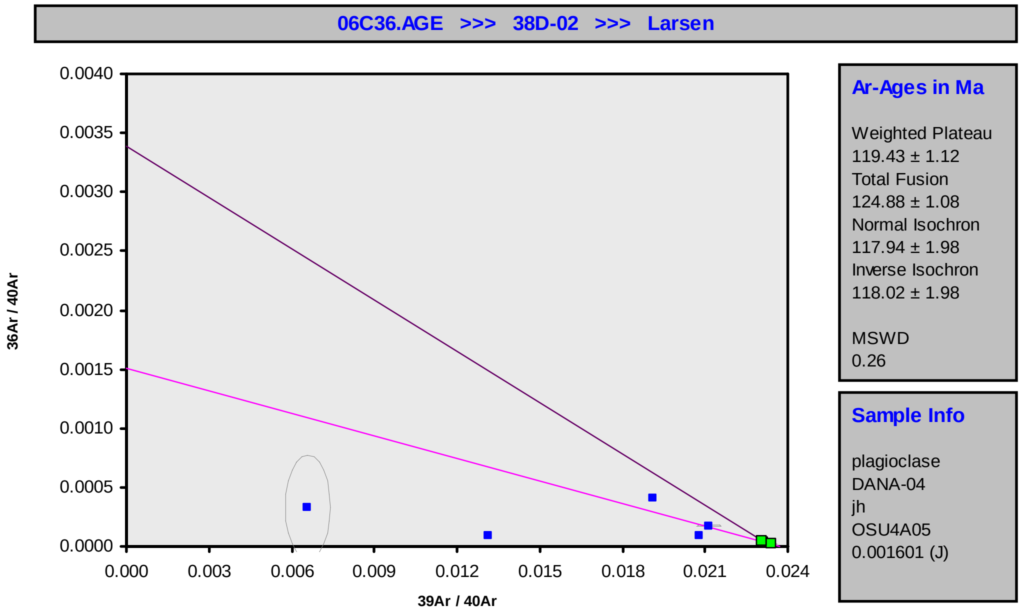

Sample Dana-04-37D-12: Type 10, Enriched basalt, Canyon A

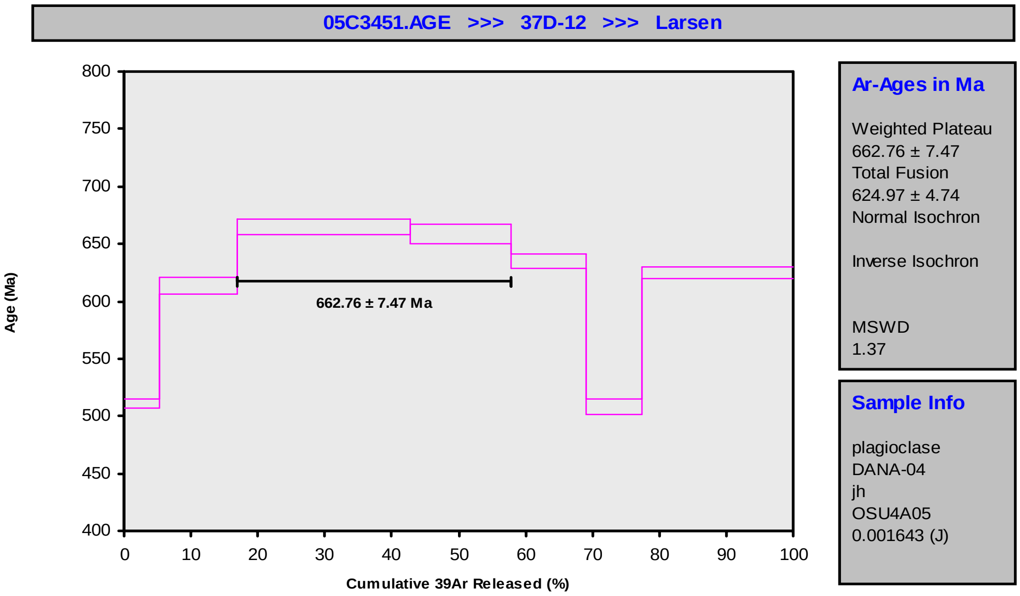

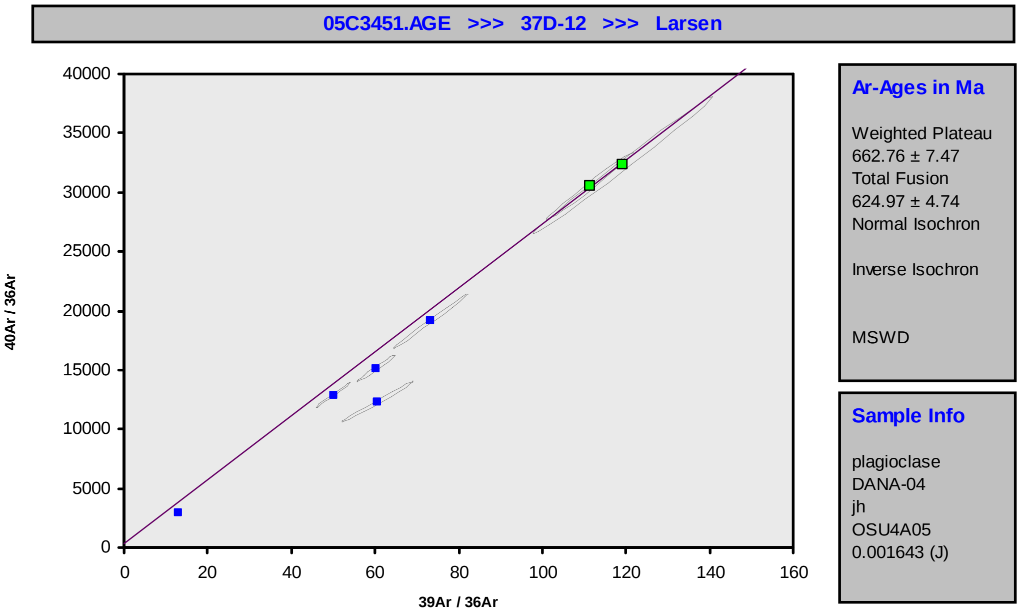

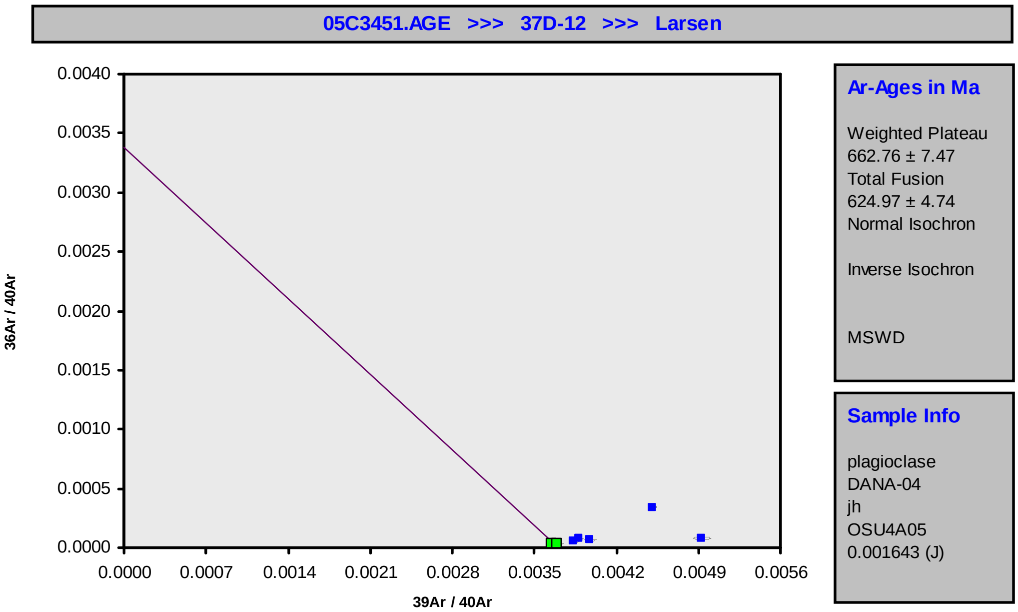

Sample Dana-04-38D-04: Type 5, Contaminated basalt, Seamount H

06C44.AGE >>> 38D-04 >>> Larsen

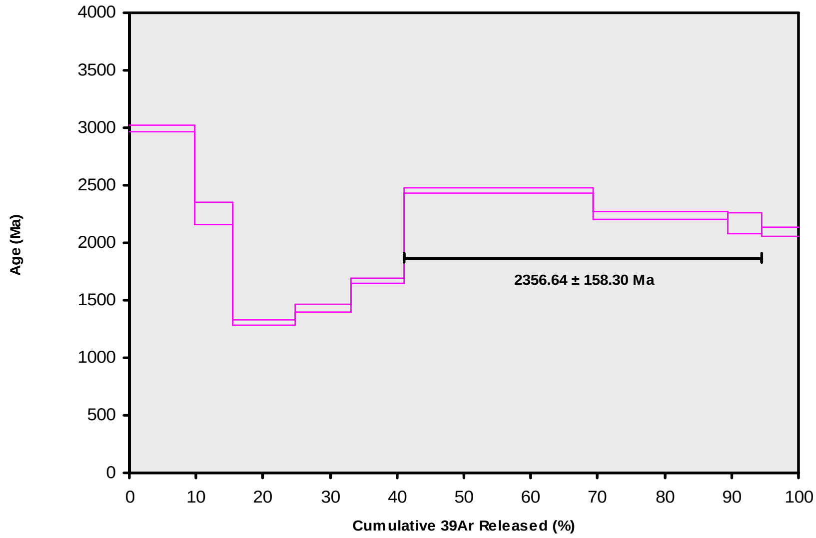

Ar-Ages in Ma

Weighted Plateau
2356.64 ± 158.30
Total Fusion
2226.77 ± 18.45
Normal Isochron
1542.58 ± 243.78
Inverse Isochron
1542.95 ± 243.14

MSWD
57.84

Sample Info

plagioclase
DANA-04
jh
OSU4A05
0.001579 (J)

06C44.AGE >>> 38D-04 >>> Larsen

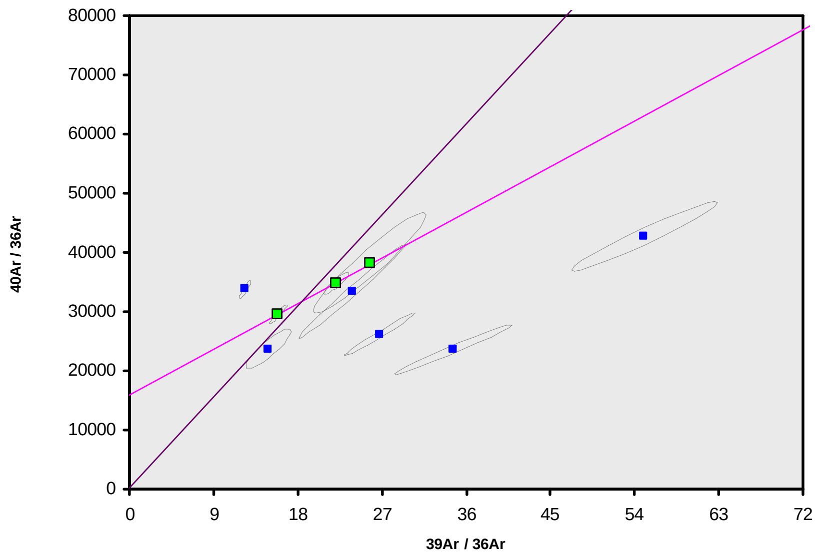

Ar-Ages in Ma

Weighted Plateau
2356.64 ± 158.30
Total Fusion
2226.77 ± 18.45
Normal Isochron
1542.58 ± 243.78
Inverse Isochron
1542.95 ± 243.14

MSWD
0.03

Sample Info

plagioclase
DANA-04
jh
OSU4A05
0.001579 (J)

06C44.AGE >>> 38D-04 >>> Larsen

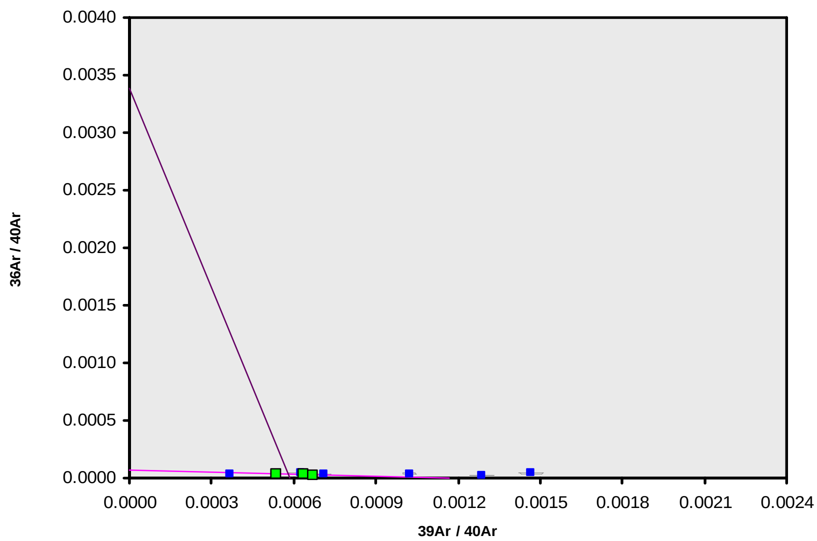

Ar-Ages in Ma

Weighted Plateau
2356.64 ± 158.30
Total Fusion
2226.77 ± 18.45
Normal Isochron
1542.58 ± 243.78
Inverse Isochron
1542.95 ± 243.14

MSWD
0.03

Sample Info

plagioclase
DANA-04
jh
OSU4A05
0.001579 (J)

Appendix 2

Analyses of dredged samples 2003–2004

Appendix 2. Analysed samples dredged 2003-2004 Major elements in wt% oxides. Analyses by XRF (X-ray fluorescence spectrometry) on fused glass discs at GEUS Rock Geochemical Laboratory.

Sample_ID	Feature	Comment	Group	SiO2	TiO2	Al2O3	Fe2O3	FeO	MnO	MgO	CaO	Na2O	K2O	P2O5	Volat	Sum	FeO*	Mg#
AT452D-04A	Seamount E	plag-phyric dolerite	12	46.92	0.91	15.52	12.95	0.00	0.18	7.28	10.21	2.27	0.558	0.107	2.53	99.43	11.66	55.81
AT452D-06A	Seamount E	pl+ol phyric	10	45.44	4.79	12.96	5.75	9.62	0.21	5.57	9.05	2.95	1.175	0.611	1.37	99.50	14.79	43.21
AT452D-08	Seamount E	plag phyric	1	48.04	2.12	13.13	5.27	7.02	0.20	7.57	9.53	3.60	0.193	0.202	2.38	99.21	11.76	56.55
AT452D-09	Seamount E	plag phyric	7	48.68	1.27	14.02	5.01	7.55	0.20	7.23	11.53	2.61	0.086	0.119	0.93	99.22	12.06	54.80
AT452D-25	Seamount E	pl+ol microphyric	1	48.15	2.31	13.69	5.01	7.98	0.20	6.72	11.26	2.68	0.270	0.238	0.88	99.37	12.49	52.13
AT452D-29	Seamount E	pl+ol microphyric	1	47.88	3.25	13.33	4.70	9.29	0.19	5.94	10.57	2.84	0.486	0.355	0.78	99.62	13.52	47.07
AT452D-30	Seamount E	ol+pl-microphyric	1	48.14	2.78	13.75	3.70	9.24	0.18	6.91	10.77	2.65	0.351	0.271	0.58	99.31	12.56	52.66
AT452D-33	Seamount E	cp+pl+ol microphyric	2	48.44	2.07	14.04	4.66	8.18	0.19	6.12	11.17	2.85	0.413	0.228	1.06	99.42	12.37	50.01
AT452D-51	Seamount E	plag phyric	5	54.84	1.70	15.82	2.98	5.44	0.12	3.74	7.58	3.76	1.147	0.343	1.98	99.44	8.13	48.20
AT452D-56	Seamount E	ol+pl microphyric	2	48.38	3.03	13.81	7.57	6.41	0.21	4.81	9.77	3.36	0.821	0.449	0.74	99.35	13.22	42.41
AT452D-57	Seamount E	pl+ol microphyric	3	47.79	2.04	14.19	3.42	8.73	0.19	6.71	12.11	2.27	0.490	0.228	1.57	99.75	11.80	53.49
AT452D-70	Seamount E	pl+ol+cp microphyric	2	47.65	2.35	14.58	6.68	5.94	0.20	6.37	10.72	3.19	0.482	0.312	1.01	99.48	11.95	51.89
AT452D-72	Seamount E	plag phyric	12	49.71	1.53	13.98	4.09	11.91	0.23	4.33	8.74	2.84	0.475	0.164	1.31	99.30	15.59	35.95
AT453D-13	Seamount B	olivine phyric	3	45.70	2.10	10.50	3.27	7.48	0.15	14.18	9.89	1.70	0.068	0.200	3.79	98.99	10.42	73.35
AT453D-20	Seamount B	plag phyric	4	47.28	2.97	13.08	5.60	8.75	0.22	6.12	10.46	2.83	0.218	0.336	0.83	98.67	13.79	47.32
AT453D-27	Seamount B	plag phyric	1	47.40	2.84	13.77	4.77	8.61	0.20	5.45	10.28	2.96	0.441	0.343	0.90	97.93	12.90	46.06
AT453D-28	Seamount B	hyaloclastite	3	45.20	3.16	11.76	9.26	5.43	0.18	6.12	5.46	3.44	0.899	0.355	7.37	98.60	13.76	47.35
AT453D-32	Seamount B	gabbro	12	44.59	3.06	17.23	3.23	8.51	0.15	4.17	7.25	4.12	1.813	1.461	3.36	98.90	11.42	42.48
AT453D-33	Seamount B	dolerite	12	48.28	2.51	12.88	3.61	13.00	0.23	5.11	9.54	2.47	0.286	0.160	1.08	99.12	16.25	38.86
AT453D-40	Seamount B	plag-rich	3	47.77	1.60	18.21	2.23	6.98	0.13	5.39	12.22	2.81	0.506	0.189	1.47	99.47	8.98	54.83
AT453D-41	Seamount B	fine grained fresh	10	50.02	3.57	13.93	2.84	9.61	0.20	3.95	8.17	4.18	1.092	0.694	0.68	98.92	12.17	39.66
AT453D-42	Seamount B	medium grained	12	44.31	1.94	12.46	3.23	6.47	0.22	4.81	11.35	2.39	0.231	0.158	11.43	98.97	9.37	50.93
AT454D-05	Seamount B	vesicular lava	11	36.02	3.97	17.90	13.72	1.07	0.35	2.98	5.96	2.20	2.791	2.648	9.37	98.96	13.41	31.03
AT454D-14	Seamount B	agglomerate	3	44.42	2.39	12.97	9.23	3.29	0.16	8.12	7.61	4.33	1.263	0.229	5.21	99.19	11.59	58.60
AT454D-16	Seamount B	aphyric	1	44.96	3.19	13.61	5.23	9.64	0.22	6.78	9.83	2.54	0.247	0.336	2.36	98.92	14.34	48.88
AT454D-20	Seamount B	vesicular lava	11	33.01	3.75	17.91	9.08	2.43	0.12	4.27	12.29	1.44	1.491	1.485	11.67	98.91	10.60	44.89
AT465D-36	Davis Strait High	coarse	8	45.26	1.54	15.92	3.92	7.48	0.15	9.37	8.92	2.65	0.068	0.166	3.73	99.14	11.01	63.27
AT465D-39	Davis Strait High	plag-rich	9	53.21	0.79	16.58	2.31	5.89	0.15	6.56	9.85	1.99	0.931	0.093	0.96	99.27	7.96	62.48
AT465D-69	Davis Strait High	vesicular lava	9	50.16	0.82	14.75	1.54	7.24	0.16	7.57	10.25	2.88	0.609	0.096	3.02	99.05	8.62	63.97
AT466D-02	Davis Strait High	oxidised olivines	9	50.51	0.85	16.17	3.78	5.54	0.11	8.18	10.34	2.65	0.277	0.099	1.00	99.47	8.94	64.92
AT466D-23	Davis Strait High	plag microphyric	7	48.75	0.74	13.95	4.08	7.87	0.19	8.30	12.46	2.06	0.047	0.060	0.94	99.42	11.54	59.25
AT466D-32	Davis Strait High	olivine phyric	8	48.78	1.29	13.32	4.55	9.08	0.20	7.23	10.79	2.69	0.056	0.096	0.91	98.98	13.18	52.61
AT466D-41	Davis Strait High	with flowage lines	8	48.05	1.15	15.04	4.28	7.19	0.17	7.43	11.76	2.55	0.073	0.097	1.54	99.31	11.04	57.65
AT484D-05	Canyon A	vesicular lava	4	47.02	1.80	14.31	5.08	5.43	0.19	4.34	11.90	2.95	0.392	0.314	5.08	98.79	10.00	46.76
AT484D-07	Canyon A	vesicular lava	3	48.82	4.14	11.20	4.76	9.24	0.21	5.53	7.80	2.91	0.558	0.500	3.03	98.67	13.52	45.28
AT484D-10	Canyon A	fresh olivine	1	47.60	2.57	13.94	5.02	8.68	0.16	5.60	11.06	2.82	0.344	0.252	1.13	99.15	13.20	46.17
AT485D-08	Canyon A	vesicular lava	1	47.18	2.72	13.60	7.23	6.37	0.20	6.92	10.96	2.69	0.264	0.262	0.79	99.16	12.88	52.10
AT485D-09	Canyon A	large	1	46.99	3.18	13.43	5.96	7.93	0.17	5.84	10.62	2.87	0.147	0.335	1.64	99.08	13.29	47.05
AT485D-23	Canyon A	aphyric	1	47.50	2.49	13.60	5.82	7.65	0.19	6.84	10.98	2.73	0.191	0.248	0.77	98.99	12.89	51.78
AT486D-06	Canyon A	plag phyric	3	47.44	2.09	16.07	5.37	5.94	0.16	5.70	10.21	3.03	0.316	0.207	2.90	99.39	10.77	51.69
AT486D-11	Canyon A	plag phyric	4	47.47	2.00	13.65	3.49	8.94	0.18	5.98	11.18	2.59	0.140	0.202	3.53	99.33	12.08	50.03
AT487D-05	Canyon A	finegrained	1	47.73	2.45	13.66	5.27	7.88	0.20	6.60	11.09	2.70	0.240	0.245	0.90	98.93	12.62	51.41
AT487D-13	Canyon A	aphyric	1	47.36	3.36	13.81	5.15	8.61	0.20	5.82	10.89	2.86	0.149	0.355	1.04	99.57	13.24	47.05
Dana-04-04D-85	Davis Strait High	vesicular lava	9	50.67	0.84	15.59	3.66	5.88	0.14	7.67	8.74	3.12	0.526	0.124	2.51	99.48	9.17	62.85
Dana-04-04D-94	Davis Strait High	plag-phyric	7	47.44	0.65	16.41	3.19	6.16	0.16	8.98	12.38	1.87	0.108	0.059	1.97	99.39	9.03	66.79
Dana-04-04D-95	Davis Strait High	plag-phyric	8	48.74	1.89	14.79	5.14	7.38	0.20	6.37	11.23	2.75	0.173	0.191	0.75	99.60	12.00	51.76
Dana-04-04D-98	Davis Strait High	vesicular lava	7	47.69	0.64	16.62	4.96	5.08	0.17	7.82	12.22	2.41	0.190	0.064	1.91	99.76	9.54	62.36
Dana-04-04D-99	Davis Strait High	picrite	7	45.57	0.67	12.67	1.91	7.97	0.16	17.00	9.68	1.79	0.128	0.063	1.69	99.30	9.69	78.02

Trace elements in ppm. Analyses by ICP-MS (inductively coupled plasma mass spectrometry) at GEUS Rock Geochemical Laboratory.

Sample_ID	Sc	V	Cr	Co	Ni	Cu	Zn	Ga	Rb	Sr	Y	Zr	Nb	Cs	Ba
AT452D-04A	39.23	206.78	117.31	64.07	147.85	126.30	88.82	16.66	18.50	289.92	14.73	55.09	7.86	0.798	217.20
AT452D-06A	32.56	395.73	127.21	49.79	86.35	387.46	157.63	26.30	18.44	402.91	44.98	360.64	48.89	0.080	282.79
AT452D-08	40.44	350.80	282.65	53.80	124.73	189.75	99.72	17.56	2.19	225.23	27.16	126.54	11.51	0.042	48.75
AT452D-09	57.79	411.26	281.04	60.67	99.97	258.37	97.21	18.24	2.13	77.08	36.03	71.33	2.42	0.174	24.11
AT452D-25	44.97	409.28	189.72	54.53	94.81	169.03	105.61	21.54	2.49	246.88	28.80	135.71	12.08	0.030	70.63
AT452D-29	44.06	432.46	175.07	51.90	91.19	295.73	131.21	23.09	8.68	269.56	39.11	208.55	21.06	0.109	100.50
AT452D-30	43.61	418.28	159.83	54.40	111.33	219.85	118.50	23.19	5.46	261.14	31.80	158.89	13.97	0.023	71.27
AT452D-33	49.27	389.85	110.65	52.95	72.55	179.08	103.65	19.80	7.30	249.13	31.17	119.05	15.37	0.053	90.04
AT452D-51	32.27	205.51	75.03	32.35	44.89	60.86	96.27	22.09	16.36	305.21	40.79	372.76	27.08	0.347	530.03
AT452D-56	45.15	443.20	39.64	49.09	36.31	152.75	129.69	21.29	14.68	353.84	39.47	207.79	36.21	0.044	272.47
AT452D-57	53.26	365.67	118.15	50.81	74.07	159.28	92.90	18.87	14.55	218.44	28.63	103.46	10.70	0.264	84.61
AT452D-70	50.11	395.23	104.39	46.98	74.22	89.64	108.45	20.73	3.95	299.64	34.95	167.23	25.20	0.013	164.57
AT452D-72	44.13	410.91	10.49	55.02	39.40	202.05	121.00	21.49	14.80	155.94	30.94	94.75	6.10	0.258	141.20
AT453D-13	36.09	284.76	1251.67	69.26	755.12	117.44	88.04	16.94	1.10	179.49	24.28	92.18	9.59	0.093	17.27
AT453D-20	43.71	506.73	68.26	91.28	62.68	218.44	128.08	23.14	5.20	257.40	40.94	182.15	10.09	0.076	58.13
AT453D-27	38.58	374.95	74.44	58.39	61.90	262.96	126.77	22.15	4.11	319.99	37.53	190.83	22.03	0.034	180.69
AT453D-28	38.05	405.24	103.02	62.93	71.64	300.32	130.56	20.51	9.43	434.31	39.36	206.17	19.07	0.315	59.11
AT453D-32	21.23	148.86	11.97	36.76	28.31	36.23	105.81	18.08	76.09	1015.84	29.38	135.98	31.27	0.880	1208.12
AT453D-33	48.11	561.19	56.25	60.46	42.38	106.74	138.93	19.95	9.08	131.61	33.74	96.91	9.61	0.162	100.94
AT453D-40	34.53	259.52	89.02	53.65	57.93	104.12	76.57	19.28	8.53	378.11	20.00	98.63	14.35	0.130	112.72
AT453D-41	25.30	236.83	0.28	54.80	4.37	22.15	153.87	26.17	20.29	455.11	51.96	360.19	47.94	0.267	230.10
AT453D-42	48.40	419.96	59.39	42.79	41.64	106.80	51.88	20.03	11.70	189.74	31.42	86.28	9.39	0.180	113.62
AT454D-05	30.42	240.93	259.91	113.59	113.48	102.23	189.97	14.80	54.62	410.43	91.41	388.00	102.90	1.103	442.65
AT454D-14	36.56	304.55	426.41	53.26	197.95	130.42	94.41	15.42	9.98	353.01	28.93	158.38	11.69	0.450	158.34
AT454D-16	43.16	407.79	178.52	54.57	93.00	179.89	128.76	23.21	3.52	245.13	36.93	209.99	21.20	0.064	83.02
AT454D-20	32.43	283.28	80.65	27.80	78.62	68.39	132.70	18.49	25.97	406.55	42.29	383.09	99.10	0.465	339.17
AT465D-36	39.86	284.70	346.39	57.82	216.28	108.80	79.25	17.44	1.55	174.60	30.54	107.16	1.62	0.077	24.29
AT465D-39	36.42	246.96	302.69	38.32	20.65	28.38	75.80	17.56	35.85	138.66	24.67	80.33	5.02	0.399	197.92
AT465D-69	37.13	236.11	259.87	44.30	36.36	56.12	74.56	15.03	15.57	231.99	24.08	87.62	5.53	0.167	123.96
AT466D-02	38.79	252.15	234.17	44.61	57.66	77.04	73.19	17.71	1.70	152.05	22.88	77.89	3.23	0.015	155.20
AT466D-23	45.79	293.91	148.14	58.28	92.47	220.66	78.60	14.88	1.73	56.55	23.17	35.22	1.59	0.019	18.14
AT466D-32	45.57	422.39	149.01	54.63	115.83	267.17	98.59	18.08	0.81	72.48	38.99	74.57	1.89	0.027	32.93
AT466D-41	42.68	312.05	253.25	51.70	77.58	100.34	75.70	16.66	1.24	124.12	27.54	64.66	1.10	0.020	19.41
AT484D-05	42.77	379.99	83.58	49.97	45.53	81.56	126.04	20.44	4.09	241.95	42.66	122.69	5.44	0.137	196.33
AT484D-07	33.34	447.36	111.41	63.07	76.83	406.89	146.89	23.08	7.97	146.69	55.63	329.02	23.49	0.036	135.36
AT484D-10	38.96	398.54	115.47	61.73	90.93	258.10	122.51	24.11	6.10	229.22	34.40	158.60	14.31	0.062	68.49
AT485D-08	34.73	368.38	211.75	51.90	113.29	222.53	117.61	23.84	3.89	251.12	32.96	177.85	17.03	0.134	64.59
AT485D-09	34.91	404.12	136.60	54.16	69.05	251.94	134.48	23.33	1.15	272.71	41.53	214.06	19.51	0.012	59.46
AT485D-23	36.10	374.41	180.34	54.37	89.12	232.66	110.11	21.67	1.31	233.40	32.13	155.68	13.08	0.005	72.55
AT486D-06	27.65	283.93	60.34	45.10	77.15	170.68	93.53	22.41	5.44	251.41	26.15	142.15	10.91	0.126	42.54
AT486D-11	41.65	362.94	164.78	49.47	77.14	203.17	116.00	19.58	1.98	160.23	38.30	133.73	7.86	0.302	50.81
AT487D-05	37.12	384.06	122.70	53.68	86.75	199.38	110.27	21.84	2.66	247.60	31.53	158.62	13.74	0.110	71.76
AT487D-13	33.97	390.28	165.53	55.34	99.72	303.73	131.64	24.03	1.38	298.93	39.13	232.90	24.59	0.092	83.04
Dana-04-04D-85	38.23	231.69	195.98	36.96	40.21	67.27	75.84	17.31	4.26	259.76	25.28	105.00	4.33	0.046	117.72
Dana-04-04D-94	41.13	236.24	259.70	50.88	111.97	122.30	59.36	13.84	1.47	60.74	19.32	27.85	0.72	0.023	20.53
Dana-04-04D-95	40.34	372.85	155.60	49.76	71.61	210.98	100.90	20.42	1.01	187.54	34.92	117.66	6.31	0.009	58.87
Dana-04-04D-98	43.82	254.85	265.89	49.53	89.81	135.32	63.02	14.52	2.55	78.46	22.51	30.67	0.53	0.260	10.23
Dana-04-04D-99	37.61	226.67	1100.75	73.46	612.45	77.58	61.87	11.80	1.18	120.71	19.25	32.66	0.54	0.021	4.98

Trace elements in ppm. Analyses by ICP-MS (inductively coupled plasma mass spectrometry) at GEUS Rock Geochemical Laboratory.

Sample_ID	La	Ce	Pr	Nd	Sm	Eu	Gd	Tb	Dy	Ho	Er	Tm	Yb	Lu	Hf	Ta	Pb	Th	U
AT452D-04A	9.54	20.68	2.77	11.73	2.51	0.98	2.68	0.427	2.57	0.526	1.46	0.230	1.46	0.227	1.31	0.616	4.852	0.801	0.168
AT452D-06A	36.48	87.91	12.17	51.84	11.38	3.55	11.36	1.667	8.92	1.594	4.11	0.589	3.47	0.521	8.87	3.324	2.518	3.117	0.994
AT452D-08	9.70	24.05	3.72	17.19	4.80	1.59	4.82	0.852	4.88	0.985	2.55	0.384	2.29	0.329	3.21	1.167	0.837	0.710	0.309
AT452D-09	2.50	6.76	1.26	7.02	2.84	1.04	3.83	0.819	5.39	1.276	3.45	0.573	3.53	0.552	2.03	1.106	0.423	0.243	0.126
AT452D-25	10.40	26.34	4.01	18.63	5.04	1.80	5.48	0.933	5.30	1.049	2.72	0.401	2.41	0.355	3.74	1.058	1.094	0.832	0.244
AT452D-29	17.73	44.20	6.73	29.84	7.43	2.45	7.97	1.263	7.26	1.373	3.62	0.519	3.26	0.489	5.58	1.628	1.653	1.468	0.442
AT452D-30	11.83	30.63	4.60	21.36	5.77	2.06	6.32	1.052	6.06	1.146	2.93	0.429	2.58	0.383	4.30	1.123	1.100	0.883	0.277
AT452D-33	12.47	29.03	4.15	18.51	4.75	1.69	5.40	0.915	5.53	1.085	2.95	0.442	2.77	0.424	3.32	1.450	0.931	0.978	0.273
AT452D-51	35.01	70.91	9.46	37.48	7.89	2.36	8.25	1.268	7.01	1.404	3.82	0.578	3.55	0.538	8.81	2.002	4.794	3.641	0.915
AT452D-56	27.77	60.48	7.84	32.88	7.35	2.41	8.00	1.221	7.07	1.375	3.57	0.535	3.40	0.513	5.20	2.650	2.205	2.312	0.611
AT452D-57	8.72	22.24	3.32	15.86	4.38	1.60	4.92	0.861	4.95	0.978	2.61	0.385	2.47	0.354	2.90	1.160	0.998	0.691	0.204
AT452D-70	20.82	46.25	6.25	26.28	6.15	2.07	6.74	1.090	6.33	1.259	3.28	0.488	2.94	0.449	4.48	1.863	2.121	1.937	0.414
AT452D-72	9.20	21.55	3.08	13.92	3.78	1.34	4.51	0.840	5.14	1.079	3.01	0.448	2.95	0.446	2.68	0.947	2.944	1.638	0.396
AT453D-13	7.97	21.83	3.60	17.52	4.95	1.69	4.88	0.847	4.61	0.887	2.12	0.293	1.69	0.245	2.59	1.081	0.664	0.410	0.118
AT453D-20	10.11	27.72	4.66	23.28	6.87	2.28	7.20	1.261	7.38	1.473	3.81	0.569	3.26	0.497	4.65	2.408	1.481	0.799	0.231
AT453D-27	19.00	44.01	6.60	29.06	7.34	2.26	7.27	1.193	6.76	1.394	3.60	0.521	3.16	0.471	4.73	2.182	2.145	1.388	0.445
AT453D-28	14.63	37.44	6.01	28.27	7.44	2.28	7.41	1.239	7.12	1.420	3.65	0.543	3.24	0.502	5.16	1.520	1.396	1.187	0.424
AT453D-32	34.25	74.97	10.89	45.41	8.84	3.04	8.00	1.087	5.62	1.048	2.67	0.375	2.24	0.343	3.21	2.280	4.944	1.739	0.747
AT453D-33	9.65	23.16	3.69	16.77	4.52	1.42	4.95	0.901	5.55	1.190	3.18	0.512	3.22	0.488	2.65	1.210	1.533	1.112	0.311
AT453D-40	11.08	24.56	3.65	16.30	4.01	1.38	4.03	0.636	3.70	0.719	1.90	0.266	1.65	0.241	2.52	2.149	1.001	0.948	0.280
AT453D-41	33.70	77.02	11.89	50.87	12.02	3.68	11.76	1.819	9.77	1.906	4.81	0.689	3.92	0.567	8.09	4.346	2.383	3.046	1.036
AT453D-42	14.20	30.25	4.65	20.59	5.35	1.79	5.32	0.915	5.39	1.148	3.07	0.491	3.06	0.470	2.32	2.659	3.514	1.067	0.314
AT454D-05	114.72	129.34	23.31	91.26	17.23	4.97	17.23	2.387	12.46	2.415	6.07	0.814	4.53	0.673	8.51	6.346	5.349	8.302	3.244
AT454D-14	10.08	26.85	4.59	21.84	5.93	1.95	6.05	0.978	5.52	1.080	2.66	0.393	2.23	0.332	4.00	0.798	0.910	0.773	0.320
AT454D-16	15.61	40.78	6.64	30.06	7.58	2.38	7.44	1.241	6.89	1.353	3.46	0.503	3.05	0.444	5.26	1.649	1.339	1.389	0.209
AT454D-20	66.68	122.56	15.96	62.40	12.52	3.80	11.65	1.604	8.07	1.429	3.42	0.449	2.50	0.356	7.94	5.937	4.729	7.610	2.362
AT465D-36	2.89	9.19	1.94	10.98	3.95	1.44	4.44	0.820	4.94	1.069	2.84	0.437	2.62	0.396	2.75	0.212	0.471	0.133	0.043
AT465D-39	10.22	21.18	2.79	11.37	2.82	0.88	3.06	0.581	3.79	0.825	2.39	0.376	2.46	0.373	2.13	0.535	4.821	2.687	0.676
AT465D-69	11.50	23.57	3.12	12.54	2.76	0.86	3.01	0.567	3.83	0.833	2.37	0.367	2.38	0.362	2.28	0.563	3.334	2.050	0.490
AT466D-02	9.23	19.61	2.63	10.86	2.67	0.93	2.90	0.572	3.65	0.795	2.27	0.354	2.31	0.337	2.00	0.886	2.393	1.355	0.185
AT466D-23	1.52	4.07	0.72	4.01	1.56	0.64	2.18	0.468	3.34	0.792	2.31	0.364	2.38	0.385	1.04	0.300	0.225	0.199	0.052
AT466D-32	3.18	8.18	1.43	7.64	2.89	1.11	3.96	0.862	5.85	1.314	3.82	0.594	3.96	0.622	2.14	0.295	1.361	0.694	0.179
AT466D-41	1.69	5.61	1.14	6.70	2.48	1.01	3.20	0.639	4.20	0.942	2.67	0.410	2.62	0.394	1.75	0.182	0.356	0.121	0.023
AT484D-05	13.03	29.94	4.53	20.70	5.23	1.68	5.77	1.056	6.79	1.439	4.03	0.613	3.85	0.595	3.25	0.554	4.085	1.220	0.655
AT484D-07	20.50	53.86	8.72	41.24	10.57	3.20	10.75	1.796	10.29	1.936	5.14	0.698	4.30	0.618	7.92	2.373	1.916	1.676	0.575
AT484D-10	11.46	29.23	4.58	21.37	5.59	1.85	5.86	1.017	6.07	1.220	3.20	0.459	2.89	0.427	3.97	1.405	1.095	0.985	0.296
AT485D-08	13.45	33.89	5.23	23.81	6.00	1.97	6.11	1.016	5.87	1.145	3.10	0.428	2.58	0.363	4.27	1.197	1.183	1.161	0.280
AT485D-09	15.97	40.40	6.34	29.08	7.55	2.38	7.49	1.304	7.45	1.454	3.81	0.543	3.31	0.475	5.33	1.674	1.522	1.396	0.504
AT485D-23	11.16	27.67	4.42	20.66	5.51	1.78	5.64	0.962	5.66	1.141	2.96	0.420	2.63	0.383	3.85	0.994	1.246	1.005	0.281
AT486D-06	9.43	23.98	3.94	18.28	4.61	1.65	4.74	0.820	4.73	0.920	2.50	0.350	2.11	0.326	3.44	0.840	1.035	0.792	0.256
AT486D-11	7.31	19.33	3.20	15.90	4.72	1.57	5.38	0.997	6.27	1.304	3.62	0.541	3.50	0.531	3.44	0.675	1.034	0.760	0.224
AT487D-05	11.38	28.36	4.49	20.69	5.37	1.87	5.54	0.979	5.61	1.120	2.93	0.413	2.59	0.388	3.92	1.687	1.224	0.985	0.284
AT487D-13	18.45	45.43	7.11	32.04	7.85	2.42	7.69	1.280	7.27	1.370	3.55	0.495	3.11	0.443	5.52	1.700	1.044	1.642	0.534
Dana-04-04D-85	15.65	31.45	3.71	14.48	3.02	0.94	3.48	0.601	3.80	0.868	2.34	0.386	2.39	0.383	2.60	0.364	3.143	2.417	0.297
Dana-04-04D-94	0.82	2.41	0.45	2.80	1.20	0.53	1.85	0.394	2.75	0.645	1.84	0.301	1.91	0.294	0.83	0.456	0.181	0.080	0.019
Dana-04-04D-95	7.51	18.08	2.69	13.40	4.24	1.51	5.00	0.896	5.47	1.217	3.22	0.489	3.07	0.464	2.96	0.498	1.067	0.641	0.213
Dana-04-04D-98	0.81	2.38	0.46	2.95	1.37	0.60	2.06	0.455	3.18	0.762	2.18	0.343	2.24	0.353	0.93	0.276	0.178	0.072	0.052
Dana-04-04D-99	0.76	2.60	0.51	3.17	1.39	0.58	1.93	0.407	2.80	0.671	1.86	0.299	1.89	0.291	0.92	0.237	0.193	0.046	0.017

Sample_ID	Feature	Comment	Group	SiO2	TiO2	Al2O3	Fe2O3	FeO	MnO	MgO	CaO	Na2O	K2O	P2O5	Volat	Sum	FeO*	Mg#
Dana-04-11D-04	Seamount C	plag-phyric	7	50.00	0.81	15.34	2.31	7.84	0.19	7.26	12.87	2.01	0.056	0.084	0.76	99.53	9.92	59.67
Dana-04-11D-10	Seamount C	plag-phyric	3	47.91	2.08	15.02	6.40	6.76	0.19	6.13	10.38	2.68	0.312	0.191	1.18	99.23	12.52	49.76
Dana-04-11D-11	Seamount C	plag-microphyric	2	48.34	2.78	13.53	4.16	9.34	0.21	5.77	10.51	2.83	0.446	0.328	0.97	99.20	13.08	47.12
Dana-04-12Gr-04	Seamount C	aphyric	1	48.28	2.34	13.97	4.67	7.78	0.20	6.49	11.32	2.87	0.350	0.280	0.93	99.48	11.98	52.29
Dana-04-12Gr-05	Seamount C	aphyric	10	48.47	3.67	13.46	4.77	8.51	0.19	5.71	10.15	2.99	0.419	0.387	0.83	99.55	12.80	47.41
Dana-04-12Gr-12	Seamount C	plag-phyric	1	47.64	2.75	13.99	6.27	7.54	0.22	6.26	10.91	2.65	0.275	0.263	0.87	99.64	13.18	48.99
Dana-04-20D-16	Canyon A	plag-phyric	1	48.26	2.76	13.73	4.00	9.22	0.19	6.38	10.76	2.63	0.221	0.273	1.02	99.44	12.82	50.17
Dana-04-20D-17	Canyon A	aphyric	1	47.70	2.71	13.83	4.75	8.21	0.20	6.66	11.10	2.54	0.175	0.257	1.10	99.24	12.48	51.92
Dana-04-20D-20	Canyon A	plag-phyric	3	49.24	3.53	12.52	4.11	11.08	0.25	3.86	8.02	3.12	1.405	0.528	1.57	99.24	14.78	34.55
Dana-04-20D-25	Canyon A	qz-fsp-phyric rhyolite	6	73.21	0.17	13.15	1.72	0.27	0.04	0.00	0.09	3.40	6.941	0.040	0.53	99.56	1.81	0.00
Dana-04-22D-14	Canyon A	med.-grained	4	48.12	0.88	14.50	3.30	6.22	0.15	6.23	11.43	2.43	0.364	0.130	5.88	99.64	9.19	57.83
Dana-04-22D-16	Canyon A	strongly plag-phyric	10	49.80	2.51	16.51	5.50	5.63	0.13	3.88	9.94	3.52	0.426	0.331	1.48	99.65	10.58	42.56
Dana-04-22D-24	Canyon A	altered, aphyric	12	50.62	1.87	14.99	3.61	7.42	0.16	5.28	7.61	4.29	0.979	0.319	2.48	99.61	10.67	50.01
Dana-04-22D-26	Canyon A	pervasively altered	12	51.00	1.10	13.54	3.45	8.39	0.21	6.87	9.87	1.77	0.600	0.086	2.73	99.61	11.50	54.74
Dana-04-23D-12	Canyon A	metasandstone	0	68.45	0.64	13.26	0.81	4.11	0.07	2.90	1.69	2.99	2.622	0.172	1.71	99.42	4.84	54.77
Dana-04-23D-15	Canyon A	picrite	3	43.71	2.38	11.48	4.25	8.93	0.19	13.80	8.60	2.44	0.426	0.363	2.43	98.99	12.75	68.64
Dana-04-23D-16	Canyon A	plag-phyric	10	45.09	5.27	12.78	6.14	9.20	0.20	5.43	9.54	2.91	0.707	0.716	1.08	99.06	14.72	42.70
Dana-04-23D-28	Canyon A	pahoehoe lava	4	44.82	1.13	12.59	3.71	7.17	0.17	14.66	8.14	3.09	0.668	0.125	3.33	99.60	10.51	73.84
Dana-04-23D-29	Canyon A	aphyric	1	48.37	2.95	13.34	2.44	10.71	0.22	5.85	10.70	2.70	0.494	0.382	0.95	99.11	12.91	47.82
Dana-04-25D-03	Canyon A	plag-phyric	1	47.04	2.97	13.63	6.24	7.83	0.24	5.77	10.30	2.95	0.503	0.342	1.59	99.41	13.45	46.44
Dana-04-27D-15	Canyon A	plag-phyric	4	48.85	1.79	14.93	3.10	8.92	0.19	6.56	11.53	2.31	0.140	0.165	0.86	99.35	11.71	53.11
Dana-04-27D-16	Canyon A	plag-phyric	1	47.23	3.37	12.94	2.99	12.48	0.24	5.83	10.29	2.36	0.245	0.333	1.04	99.34	15.17	43.72
Dana-04-28D-09	Canyon A	aphyric	1	47.73	2.64	13.84	4.99	7.96	0.19	6.93	10.87	2.56	0.156	0.251	1.26	99.38	12.45	52.97
Dana-04-28D-11	Canyon A	plag-phyric	3	47.50	2.06	16.29	4.27	6.70	0.17	5.82	11.88	2.56	0.526	0.255	1.38	99.40	10.54	52.74
Dana-04-29D-12	Canyon A	aphyric	4	46.30	1.62	15.30	5.03	5.74	0.15	9.23	11.61	1.96	0.224	0.150	2.39	99.70	10.26	64.53
Dana-04-29D-13	Canyon A	aphyric	1	48.07	2.55	13.85	6.70	6.22	0.23	6.10	10.99	2.88	0.330	0.279	0.96	99.16	12.24	50.20
Dana-04-29D-14	Canyon A	aphyric, altered, PC?	12	48.78	1.55	13.92	2.93	11.12	0.23	6.15	10.83	2.36	0.223	0.117	0.95	99.16	13.76	47.47
Dana-04-29D-15	Canyon A	plag-phyric	1	47.74	3.48	13.20	4.43	9.35	0.19	6.42	9.91	2.67	0.498	0.344	0.85	99.08	13.34	49.34
Dana-04-32D-01	Seamount C	aphyric	1	46.30	2.52	13.68	2.30	10.50	0.21	6.79	9.35	3.17	0.206	0.238	3.94	99.21	12.57	52.20
Dana-04-34D-01	Canyon A	red-oxidised lava top	1	46.67	2.66	13.50	11.89	1.97	0.19	4.88	9.57	4.21	0.243	0.298	3.08	99.15	12.67	43.78
Dana-04-36D-15	Canyon A	carbonate sediment	0	7.07	0.12	2.68	5.49	38.15	0.43	4.72	4.06	0.23	0.311	0.635	34.91	98.79	43.09	18.14
Dana-04-36D-16	Canyon A	plag-phyric	1	47.45	3.16	13.26	5.94	7.97	0.21	5.74	10.62	2.76	0.379	0.410	1.43	99.33	13.31	46.58
Dana-04-36D-17	Canyon A	nearly aphyric	1	48.07	2.89	13.24	5.36	8.24	0.24	6.38	10.23	2.77	0.212	0.295	1.25	99.17	13.06	49.69
Dana-04-36D-18	Canyon A	plag-phyric	1	47.47	3.16	13.12	5.51	8.57	0.22	5.85	10.55	2.74	0.388	0.407	1.27	99.26	13.53	46.67
Dana-04-37D-08	Canyon A	aphyric	1	43.85	3.22	13.82	6.67	10.17	0.23	6.65	8.58	2.04	0.178	0.340	3.53	99.27	16.17	45.40
Dana-04-37D-09	Canyon A	olivine-phyric	2	47.03	2.03	13.53	3.96	7.59	0.22	9.98	10.79	2.36	0.110	0.229	2.10	99.92	11.15	64.41
Dana-04-37D-12	Canyon A	gabbro/dolerite	10	47.87	4.92	13.25	4.53	8.27	0.16	6.23	8.40	2.72	0.606	0.534	1.67	99.17	12.35	50.52
Dana-04-38D-01	Seamount H	greenschist-PC?	12	50.51	1.15	13.76	2.49	10.28	0.21	6.19	10.72	1.99	0.403	0.118	1.51	99.33	12.52	49.98
Dana-04-38D-02	Seamount H	med.-grained	4	49.53	3.53	12.16	4.05	12.57	0.23	4.49	8.68	2.70	0.694	0.373	0.88	99.88	16.21	35.91
Dana-04-38D-03	Seamount H	plag-phyric	3	49.21	2.52	14.03	5.24	7.17	0.19	6.95	10.47	2.73	0.259	0.246	0.79	99.79	11.88	54.20
Dana-04-38D-04	Seamount H	gabbro/dolerite	12	48.12	1.99	16.18	3.11	10.33	0.18	5.68	7.70	3.14	1.657	0.422	0.81	99.32	13.12	46.66
Dana-04-39D-13	Seamount H	aphyric	1	46.91	2.28	14.35	6.77	5.81	0.21	6.71	11.31	2.38	0.213	0.232	2.37	99.55	11.90	53.30
Dana-04-39D-14	Seamount H	plag-microphyric	1	46.81	3.03	13.13	6.04	8.92	0.22	6.18	10.54	2.82	0.177	0.298	1.11	99.28	14.36	46.55
Dana-04-39D-15	Seamount H	weakly plag-phyric	2	46.60	2.63	14.25	4.63	8.56	0.20	6.66	10.92	2.86	0.624	0.334	1.47	99.74	12.73	51.40
Dana-04-39D-18	Seamount H	plag-phyric	5	51.68	2.49	14.46	6.11	6.63	0.20	3.96	7.91	3.91	1.225	0.406	0.82	99.80	12.13	39.78
Dana-04-39D-19	Seamount H	plag-phyric	1	48.18	2.82	13.83	5.13	8.70	0.19	5.55	10.39	2.94	0.434	0.328	1.18	99.67	13.31	45.76
Dana-04-39D-21	Seamount H	gabbro/dolerite-PC?	12	49.24	2.37	12.07	3.00	13.53	0.25	4.96	9.15	2.37	0.439	0.243	1.43	99.04	16.23	38.19
Dana-04-39D-25	Seamount H	amphibole-PC?	12	52.55	0.79	16.79	1.05	7.80	0.15	5.45	7.92	3.51	1.488	0.305	1.62	99.42	8.74	55.76
Dana-04-39D-28	Seamount H	hydroth. leached	6	76.62	0.19	12.10	0.00	3.11	0.06	0.38	0.04	3.31	1.654	0.040	1.94	99.45	3.11	19.93

Sample_ID	Sc	V	Cr	Co	Ni	Cu	Zn	Ga	Rb	Sr	Y	Zr	Nb	Cs	Ba
Dana-04-11D-04	45.33	269.92	321.86	51.39	105.01	131.92	73.99	14.95	1.00	82.09	22.20	43.68	1.71	0.021	18.15
Dana-04-11D-10	38.43	382.83	169.34	52.32	88.56	254.11	118.59	21.42	2.49	197.57	28.82	129.62	9.97	0.027	67.47
Dana-04-11D-11	35.68	376.61	91.95	51.45	72.73	212.43	125.88	21.66	3.53	327.15	36.82	197.00	21.88	0.034	203.72
Dana-04-12D-04	38.09	361.04	138.64	50.50	79.42	165.85	110.91	20.24	4.87	337.76	32.97	165.33	24.80	0.113	156.44
Dana-04-12D-05	29.86	398.96	109.66	50.43	79.63	202.84	132.00	24.38	2.73	432.96	34.13	274.74	26.72	0.019	179.13
Dana-04-12D-12	39.40	414.34	213.10	50.88	94.72	248.46	119.81	21.95	2.88	227.43	37.02	174.98	14.15	0.248	70.33
Dana-04-20D-16	37.29	395.31	145.42	51.48	97.74	239.16	121.20	22.95	1.16	263.42	34.04	181.89	15.55	0.021	78.37
Dana-04-20D-17	35.99	386.73	241.41	53.29	115.42	181.01	117.09	22.40	2.59	266.04	31.27	168.89	14.02	0.059	48.84
Dana-04-20D-20	31.33	340.44	7.14	43.88	24.02	259.04	159.71	23.68	35.75	329.47	59.43	317.67	49.80	0.495	337.13
Dana-04-20D-25	4.04	1.63	0.45	60.53	2.32	4.80	135.68	21.32	225.86	4.93	66.11	446.00	37.49	0.462	101.83
Dana-04-22D-14	36.86	252.25	248.71	45.35	85.26	108.10	90.85	15.10	3.58	423.03	19.69	48.60	1.79	0.190	208.53
Dana-04-22D-16	24.62	315.48	42.04	41.86	51.63	79.28	106.45	25.06	2.69	451.78	28.51	222.15	17.35	0.010	233.45
Dana-04-22D-24	25.24	259.44	31.32	42.41	47.03	43.24	107.81	20.81	7.24	505.88	23.96	144.06	13.65	0.011	602.21
Dana-04-22D-26	48.96	340.70	98.20	48.38	55.10	38.77	96.77	15.77	32.78	105.76	28.67	54.98	4.42	0.873	83.92
Dana-04-23D-12	13.38	89.79	123.56	23.29	48.13	20.48	85.78	15.07	105.06	218.52	24.43	192.74	11.25	4.468	819.76
Dana-04-23D-15	28.93	298.01	890.49	72.94	442.67	141.44	99.88	15.37	5.25	341.28	22.36	105.16	15.45	0.053	338.42
Dana-04-23D-16	30.52	379.98	153.15	49.02	97.01	477.66	176.92	27.19	13.87	315.75	58.24	453.75	57.40	0.061	168.20
Dana-04-23D-28	33.00	273.33	886.52	68.77	522.74	141.11	73.91	12.43	4.83	307.33	20.34	70.75	4.42	0.048	52.72
Dana-04-23D-29	39.90	419.16	84.42	47.30	59.71	247.41	126.13	20.64	10.69	243.91	46.81	216.89	30.34	0.141	148.89
Dana-04-25D-03	37.69	421.50	62.26	53.19	57.39	227.56	130.96	21.06	6.20	320.80	36.96	195.21	22.03	0.201	141.04
Dana-04-27D-15	39.01	363.47	138.07	52.38	107.76	202.44	98.28	19.66	2.12	199.11	26.49	107.75	8.24	0.037	51.63
Dana-04-27D-16	38.91	432.66	109.92	53.38	81.76	327.06	142.25	22.60	4.79	226.26	43.34	231.84	20.10	0.070	69.35
Dana-04-28D-09	35.44	368.31	179.23	50.01	108.92	211.75	112.15	21.83	1.40	257.53	30.95	165.38	13.81	0.038	40.33
Dana-04-28D-11	36.61	299.28	68.85	46.62	56.69	149.00	91.61	18.82	10.48	344.28	25.31	138.10	23.53	0.060	146.50
Dana-04-29D-12	44.27	344.44	343.39	53.82	172.62	147.90	74.78	18.07	1.83	183.44	24.46	73.13	5.26	0.025	71.02
Dana-04-29D-13	44.08	419.05	106.05	46.96	65.67	205.02	115.80	21.00	25.61	232.83	42.87	183.55	19.24	1.523	64.76
Dana-04-29D-14	41.87	408.56	41.82	62.17	53.37	128.80	105.38	18.33	5.38	164.89	24.76	79.81	7.60	0.073	89.47
Dana-04-29D-15	35.73	435.51	142.50	51.27	87.65	261.29	130.45	23.84	8.98	303.62	38.13	242.58	22.96	0.037	110.85
Dana-04-32D-01	37.89	384.78	157.69	48.29	96.63	83.38	114.17	20.97	4.32	322.24	32.71	160.86	13.55	0.152	55.20
Dana-04-34D-01	37.04	354.14	87.84	46.34	76.68	212.03	109.78	20.21	9.54	318.52	34.84	174.50	15.02	0.048	32.95
Dana-04-36D-15	4.30	32.22	16.45	3.47	8.35	7.40	14.39	3.54	17.19	140.67	16.99	26.72	2.13	0.956	125.19
Dana-04-36D-16	39.49	426.20	99.95	46.04	63.27	248.68	133.55	20.93	2.79	293.22	45.33	219.82	33.05	0.034	163.14
Dana-04-36D-17	36.66	394.42	103.96	49.90	80.13	131.89	124.71	21.84	1.71	248.56	36.39	195.52	17.05	0.036	77.62
Dana-04-36D-18	39.26	421.58	97.91	47.55	63.68	247.54	134.73	21.34	3.28	294.88	45.14	221.91	33.10	0.046	161.69
Dana-04-37D-08	39.35	419.61	169.79	55.25	90.18	212.96	138.15	23.11	1.35	184.15	39.37	220.16	20.52	0.030	46.27
Dana-04-37D-09	38.13	329.51	468.61	54.61	262.56	76.91	93.38	17.87	0.60	258.12	25.95	116.21	16.42	0.012	69.35
Dana-04-37D-12	30.14	495.06	122.50	41.98	87.17	305.09	90.42	28.96	16.90	512.69	43.32	413.44	30.46	0.590	154.12
Dana-04-38D-01	43.52	321.14	69.79	54.32	60.49	147.34	101.23	16.94	8.46	128.53	25.40	28.33	4.12	0.112	67.69
Dana-04-38D-02	40.77	513.58	36.72	52.63	46.81	251.60	162.48	23.26	21.50	201.06	63.83	274.14	18.95	0.361	139.04
Dana-04-38D-03	35.43	361.97	332.35	52.56	131.06	187.75	126.77	22.25	2.19	277.25	31.32	168.58	11.40	0.056	82.00
Dana-04-38D-04	27.30	213.58	44.13	60.70	76.42	51.38	130.70	21.03	24.24	455.11	30.19	143.82	5.24	0.432	805.55
Dana-04-39D-13	39.40	357.36	267.42	48.22	117.47	155.08	107.04	22.19	5.80	202.30	31.32	141.76	12.57	0.708	29.09
Dana-04-39D-14	44.86	454.17	89.51	50.20	65.92	215.89	129.90	22.20	0.72	210.11	45.13	186.87	16.19	0.003	58.06
Dana-04-39D-15	34.23	358.53	102.07	49.76	89.54	229.65	102.34	20.07	10.27	402.81	26.13	137.09	18.54	0.114	244.55
Dana-04-39D-18	28.86	319.58	11.02	45.55	18.39	73.40	116.65	22.69	20.47	414.20	32.08	233.70	26.56	0.088	461.70
Dana-04-39D-19	35.98	354.05	71.69	48.62	59.63	224.89	124.30	21.79	3.19	317.75	37.06	189.62	21.45	0.021	187.16
Dana-04-39D-21	44.52	456.63	71.33	57.23	96.16	484.68	143.02	19.67	12.58	126.57	43.37	127.85	11.30	0.321	133.12
Dana-04-39D-25	23.65	181.19	57.19	29.82	21.79	4.81	82.28	17.89	39.74	683.11	16.02	79.07	3.48	0.799	779.66
Dana-04-39D-28	2.46	1.81	0.02	21.74	1.29	3.04	24.61	37.30	66.05	26.48	55.69	421.36	153.00	0.596	118.38

Sample_ID	La	Ce	Pr	Nd	Sm	Eu	Gd	Tb	Dy	Ho	Er	Tm	Yb	Lu	Hf	Ta	Pb	Th	U
Dana-04-11D-04	2.30	5.78	0.90	4.81	1.73	0.68	2.30	0.485	3.17	0.766	2.08	0.353	2.23	0.356	1.20	0.668	0.351	0.158	0.039
Dana-04-11D-10	8.92	21.89	3.26	15.66	4.33	1.51	4.77	0.828	4.88	1.028	2.73	0.401	2.49	0.382	3.21	0.703	1.017	0.754	0.190
Dana-04-11D-11	19.64	44.86	6.22	27.74	6.73	2.16	7.05	1.121	6.47	1.294	3.41	0.500	3.06	0.465	4.79	1.471	2.474	1.519	0.448
Dana-04-12D-04	20.39	43.70	5.75	24.32	5.69	1.91	6.12	0.955	5.71	1.169	3.09	0.450	2.82	0.425	3.98	1.590	1.885	1.712	0.417
Dana-04-12D-05	23.42	56.74	8.15	36.63	8.44	2.72	8.29	1.232	6.69	1.236	2.99	0.407	2.48	0.343	6.39	1.745	2.064	1.695	0.495
Dana-04-12D-12	12.12	30.22	4.65	21.98	6.01	2.04	6.36	1.115	6.49	1.319	3.45	0.500	3.15	0.473	4.35	1.022	1.219	1.016	0.278
Dana-04-20D-16	13.26	32.72	4.95	23.03	6.11	2.06	6.37	1.073	6.16	1.240	3.14	0.458	2.81	0.423	4.62	1.232	1.326	1.057	0.310
Dana-04-20D-17	11.94	30.15	4.67	22.12	5.81	2.00	6.08	1.012	5.90	1.169	2.93	0.424	2.56	0.383	4.21	1.047	1.088	0.922	0.280
Dana-04-20D-20	41.46	86.71	11.31	47.14	10.71	3.18	11.40	1.790	10.66	2.159	5.65	0.853	5.35	0.792	7.79	3.423	3.713	4.012	0.989
Dana-04-20D-25	43.35	68.06	10.27	37.16	7.53	0.45	8.69	1.635	10.44	2.352	6.34	0.996	6.02	0.866	12.16	3.190	23.357	11.627	0.777
Dana-04-22D-14	5.89	13.00	1.99	9.13	2.47	0.92	2.89	0.496	3.26	0.700	1.92	0.305	1.90	0.294	1.35	0.144	2.197	0.265	0.127
Dana-04-22D-16	21.01	49.40	6.74	29.61	6.76	2.17	6.57	0.955	5.16	0.995	2.53	0.350	2.14	0.313	5.21	1.193	2.176	1.342	0.404
Dana-04-22D-24	22.68	49.18	6.52	27.39	5.88	1.78	5.87	0.812	4.41	0.843	2.14	0.298	1.86	0.264	3.78	0.841	3.726	0.876	0.251
Dana-04-22D-26	5.43	13.04	1.90	9.31	2.80	0.92	3.49	0.657	4.34	0.974	2.74	0.432	2.79	0.422	1.65	0.449	2.794	0.612	0.159
Dana-04-23D-12	30.84	60.51	7.37	27.27	5.18	1.02	5.05	0.706	4.04	0.807	2.28	0.358	2.29	0.367	5.02	1.793	19.027	9.410	2.612
Dana-04-23D-15	13.46	31.51	4.40	19.94	4.68	1.58	4.88	0.718	4.00	0.755	1.98	0.276	1.69	0.257	2.63	1.389	0.944	0.716	0.185
Dana-04-23D-16	40.94	96.84	13.33	58.08	13.24	3.86	13.11	1.957	10.79	2.022	5.23	0.730	4.32	0.640	10.35	3.746	2.464	3.378	1.053
Dana-04-23D-28	4.91	12.13	1.83	8.94	2.76	0.98	3.15	0.544	3.36	0.708	1.89	0.281	1.74	0.253	1.90	0.359	0.798	0.532	0.106
Dana-04-23D-29	22.94	51.12	6.89	29.85	7.17	2.20	7.88	1.297	7.76	1.604	4.36	0.661	4.02	0.612	5.27	2.451	1.861	1.984	0.547
Dana-04-25D-03	19.12	44.52	6.39	28.41	6.95	2.24	7.23	1.166	6.69	1.302	3.42	0.483	2.96	0.436	4.94	1.555	2.018	1.503	0.536
Dana-04-27D-15	7.67	19.06	2.92	14.06	4.02	1.37	4.46	0.742	4.60	0.930	2.58	0.375	2.29	0.350	2.82	1.064	0.890	0.630	0.183
Dana-04-27D-16	15.83	40.39	6.21	29.16	7.69	2.42	8.20	1.332	7.92	1.536	4.07	0.598	3.56	0.534	5.85	1.387	1.254	1.306	0.431
Dana-04-28D-09	11.51	29.30	4.55	21.70	5.73	1.95	6.16	0.991	5.73	1.129	2.88	0.418	2.47	0.365	4.30	0.955	1.025	0.893	0.287
Dana-04-28D-11	17.62	37.81	5.02	21.98	5.09	1.69	5.24	0.800	4.58	0.913	2.40	0.341	2.04	0.307	3.44	1.491	1.116	1.596	0.434
Dana-04-29D-12	5.05	13.15	2.12	10.85	3.42	1.26	3.93	0.688	4.15	0.870	2.32	0.343	2.02	0.300	2.15	0.701	0.651	0.396	0.098
Dana-04-29D-13	15.53	35.10	5.03	23.53	5.97	1.98	7.18	1.173	7.02	1.462	4.02	0.593	3.62	0.541	4.57	1.273	1.192	1.374	0.346
Dana-04-29D-14	7.69	18.36	2.64	12.28	3.22	1.05	3.66	0.637	3.90	0.842	2.40	0.361	2.25	0.337	2.08	0.704	1.257	0.815	0.202
Dana-04-29D-15	18.33	44.88	6.69	31.25	7.71	2.43	8.02	1.228	6.91	1.368	3.46	0.490	2.90	0.443	5.95	1.782	1.686	1.478	0.436
Dana-04-32D-01	11.59	29.21	4.25	20.53	5.41	1.72	6.06	0.960	5.53	1.135	3.04	0.427	2.65	0.380	4.02	0.894	1.686	0.884	0.253
Dana-04-34D-01	13.48	32.48	4.87	23.09	5.88	1.95	6.59	1.019	5.94	1.225	3.24	0.448	2.83	0.412	4.35	1.003	1.444	1.140	0.579
Dana-04-36D-15	10.22	19.55	2.38	9.67	1.95	0.50	2.34	0.369	2.04	0.422	1.12	0.145	0.90	0.141	0.59	0.165	3.818	1.664	0.541
Dana-04-36D-16	25.11	55.40	7.52	32.84	7.43	2.28	8.20	1.310	7.74	1.588	4.34	0.630	3.91	0.596	5.45	2.141	1.934	2.138	0.613
Dana-04-36D-17	15.02	36.54	5.31	25.29	6.39	2.08	7.12	1.112	6.31	1.283	3.43	0.492	2.88	0.435	4.86	1.101	1.965	1.302	0.348
Dana-04-36D-18	25.43	55.73	7.37	32.42	7.24	2.28	8.23	1.271	7.68	1.591	4.29	0.632	3.91	0.583	5.40	2.031	1.898	2.142	0.595
Dana-04-37D-08	18.14	43.27	6.57	30.59	7.58	2.41	8.24	1.236	7.14	1.429	3.72	0.516	3.13	0.464	5.52	1.357	1.124	1.393	0.294
Dana-04-37D-09	13.63	31.90	4.52	20.61	4.91	1.64	5.35	0.827	4.76	0.926	2.44	0.343	2.07	0.297	3.06	1.052	1.037	1.032	0.170
Dana-04-37D-12	29.09	79.26	12.40	58.82	13.09	4.02	12.70	1.744	9.05	1.606	3.97	0.517	2.99	0.417	9.87	2.053	2.008	2.124	0.731
Dana-04-38D-01	5.24	13.41	2.10	10.34	2.99	1.02	3.71	0.662	4.18	0.906	2.51	0.383	2.39	0.361	0.93	0.580	4.961	0.516	0.155
Dana-04-38D-02	19.39	46.65	7.06	33.98	9.39	2.80	10.81	1.797	10.80	2.254	6.10	0.891	5.47	0.824	7.05	1.329	2.568	2.322	0.639
Dana-04-38D-03	11.38	29.37	4.47	22.00	5.77	1.93	6.40	0.995	5.79	1.144	2.92	0.410	2.49	0.350	4.36	0.914	2.623	0.938	0.306
Dana-04-38D-04	15.75	35.12	5.33	24.26	5.55	2.11	5.68	0.899	5.22	1.067	2.91	0.426	2.63	0.406	3.54	0.588	5.272	1.120	0.450
Dana-04-39D-13	10.28	25.68	4.06	18.63	5.05	1.68	5.30	0.913	5.33	1.099	2.80	0.420	2.54	0.383	3.66	0.916	0.910	0.817	0.288
Dana-04-39D-14	14.18	33.53	5.25	24.45	6.66	2.14	7.06	1.268	7.64	1.590	4.27	0.646	3.94	0.593	5.00	1.303	1.132	1.127	0.332
Dana-04-39D-15	15.92	36.67	5.45	24.65	5.75	1.93	5.60	0.890	4.82	0.943	2.41	0.343	2.06	0.313	3.53	1.215	1.728	1.215	0.313
Dana-04-39D-18	30.82	66.33	9.09	37.51	7.59	2.24	7.41	1.070	5.93	1.149	2.97	0.424	2.64	0.390	5.86	2.124	3.497	2.338	0.550
Dana-04-39D-19	19.14	43.81	6.32	27.89	6.66	2.12	7.09	1.134	6.59	1.317	3.46	0.524	3.10	0.473	4.80	1.544	1.947	1.488	0.427
Dana-04-39D-21	13.05	30.83	4.47	20.64	5.40	1.67	6.24	1.118	6.90	1.509	4.15	0.627	4.04	0.622	3.51	0.948	2.497	1.509	0.360
Dana-04-39D-25	15.92	35.26	5.13	21.76	4.41	1.32	4.09	0.539	2.95	0.580	1.51	0.227	1.42	0.220	2.12	0.250	4.055	0.939	0.451
Dana-04-39D-28	116.77	231.67	27.61	95.77	15.95	0.57	13.99	1.876	9.90	1.910	5.28	0.794	5.32	0.718	12.18	11.435	6.280	24.059	4.630